MECHANISMS OF PHOSPHORUS STABILIZATION IN THE SOIL ENVIRONMENT: A MOLECULAR SCALE EVALUATION

by

Stefan Hunger

A dissertation submitted to the faculty of the University of Delaware in partial fulfillment of the requirements for the degree of Doctor of Philosophy in Plant and Soil Sciences

Fall 2003

UMI Number: 3112674

UMI Microform 3112674

ProQuest Information and Learning Company
300 North Zeeb Road
P.O. Box 1346
Ann Arbor, MI 48106-1346

MECHANISMS OF PHOSPHORUS STABILIZATION IN THE SOIL ENVIRONMENT: A MOLECULAR SCALE EVALUATION

by

Stefan Hunger

Approved: Donald L. Sparks

Donald L. Sparks, Ph.D.
Chair of the Department of Plant and Soil Sciences

Approved: Robin W. Morgan

Robin W. Morgan, Ph.D.
Dean of the College of Agriculture and Natural Resources

Approved:

Conrado M. Gempesaw II, PhD.
Vice Provost for Academic and International Programs

I certify that I have read this dissertation and that in my opinion it meets the academic and professional standard required by the University as a dissertation for the degree of Doctor of Philosophy.

Signed: 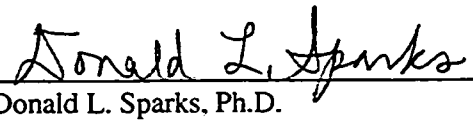

Donald L. Sparks, Ph.D.
Professor in charge of dissertation

I certify that I have read this dissertation and that in my opinion it meets the academic and professional standard required by the University as a dissertation for the degree of Doctor of Philosophy.

Signed: 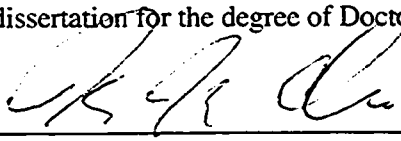

Herman M. Cho, Ph.D.
External member of dissertation committee

I certify that I have read this dissertation and that in my opinion it meets the academic and professional standard required by the University as a dissertation for the degree of Doctor of Philosophy.

Signed: 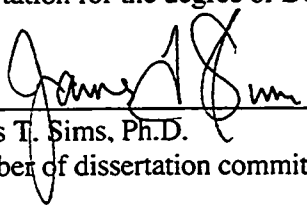

James T. Sims, Ph.D.
Member of dissertation committee

I certify that I have read this dissertation and that in my opinion it meets the academic and professional standard required by the University as a dissertation for the degree of Doctor of Philosophy.

Signed: 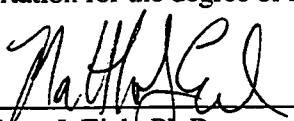

Matthew J. Eick, Ph.D.
Member of dissertation committee

ACKNOWLEDGMENTS

First and foremost I wish to thank my advisory committee, Dr. Matthew J. Eick, Dr. Herman Cho, Dr. J. Thomas Sims and Dr. Donald L. Sparks, for their guidance with the conception and development of this work. I am especially grateful to Dr. Sparks for giving me the freedom and making available the resources to pursue this project.

I am also indebted to the scientific staff at the National Laboratories where the spectroscopic work was performed, especially Drs. Sarah Burton and Joseph Ford of Environmental Molecular Science Laboratory for their assistance with the NMR experiments, and Dr. Wolfgang Caliebe of the National Synchrotron Light Source for his assistance at beamline X-19A. I wish to thank all of them for their patience, their helpful explanations, and their support at almost every hour of the day.

The NMR experiments were performed in the Environmental Molecular Sciences Laboratory (a national scientific user facility sponsored by the U.S. DOE Office of Biological and Environmental Research) located at Pacific Northwest National Laboratory, operated by Battelle for the DOE. XAS work was performed at beamline X-19A of the National Synchrotron Light Source, which is part of the Brookhaven National Laboratory, Upton, NY.

I appreciate the support of a Delaware Water Resources Center (DWRC) graduate research fellowship.

I wish to thank the former and current members of the Soil Chemistry Research Group of the University of Delaware for the friendly atmosphere and a stimulating scientific environment, which made my time with them a pleasant experience. I am especially grateful to Yuji Arai, Eef Elzinga, Maarten Nachtegaal, Derek Peak, and Darryl Roberts for interesting discussions, scientific and otherwise, and their support. I am also grateful to all the friends I made in Delaware for making this great adventure of mine bearable.

I dedicate this work to Johanna Büchner and our son Karl Friedrich Büchner, who have been waiting patiently for me. Their love was my greatest motivation.

TABLE OF CONTENTS

LIST OF TABLES

LIST OF FIGURES

ABSTRACT

The mobility and bioavailability of phosphorus, an element widely considered to be the limiting nutrient for eutrophication in fresh water, is determined by its speciation in the natural environment. The speciation of phosphate in model systems of increasing complexity and in poultry litter was investigated using solid-state ^{31}P Nuclear Magnetic Resonance (NMR) and P K-edge X-ray Absorption Near Edge Structure (XANES) spectroscopy as molecular tools. The sorption kinetics and isotherms of phosphate were also investigated in these model systems.

The spectroscopic results indicate that phosphate sorbs to the gibbsite surface as a combination of binuclear, bidentate surface complexes and amorphous aluminum phosphate surface precipitates in the presence and absence of the competing organic acid citric acid and of the cooperatively adsorbing calcium cation. No aluminum phosphate surface precipitates are however observed in the model system containing both gibbsite and calcite as sorbents, but rather ternary surface complexes at the gibbsite surface at low surface concentrations, and a mixture of surface complexes at the gibbsite surface and a calcium phosphate precipitate at the calcite surface at elevated concentrations.

The results of the ^{31}P-NMR-spectroscopic investigation of unamended and alum-amended poultry litter (PL) indicate that on average 40 ± 14 % of the phosphate in alum-amended PL are bound either as surface complexes on aluminum hydroxide or as an uncondensed aluminum hydroxyphosphate precipitate. In both alum-amended PL and unamended PL, phosphate is present as a calcium phosphate phase, probably a surface precipitate at calcium carbonate surfaces or tribasic calcium phosphate. Only a minor

proportion can be clearly identified as inorganic orthophosphate bound by hydrogen bonds and is expected to be readily water-soluble. A large proportion (= 50 %) of the phosphate species cannot be resolved by ^{31}P-NMR. These species are probably organic and inorganic orthophosphate complexed by a variety of cations in an inhomogeneous environment.

This research demonstrates the scope and limitations of solid-state ^{31}P-NMR spectroscopy for the analysis of heterogeneous materials such as poultry litter. It further provides a basis for the interpretation of solid-state ^{31}P-NMR spectra of other environmental samples, e.g. whole soils or size fractions of soils, composts, sewage sludge, or animal wastes.

Chapter 1

INTRODUCTION

Phosphorus has been recognized as the limiting nutrient for eutrophication in fresh water because it is supplied through equilibria with solid phases, whereas other macronutrients such as carbon and nitrogen are also supplied by atmospheric sources (Sharpley et al., 1994). Although a naturally occurring aging phenomenon of surface water, eutrophication is accelerated by anthropogenic nutrient inputs and therefore poses a severe threat to water quality worldwide (Sharpley et al., 1994, 1999, 2000). An over-supply of nutrients triggers an increased growth of algae and other water plants. The decaying plant matter causes turbidity and reduces the oxygen content, severely disrupting the aquatic ecosystem and causing fish kills. This reduces the water quality for use and poses severe health threats. Elevated concentrations of phosphorus have also been associated with the outbreak of the dinoflagellate *Pfiesteria piscicida* in estuaries on the Atlantic coast of the U.S., which produces a toxin lethal to fish and hazardous to the health of humans (Burkholder and Glasgow Jr, 1997; Burkholder et al., 1992, 1997). With rapidly diminishing fresh water supplies and the accompanying political and social problems expected or already encountered worldwide, the management and protection of fresh water supplies have become environmental challenges for the immediate future and play an important role towards sustainable development.

After decades of regulating phosphorus point-sources and decreasing inputs into lakes, streams and estuaries from industry and municipal waste water treatment plants, inputs of phosphorus from agriculture have remained as an important non-point-source.

Modern intensive agriculture relies heavily on the input of nutrients in the form of mineral fertilizers or as animal manure to ensure food and fiber production. Animal manure has been extensively utilized as an inexpensive and effective method to improve soil quality by adding organic matter and enhancing soil fertility. In areas with industrialized poultry production such as the Delmarva Peninsula, however, the practice of soil-application as a cheap way of disposal of the animal wastes has led to a net accumulation of nutrients, especially phosphorus, in the soils. This is mainly caused by the sheer mass of animal wastes applied to the soils. Another reason is the low N : P ratio of the poultry litter in combination with an application practice to meet the N requirements of the soils. In other areas, centuries of application of fertilizers has caused enrichment of the soils with phosphorus.

Phosphorus can be lost from soils by erosion (particulate phosphorus) and by surface run-off and leaching (primarily soluble phosphorus). A research effort has been undertaken to establish a general model linking such soil-P properties as the P-saturation or soil-P test values to the concentration of P in run-off and provide a tool to better predict P-losses from soils (Maguire and Sims, 2002; McDowell and Sharpley, 2003; Pautler and Sims, 2000). P-saturation has been defined as the maximum amount of P that can be immobilized in a soil, assuming that inorganic phosphate mainly adsorbs to the amorphous or oxalate-extractable Fe- and Al- hydroxides (Freese et al., 1995). In reality,

the definition of a soil-P level, at which saturation occurs, is not trivial due to the complexity of P reactions in soils and the number of different species controlling P concentrations.

In acid to neutral agricultural soils, inorganic orthophosphate is primarily associated with secondary Al and Fe minerals, which are either present as distinct metal (oxy)hydroxide particles in the clay-fraction or as coatings on primary mineral grains. It has been found that even in neutral to basic soils, which contain considerable amounts of Ca and Mg as free cations or as calcite and dolomite, only part of the soil-P is present as Ca or Mg phosphate phases (Castro and Torrent, 1998, 2000; Delgado et al., 2000; Hamad et al., 1992). Phosphate has been found to be either predominantly associated with Fe (oxy)hydroxide coatings (Hamad et al., 1992) or to be distributed between calcium phosphate precipitates and sorbates on variably charged mineral surfaces (Castro and Torrent, 1998, 2000), depending on the relative amounts of the soil components.

Up to 80% of the soil-P compounds are organic phosphates or phosphonates (Dalal, 1977), the sorption reactions of which have not been studied as extensively as those of inorganic orthophosphate (Parfitt, 1978). Organic P compounds in soils show a broad range of solubility and therefore mobility: Small phosphate monoester or diester molecules, products of metabolic processes in microorganisms, are readily soluble, whereas phosphates or phosphonates incorporated in soil organic matter (SOM) or microbial biomass are more slowly mobilized or virtually insoluble.

Of the phosphate species in soils, dissolved inorganic orthophosphate, which is present as hydrogen phosphate and dihydrogen phosphate at typical soil pH values, has

been assumed to be the predominantly bioavailable form. It is however also known that soluble organic phosphate esters are taken up by microorganisms and that soil bacteria (Paul and Clark, 1996) and mycorrhizal fungi (Smith and Read, 1997) have developed mechanisms of acquiring phosphate from mineral phases, providing symbiotic plants with phosphorus. Mineral phosphate is further solubilized in the rhizosphere due to changes in the soil chemistry caused by the plant roots. Some plants excrete low molecular weight organic acids to make metal cations available for uptake or to detoxify high metal concentrations, at the same time dissolving phosphate associated with those metal cations. Roots also lower the pH in the rhizosphere by exuding protons, which also dissolves mineral phosphate phases (Jones, 1998; Jones and Darrah, 1994).

Organic ligands in soils not only affect desorption of phosphate but also its adsorption. Organic amendments to various soils, such as manure and crop residues, have been shown to increase the solution concentration of phosphate (see for example (Iyamuremye et al., 1996a, b, c; Ohno, 1997; Ohno and Crannell, 1996; Sibanda and Young, 1986; Staunton and Leprince, 1996)). This has been explained by competition between phosphate anions and organic acids for surface sites (Traina et al., 1986).

The reactions determining phosphorus mobility and bioavailability in soils are therefore complex and no simple correlation with easily attainable soil-P parameters such as soil-test P or total P level exists. A more complex approach is the study of phosphate sorption to soils or single soil minerals to determine the dependence of the amount of phosphate sorbed by the solid phase on pH (sorption envelopes); on solution concentration (sorption isotherms); or on time (sorption kinetics). Although great

advances have been made in modeling sorption envelopes and isotherms numerically, their results have only limited applicability, mostly due to the fact that soils are too heterogeneous to allow for generalization and phosphate sorption itself is affected by too many parameters.

P mobility and bioavailability are generally determined by P speciation. Although certain phosphate species such as mono- and bi-dentate surface complexes have been successfully used to model the pH dependence of phosphate sorption to soil minerals, P speciation can only be unambiguously studied using molecular spectroscopy. Furthermore, no correlations exist between P speciation, the molecular scale of P sorption, and sorption kinetics and isotherms on a macroscopic scale.

The molecular spectroscopic methods nuclear magnetic resonance (NMR) and x-ray-absorption (XAS) spectroscopy are standard analytical methods in chemistry, biology, medicine and materials science. Improvements in technology, such as the availability of stronger magnets for NMR and 3rd generation synchrotron radiation facilities for XAS, and development of advanced techniques have made them suitable for studying environmental samples as well, which usually pose greater difficulties to the spectroscopist due to low concentrations or sample heterogeneity (See for example: (Bertsch and Hunter, 2001; Fendorf et al., 1994; Lookman et al., 1997; Nanny et al., 1997; Wilson, 1987)).

Attempts have been made to combine information on the molecular scale from spectroscopic investigations with macroscopic information to link speciation with solubility, desorbability and mobility. This approach allows for a better understanding of

sorption and desorption reaction mechanisms of metals on soil minerals and thus for generalizations and predictions of their fate and mobility in soils (Guest et al., 2002; Scheidegger et al., 1996, 1998). Similarly, Frossard et al. (1994) combined high-resolution solid-state ^{31}P NMR spectroscopy with a sequential chemical extraction technique for the analysis of urban sewage sludge to identify P-species and gain insight in their mobility and availability.

The objectives of the research presented here are the investigation of P species in model systems and in natural systems using a combination of spectroscopic techniques and macroscopic determination of solubility, sorption kinetics and isotherms. On the molecular scale, novel spectroscopic techniques are being employed and established methods are put to novel uses.

Chapter 2

PHOSPHATE SPECIATION IN MODEL SYSTEMS

2.1. Abstract

The sorption of phosphate was investigated in systems of increasing complexity modeling the soil environment using spectroscopic (^{31}P-NMR and P K-edge XANES) and macroscopic tools (sorption isotherms, kinetics and pH-envelope). Phosphate sorbs to the gibbsite surface as binuclear, bidentate inner-sphere surface complexes and aluminum phosphate surface precipitates between pH 4 and pH 8. ^{31}P-NMR and P K-edge XANES results indicate that the surface precipitates are amorphous and have a close-range ordering similar to variscite ($AlPO_4 \cdot 2\ H_2O$) and wavellite ($Al_3(OH)_3(PO_4)_2 \cdot 5\ H_2O$). They predominate at low pH values, whereas surface complexes dominate above pH 7.

Both surface complexes and surface precipitates remain important over reaction times up to 100 days, indicating that both diffusion into micropores of the sorbent with subsequent adsorption and growth of the surface precipitate can be proposed as mechanisms for the slow phosphate sorption reaction.

Competition between phosphate and citric acid is greatest at pH 6, whereas phosphate sorption is less affected by equimolar concentrations of citric acid at pH 4 and pH 7. The spectroscopic results indicate that citric acid not only competes with

phosphate for sorption sites at the gibbsite surface but also reduces the formation of the surface precipitate with a structure similar to variscite.

Calcium and phosphate exhibit cooperative sorption to the gibbsite surface in suspensions that are undersaturated with respect to apatite, *i.e.* phosphate sorption increases in the presence of calcium, and the calcium sorption pH envelope is extended to lower pH values in the presence of phosphate. However, no spectroscopic evidence exists for calcium phosphate surface precipitates or ternary complexes of calcium with surface-bound phosphate. This synergistic sorption behavior can be explained with a more negative surface charge of the phosphated gibbsite surface and thus reduced electrostatic repulsion, which allows more calcium adsorption. Adsorption of calcium, in turn, reduces the negative surface charge, allowing more phosphate to adsorb.

The suspensions containing both gibbsite and calcite as sorbents, on the other hand, are oversaturated with respect to solid calcium phosphate phases. The ^{31}P-NMR-spectroscopic results therefore indicated the presence of both a calcium phosphate surface precipitate at the calcite surface and bidentate, binuclear surface complexes at the gibbsite surface. No aluminum phosphate surface precipitates were observed. The downfield shift of the peak assigned to the phosphate surface complexes furthermore indicated a stabilization of the surface complexes as ternary complexes.

These results are important in laying a foundation for spectroscopic investigations of soil samples and other complex sample matrices. Although aluminum minerals are of less importance in the soil environment as sorbents for phosphate than iron minerals, sorption reactions with both sorbents are similar. The information about phosphate

speciation in the model systems is therefore applicable to phosphate speciation in slightly acid to acid soils, limed soils, and neutral to alkaline soils that contain aluminum and iron hydroxide phases.

2.2. Literature Review

2.2.1. Spectroscopic investigations of the influence of pH and time on the binary system phosphate/ gibbsite

Phosphorus is retained by aluminum and iron minerals in slightly acid to acid soils. The two mechanisms involved differ in time-scale, over which they take place, and the stability of the products formed. The initial fast reaction appears to be related to an exchange of a surface hydroxyl group for a phosphate ion, leading to the formation of a surface complex (Parfitt, 1978; Sparks, 1995; Sposito, 1984, 1989). The Constant Capacitance Model (Goldberg, 1992; Goldberg and Sposito, 1984a, b) and the Triple Layer Model (Goldberg, 1992; He et al., 1997) describe the changes in adsorption with changing pH, ionic strength and phosphate concentration well. However, the precise nature of these complexes has not been proven, since compliance of the macroscopic sorption data with a model assuming the formation of certain complexes does not reveal structural information on a molecular level.

Different variations of Fourier Transform Infrared Spectroscopy (FTIR) sensitive for species at the solid-solution interface have been applied to determine the structure of phosphate surface complexes on soil minerals. The formation of a monodentate, nonbridging surface complex was determined from diffuse reflectance FTIR spectroscopy (Laiti et al., 1996, 1998; Persson et al., 1996). Changes in the spectra with increasing pH were attributed to decreasing protonation of the surface-bound phosphate anions. An *in-situ* ATR-FTIR study of phosphate sorption to hydrous ferric oxide (Arai and Sparks, 2001), however, proposed a mixture of monodentate and bidentate inner-

sphere surface complexes with various degrees of protonation depending on the pH of the suspension, of which only the bidentate complexes could be confirmed unambiguously, mainly due to limitations of the method.

Furthermore, evidence was presented, that at higher phosphate concentrations and longer reaction times a new solid phase is formed at the surface (Laiti et al., 1996, 1998; Nanzyo, 1984, 1986). It has been hypothesized, that the metal hydroxide surface weathers and that the released metal ions reprecipitate to form metal phosphates. This is in agreement with thermodynamic predictions that the aluminum and iron phosphates in these systems are more stable than the hydroxides (Lindsay, 1979; Stumm and Morgan, 1996).

The formation of amorphous metal phosphates has been suggested as the mechanism of the second, slow sorption reaction. This reaction takes place over a longer time than the ligand exchange reaction and may be the cause for the increasing stability of the sorption products with time, which has been reported by Barrow (Barrow, 1983b). The slow diffusion of phosphate into the mineral or through a surface coating of metal phosphate has alternatively been suggested (Barrow, 1983a, b, 1984; Bolan et al., 1985; van Riemsdijk et al., 1984), and could not be excluded as a possible mechanism for the slow phosphate sorption. The fact that the products of these reactions have only short-range ordering prevents the application of X-ray diffraction, the most commonly used method to identify mineral components in soils. A very recent study by Arai and Sparks (2002, unpublished data) has placed in doubt the theory of the precipitate formation by showing very clearly using P K-edge X-ray Absorption Near Edge Spectroscopy

(XANES) that no crystalline metal phosphate phase is formed during the sorption of phosphate to soils and hydrous ferric oxide.

However, evidence was presented in support of the formation of a surface precipitate on goethite upon phosphate sorption by Li and Stanforth (2000) and Ler and Stanforth (2003) from an investigation of the ?-potential of goethite particles during phosphate sorption and co-sorption of phosphate and iron or lead. Particularly the slow increase of the ?-potential over time lead to the conclusion that iron dissolves from the goethite crystal and re-adsorbs to the phosphated surface, forming ternary surface complexes that slowly transform into a surface precipitate.

The mechanisms of the initial fast reaction involved in the fixation of phosphate to aluminum and iron minerals in soils is thus not completely understood, while the mechanism of the slow consecutive sorption reaction and the structure of the products formed is still elusive.

Magic-angle-spinning Nuclear Magnetic Resonance (MAS NMR) Spectroscopy, a powerful technique to determine structures of materials, which have short-range, but no long-range ordering, has been employed to investigate the sorption reaction of phosphate to soils and to discrete soil minerals, mainly aluminum hydroxides. Lookman and coworkers (1996, 1997) identified phosphate species associated with aluminum and calcium in soils. Bleam et al. (1991) used cross-polarization magic-angle-spinning (CP-MAS) NMR experiments to discriminate protonated from deprotonated phosphate species attached to the mineral surface and distinguish between sorbed species and

phosphate incorporated into a surface precipitate. Unambiguous spectral assignment and identification of species was however not possible.

The CP-MAS NMR pulse sequence transfers magnetization from an abundant nucleus such as the proton to a dilute nucleus, thereby selectively enhancing its signal compared to the classical MAS-NMR experiment (Hartmann and Hahn, 1962; Pines et al., 1973). This improves resolution and signal to noise ratio as well as aiding spectral assignment.

In an investigation of phosphate sorption to amorphous aluminum hydroxide (Lookman et al., 1994), ^{31}P-MAS-NMR did not provide precise information because the peaks due to the diverse chemical environments of P were unresolved. The ^{27}Al-MAS-NMR spectra, on the other hand, showed distinct peaks for the three different coordination polyhedra of aluminum in synthetic amorphous aluminum phosphate and in amorphous aluminum hydroxide reacted with phosphate. The formation of aluminum phosphate minerals, which had been characterized by solid state NMR, was not observed (Bleam et al., 1989a, b). Amorphous aluminum-phosphate, however, could be detected after reacting amorphous aluminum hydroxide with phosphate (Lookman et al., 1994). From these findings, the phosphate promoted weathering of the hydroxide was proposed as a mechanism to describe phosphate sorption to amorphous aluminum hydroxides at high phosphate concentrations.

Other studies using solid state MAS-NMR were only able to assign qualitatively the phosphate present in fertilized soils or soils amended with bio-solids to different P-pools characterized by their ease of desorption (Hinedi and Chang, 1989; Hinedi et al.,

1989a, b; Leinweber et al., 1997). Due to the heterogeneity of soils and the presence of a range of different environments of the NMR-sensitive nuclei the spectra are not easy to interpret (Lookman et al., 1997). Conducting NMR spectroscopy with soil samples suffers further from the presence of paramagnetic cations, such as Fe and Mn. When close to the P nucleus their influence on the local magnetic field accelerates the relaxation of the P magnetization, broadening the resonance signal beyond detection (Blumberg, 1960; Lookman et al., 1997; Smernik and Oades, 2002; Wilson, 1987). Consequently, removing these metals from soil samples prior to the experiments is important but may change the amount of Al present and the speciation of phosphate associated with Al as well.

McDowell and coworkers (2002) used MAS ^{31}P-NMR with and without cross-polarization to investigate P-species in soil samples before and after extraction of labile P-species with 0.01 M $CaCl_2$ or DI H_2O. They identified several phosphate phases associated with Ca and Al, including the aluminum phosphate minerals berlinite (-25 ppm), variscite (-19 ppm) and wavellite (-13 to -11 ppm), and the calcium phosphate minerals monetite (-2 ppm), octacalcium phosphate (3.4 ppm), hydroxyapatite and amorphous calcium phosphate (3.0 ppm), of which the last two are indistinguishable from each other. This assignment was, however, only based on literature values of chemical shifts of the minerals, completely disregarding the possible formation of surface complexes, and without discussion on whether the proposed mineral phases could have formed under these conditions.

Al and P MAS NMR have been used successfully in the investigation of the structures of amorphous materials, namely aluminum-phosphate glasses, molecular sieves and alumina catalyst precursors (Fernandez and Amoureux, 1995; Fernandez et al., 1996; Fyfe et al., 1995; Kraus et al., 1993; Rong et al., 1998; Schaller et al., 1999; van Eck et al., 1995). New methods, which have been developed recently, are especially suited for this purpose. The weak heteronuclear dipolar coupling of nuclei in close contact to each other can be detected by the techniques Rotational Echo Double Resonance (REDOR) and Transfer of Population in Double Resonance (TRAPDOR). The first method (REDOR) has been developed to investigate the usually very weak ^{15}N-^{13}C heteronuclear coupling in amino-acid crystals and has been used to measure inter-atomic distances (Gullion and Schaefer, 1989a, b). The latter method (TRAPDOR) is an application to quadrupolar nuclei. Both can be used to detect pairs of aluminum and phosphorus atoms not farther apart than 500 pm (5 Å) (van Eck et al., 1995). Combining this information with the chemical shift of the aluminum nucleus reveals the coordination polyhedron of aluminum phosphate. A combination of both methods revealed the formation of aluminum phosphate on the surface of γ-alumina, which had been impregnated with phosphate at elevated temperatures (Fyfe et al., 1993; van Eck et al., 1995).

The above two methods, have been shown to reveal valuable structural information in a system very similar to those involved in the retention of phosphate in acid to neutral soils. They are expected to give better insight into the coordination geometries of aluminum and phosphate in samples of common soil minerals reacted with phosphate or more heterogeneous systems. It should be possible to distinguish between

phosphate adsorbed to external or internal surfaces and phosphate in a bulk aluminum phosphate precipitate by direct comparison with synthetic aluminum phosphate and with materials only briefly reacted with phosphate, in which the phosphate should be predominately present as surface complexes. Due to the unfavorable influence of paramagnetic cations on the spectral quality, sorption experiments will be conducted using the aluminum hydroxide mineral gibbsite. This is only present as a distinct phase in the clay fraction of highly weathered tropical soils, but it is structurally analogous to the ubiquitous amorphous $Al(OH)_3$ coatings and easier to characterize. The number of different surface complexes will be therefore limited, simplifying the interpretation of the spectra.

2.2.2. Investigation of P reactions and speciation in the ternary system phosphate/ citrate/ gibbsite

In general, the introduction of organic acids into the sorption reaction of phosphate to soil minerals complicates the system by creating more reaction pathways: being anions, phosphate and organic acids can compete for surface sites. This has been shown for phosphate sorption to goethite and gibbsite in the presence of simple anions such as citric acid (Geelhoed et al., 1998, 1999), *o*-phthalate (Nilsson et al., 1996), and humic acids (Sibanda and Young, 1986). It is however not known whether they generally adsorb to the same sites or whether they prefer different sites. Surface complexation modeling of the competitive adsorption of phosphate and citrate on goethite proposed inner-sphere complexes for both anions and ligand exchange with the same surface hydroxyls (Geelhoed et al., 1998). The model described the experimental data well.

Besides competition, organic acids can influence the sorption reaction by ligand-promoted dissolution of the mineral surface or of hydrolyzed Al or Fe-polymers on the surface (Traina et al., 1986). This causes higher concentrations of metal species in solution, primarily as metal complexes with the organic acid and phosphate, and an alteration of the surface.

Alteration of the surface occurs during ligand-promoted dissolution. Adsorption of the organic acid and formation of a surface complex is usually considered the initial step of dissolution, followed by detachment of the metal-complex (Stumm, 1986, 1997). The detachment of the metal complex is faster at kinks and edges of the mineral surface, because less metal-oxygen bonds have to be broken. These surface inhomogeneities will therefore dissolve faster. Amorphous aluminum hydroxide fragments, which provide a large part of the surface area when present in the material, are also likely to be predominantly dissolved. Whether or not ligand-promoted dissolution influences phosphate sorption by reducing the reactive surface sites, has not yet been established.

2.2.3. Investigation of P reactions and speciation in the ternary system phosphate/ calcium/ gibbsite

Other than with introducing organic acids into the sorption reaction, the phosphate anion does only compete to a minor extent for sorption sites with the calcium cation in the ternary system phosphate/calcium/gibbsite. In this ternary system the sorbent gibbsite primarily competes with calcium for the phosphate anion. Three possible reaction pathways can be proposed: a) calcium forms a calcium phosphate surface precipitate; b) calcium rather adsorbs to the phosphate inner-sphere complexes on the gibbsite surface, forming a ternary complex; c) calcium adsorbs as outer-sphere complexes on the phosphated gibbsite surface. The adsorbed phosphate anions decrease the surface charge, thus lowering the PZC and generally facilitating cation adsorption at lower pH values. It is not verified whether cations are preferentially attracted by localized surface charge in the phosphate inner-sphere complexes (forming ternary outer-sphere complexes), or whether the increase in negative surface charge is delocalized over the whole surface and cation-adsorption is more evenly distributed over the surface. For simulations employing the charge-distribution, multi-site complexation (CD-MUSIC) model, a delocalization of the charge is usually assumed. Evidence for changes in the electronic structure of iron oxide sorbents upon sorption of anions was presented using X-ray photoelectron spectroscopy (XPS) (Ding et al., 2000), but it is debatable whether these findings are applicable to gibbsite.

A recent study of the interaction between phosphate and Ca at the goethite surface by Rietra et al. (2001) showed that more Ca is adsorbed at pH values below the PZC of

goethite in the presence of phosphate than it is in its absence, while more phosphate is adsorbed at pH values above the PZC in the presence of Ca. Although the concentrations of phosphate and calcium were kept below the solubility limit for apatite, the formation of a surface precipitate could not be excluded because of the possibility of surface-induced reactions. The overall results showed, however, that Ca and PO_4 adsorption to goethite could be modeled sufficiently well using affinity constants adapted from the single-ion sorption experiments in the CD-MUSIC model. No ternary complexes or surface precipitates had to be introduced into the electrostatic model. Similarly, Cd and PO_4 showed cooperative sorption behavior on goethite (Venema et al., 1997) and hydrous ferric oxide (Kuo and McNeal, 1984), which was modeled using simple electrostatic models without the introduction of ternary complexes.

2.2.4. Investigation of phosphate speciation in the ternary system phosphate/ gibbsite/ calcite

As mentioned in the introduction, phosphate sorption in calcareous soils is not limited to the precipitation of calcium phosphate phases, but can even be dominated by sorption to Fe (oxy)hydroxide coatings on mineral grains (Castro and Torrent, 1998; Delgado and Torrent, 2000; Hamad et al., 1992). The sorption reaction of phosphate to calcite has been extensively investigated using both macroscopic (Griffin and Jurinak, 1973, 1974; Kuo and Lotse, 1972; Millero et al., 2001; Parfitt, 1978; Tunesi et al., 1999) and spectroscopic methods (Hinedi et al., 1992). It has been established that phosphate sorption proceeds in three steps: 1) adsorption of phosphate to the calcite surface accompanied by the heterogeneous formation of nuclei of amorphous calcium phosphate; 2) a slow transformation of these nuclei to crystalline apatite; 3) crystal growth of apatite. Using solid-state ^{1}H and ^{31}P NMR spectroscopy, Hinedi and coworkers (1992) determined that the solid calcium phosphate phase formed at the surface is a carbonate apatite.

Although phosphate sorption in binary systems has been extensively studied, no detailed information is available on the species that are formed when calcite and gibbsite compete for phosphate.

2.3. Objectives

Despite decades of research about phosphate reactions in soils and related systems, a true understanding of the influence of the reaction conditions (time, pH, concentrations of phosphate and competing anions or cations) on the phosphate speciation is still lacking. The objectives of the research presented here are therefore to:

a. Investigate the influence of reaction conditions on the phosphate speciation at the gibbsite surface in model systems of increasing complexity. The reaction parameters chosen for investigation are: pH, time, concentrations of phosphate, citric acid (chosen as a competing anion), and calcium (chosen as a co-adsorbing cation);

b. Investigate the phosphate speciation in a model system containing gibbsite and calcite as competing sorbents;

c. Employ P K-edge XANES and solid-state ^{31}P-NMR spectroscopy as molecular tools in combination with the macroscopic determination of sorption isotherms, sorption kinetics and sorption envelopes.

2.4. Materials and Methods

2.4.1. Sample Preparation

Calcite was purchased from Fisher Scientific (Fair Lawn, NJ) and used as received. Gibbsite was prepared following a method published by Hiemstra et al. (1999). A 1 *M* $AlCl_3$ solution was slowly titrated to pH 4.6 with 4 N NaOH and allowed to settle over night. The colorless gel was dialyzed against DI water at 50 °C for 30 d. An aliquot of the suspension was then freeze-dried and characterized by FTIR, XRD, and TGA. XRD and FTIR confirmed that the material as crystalline gibbsite. The TGA spectrum showed a single peak at 215 °C, indicating the loss of structural water and transformation to Al_2O_3. The BET surface area was determined to be 40 m^2g^{-1}. The point of zero salt effect (PZSE), which is equal to the point of zero charge (PZC) in the absence of specifically adsorbing ions (Parker et al., 1979; Sposito, 1981), was determined to be 10.5 by potentiometric titration.

Samples of phosphate sorbed to gibbsite were prepared by first equilibrating a gibbsite suspension in a background electrolyte at the desired pH. Suspension densities between 1.0 and 2.5 g/L and pH values between pH 4 and pH 8 were chosen for most sorption samples. To maintain an approximately constant ionic strength over the course of the reaction, a background electrolyte of 0.1 M NaCl was chosen. Both Na and Cl interact only weakly with the gibbsite surface and are easily replaced by phosphate, calcium or organic acids. To the pre-equilibrated suspension an appropriate volume of a phosphate stock solution (0.1 – 0.15 *M*) was added at approximately the same pH value to avoid any changes of the gibbsite surface due to a rapid change in pH. For sorption

experiments in the presence of citric acid and calcium, an appropriate volume of either citric acid or $CaCl_2$ stock solution was also added. The order of addition was varied by either adding phosphate or citric acid first, or both simultaneously in a mixture of the appropriate volumes of phosphate and citric acid stock solutions. The time between the consecutive addition steps of calcium was chosen to be one hour because after this time the initial fast sorption reaction would be mostly over. In the case of Ca, the reagents had to be added in intervals of 30 s for "simultaneous" addition to allow for complete mixing and to avoid local supersaturation.

The pH of the reaction was maintained constant, first by means of an automated titrator (Radiometer, Copenhagen/ Denmark, or Metrohm, Switzerland) and later by adding small quantities of dilute (0.1 *N* or 0.01 *N*) HCl or NaOH as appropriate. Mixing was conducted using a magnetic stirrer (300 rpm) or a rotary shaker (120 rpm). After reaction times between 10 min and 90 d, the solids were recovered by centrifugation using a standardized procedure of 10,000 rpm and 10 min. They were washed once with either deionized water or ethanol to remove entrained phosphate solution and effectively stop the sorption reaction, and then freeze-dried. Ethanol was used to avoid desorption of phosphate from the surface. Preliminary experiments have shown that filtration of the gibbsite suspension is not possible in batches larger than 10 ml due to the small particle size necessary to achieve the high surface area. The small particle size leads to clogging of the filter paper, making it impossible to recover the solid samples by filtration.

The supernatant was filtered through 0.2 μm Supor® filter paper (Gelman Laboratories, Ann Arbor, MI) to minimize interference from colloidal material in the

determination of solution concentrations (Anderson et al., 1996). Phosphorus concentrations were measured using a variation of the colorimetric method described by Murphy and Riley (1962) that was developed to avoid interference from the organic acids present in some samples (He et al., 1998). Al and Ca concentrations were determined using Inductively Coupled Plasma Atomic Absorption Spectroscopy (ICP-AAS). Citric acid concentrations were determined by High Performance Liquid Chromatography (HPLC).

Samples of phosphate sorbed to either calcite or a mixture of calcite and gibbsite were prepared in a similar manner using 5 g/L calcite and 2.5 g/L of each calcite and gibbsite, respectively, in a background electrolyte of 0.1 *M* NaCl. The sorption reactions were conducted at pH 8 for 48 h in the binary system and pH 7, 8 and 9 for 24 h in the ternary system. The reaction times were chosen in accordance with the common practice reported in the literature to conduct sorption reactions for 24 h. Initial phosphate concentrations of 0.48 m*M* and 1.2 m*M* were used.

The amount of phosphate, calcium or citrate sorbed to the surface was calculated by mass balance (Sparks, 1995) and normalized to the surface area to account for different specific surface areas of different gibbsite preparations.

Reference phosphate compounds were purchased and analyzed for comparison. $CaHPO_4$ and $Ca_5(PO_4)_3OH$ were purchased from Fisher Scientific (Fair Lawn, NJ). Calcium phytate and sodium phytate were purchased from Aldrich. Mineral samples of Wavellite ($Al_3OH_3(PO_4)2 \cdot H_2O$) and Variscite ($AlPO_4 \cdot 2H_2O$) were provided by the

Excalibur Mineral Company. Reagents were prepared from analytical grade chemicals, that were used as received without further purification, and deionized water (>16 MΩ).

2.4.2. Macroscopic experiments

The kinetics of sorption, sorption isotherms and pH envelopes were determined in batch experiments following a similar procedure as the preparation of sorption samples. For kinetic measurements, the suspension was equilibrated at the desired pH for at least 24 hrs and then spiked with the reagent solution, either phosphate alone or phosphate together with citrate.

The pH of the reaction was maintained constant, first by means of an automated titrator (Radiometer, Copenhagen/ Denmark, or Metrohm, Switzerland) and later by adding small quantities of dilute HCl or NaOH as appropriate. Mixing was effected using a magnetic stirrer (300 rpm) over the first ten hours and afterwards using a rotary shaker (120 rpm). Sample volumes of 10 ml were withdrawn from the vessel in increasing intervals by means of a pipette and immediately filtered through 0.2 μm Supor® filter paper (Gelman Laboratories, Ann Arbor, MI) and stored below 4 °C until analysis for phosphate, Al, and citric acid.

Sorption isotherms and pH envelopes were determined in a similar fashion using small batches with individually chosen sets of pH and concentrations of reagents.

All reactions involving Ca or pH values above pH 7 were conducted in a nitrogen-filled glove box to minimize the influence of dissolved carbon dioxide and competing reactions with carbonate. The carbonate anion is present in all natural systems and ought

to be taken into account for the assessment of phosphate sorption reactions at high pH values or in the presence of Ca, but was omitted here for simplicity.

2.4.3. NMR experiments

All NMR experiments were conducted at the Environmental Molecular Science Laboratory, which is part of the Pacific Northwest National Laboratory in Richland, Washington.

Solid-state ^{31}P-NMR spectra were recorded on a Chemagnetics CMX Infinity spectrometer with an Oxford 300 MHz wide-bore magnet operating at a magnetic field of 7.04 Tesla, corresponding to resonance frequencies of 78.16 MHz for ^{27}Al, 121.4 MHz for ^{31}P and 299.9 MHz for ^{1}H. To afford uniform distribution and homogeneous spinning of the rotor in the MAS probe, dried and ground samples were used. Spinning speeds were maintained constant at values from 7 to 10 kHz ± 5 Hz.

CP-MAS experiments used a proton p/2-pulse of 3.5 μs, a contact time of 1.3 ms and a pulse delay of 2 s. Depending on the P concentration, 2000 to 4000 scans were accumulated to give a signal to noise ratio of at least 30 : 1. Single-pulse, proton-decoupled spectra were recorded using a ^{31}P p/2-pulse of 3.7 μs and a relaxation delay of 60 s. For these experiments up to 512 scans were accumulated.

The spectra were processed using the NUTS NMR utility transform software by Acorn NMR. A line broadening of 50 – 100 Hz was applied prior to Fourier Transformation and phase correction. The complex signals were deconvoluted using a minimal set of peaks. The quality of the fit increased when Lorentzian peaks for narrow

peaks and Gaussian peaks for broad peaks were used. No other constraints were employed. Isotropic chemical shifts are all reported in parts per million (ppm) relative to the signal of 85% H_3PO_4 as an external reference; positive values correspond to low-field or high-frequency shifts.

2.4.4. XANES experiments

All XANES spectroscopic studies were conducted at beamline X19-A of the National Synchrotron Light Source at Brookhaven National Laboratory in Upton NY. Samples were covered with a thin mylar film and placed inside a helium-purged sample compartment. A solid state PIPS detector collected spectra in fluorescence mode. Reference spectra were collected of samples with a known structure and compared to the sorption samples. XANES spectra were collected from 10 eV below the P K-edge until 50 eV beyond the edge, which encompasses the near edge region. Limitations of the beamline prohibited going further below the P edge, making background subtraction sometimes a challenge for more dilute samples. Multiple scans of each sample were collected and averaged together to improve the signal to noise ratio. Data reduction was done with WinXAS 2.1. The background was removed with a linear fit, and the spectra were all normalized to the energy of the absorption edge, which is defined as the inflection point.

2.5. Results and Discussion

2.5.1. Influence of pH and time on the phosphate speciation at the gibbsite-water interface

Preliminary NMR-experiments of the sorption samples showed no differences between the single-pulse MAS and the CP-MAS NMR spectra, neither in resolution nor in the distribution of peak-intensities. In order to take full advantage of the shorter repetition time of the CP-MAS experiments, no further single-pulse experiments were conducted.

2.5.1.1. pH effects

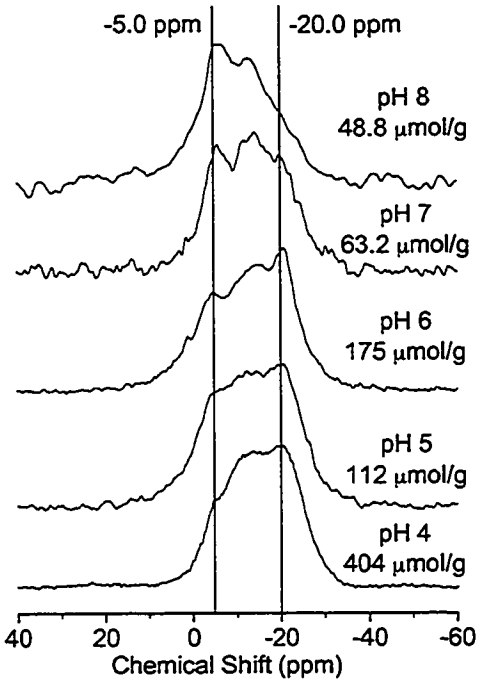

Figure 1. pH dependence of the CP-MAS NMR spectra of phosphate sorbed to gibbsite.

Figure 1 shows the CP-MAS NMR spectra of phosphate sorbed to gibbsite at pH values from 4 through 8. A minimum of three overlapping peaks can be discerned at chemical shifts d?= -5 ± 1 ppm, d_2 = -13 ± 1 ppm and d_3 = -20 ± 1 ppm. Even without deconvolution, an increase of the relative intensity of peak 1 and a concomitant decrease of the relative intensity of peaks 2 and 3 with increasing pH can be seen. The deconvolution of the samples taken at pH 4, 6 and 8 is illustrated in Figure 2 a through c, respectively. The deconvolution results are summarized in Table 1 and plotted against the pH in Figure 3. The intensities of Peaks 2 and 3 decrease linearly with pH relative to peak 1, suggesting a change in the surface-species with pH. Apparently, peak 1 dominates the NMR spectra above pH 7, while at lower pH values peaks 2 and 3 gain importance.

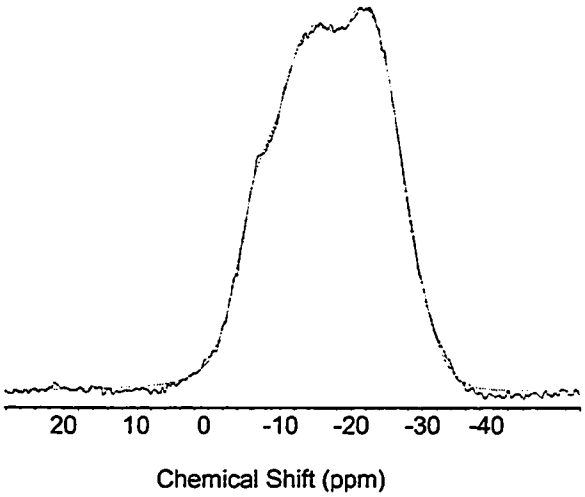

Figure 2a. Deconvolution of the CP-MAS spectrum of phosphate sorbed to gibbsite at pH 4, 24 hrs.

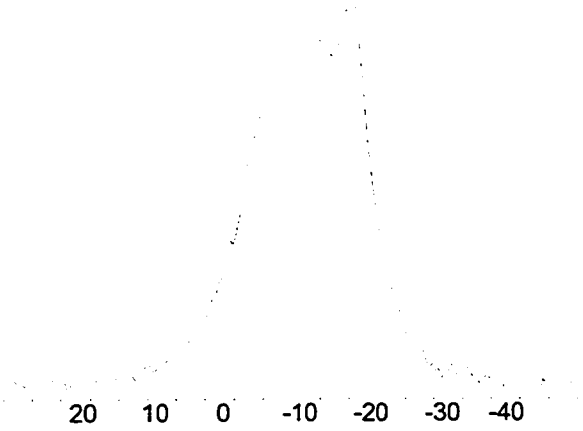

Figure 2b. Deconvolution of the CP-MAS spectrum of phosphate sorbed to gibbsite at pH 6, 24 hrs.

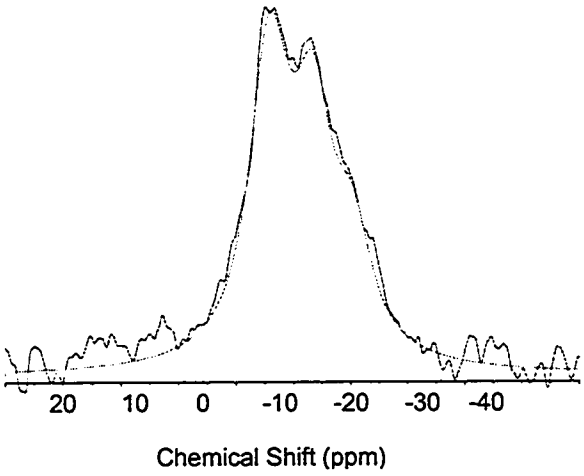

Figure 2c. Deconvolution of the CP-MAS spectrum of phosphate sorbed to gibbsite at pH 8, 24 hrs.

Table 1. Deconvolution results for the CP-MAS spectra of Figure 1. The error margins are ± 1 ppm and ± 10 %, respectively.

pH	Chemical Shift (ppm)	Relative Intensity
8	-6.0	1.0
	-13.6	0.6
	-20.4	0.3
7	-5.5	1.0
	-13.5	1.6
	-20.8	1.1
6	-3.8	1.0
	-13.3	3.5
	-21.2	1.8
5	-3.6	1.0
	-11.3	1.6
	-20.8	2.1
4	-3.4	1.0
	-11.7	5.5
	-21.2	4.9

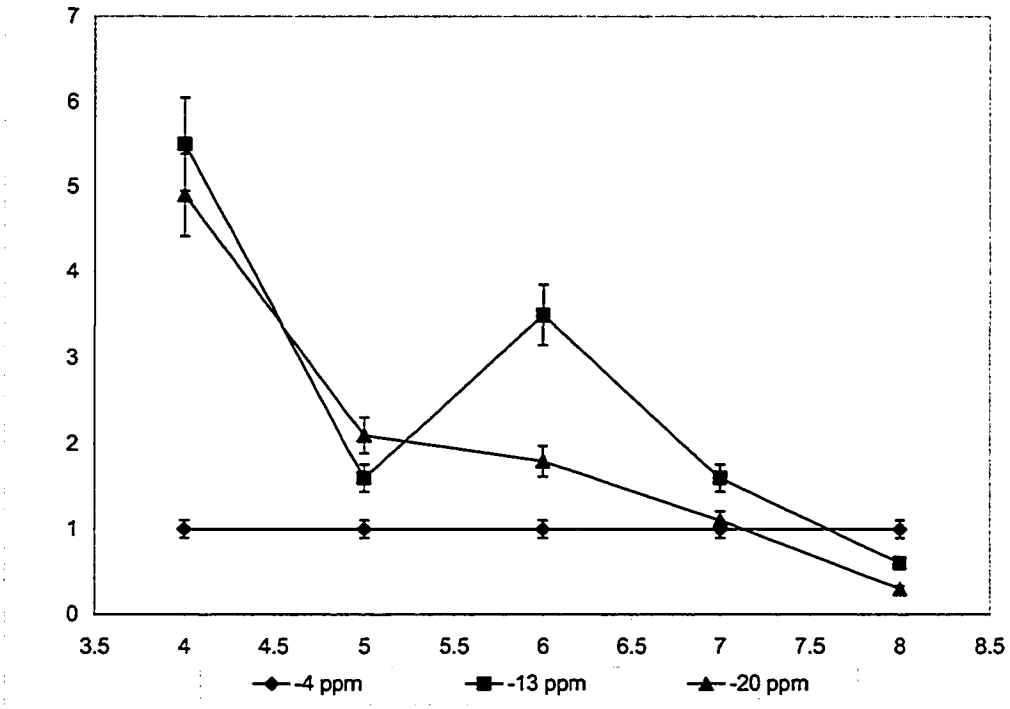

Figure 3. Relative intensities of the peaks at -5 ppm, -13 ppm and -20 ppm. The error margins for the chemical shifts and the relative intensities are ± 1 ppm and ± 10 %, respectively.

While the positions of peaks 2 and 3 remain constant within the margins of error, peak 1 shows a slight pH-dependence (Figure 4), indicating that this species is protonated. The chemical shift trend of this species, however, is opposite to the expected trend (Cody et al., 2001). A protonated phosphate species on the surface is expected to be increasingly deprotonated with increasing pH value, resulting in a downfield shift (shift to more positive chemical shift values). The observed behavior cannot be explained at this point, but remains within the margin of error and is therefore insignificant.

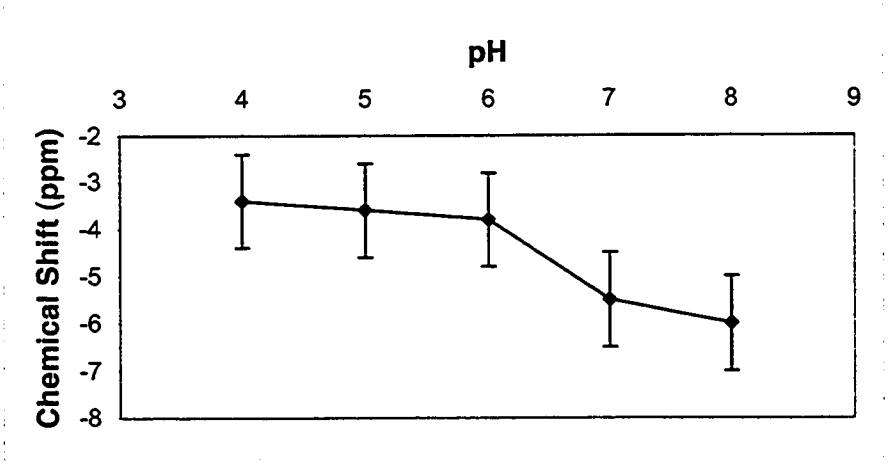

Figure 4. Correlation of the chemical shift of peak 1 with pH.

Bleam and coworkers (1991) conducted a ^{31}P-NMR investigation of the phosphate sorption reaction to the boehmite (γ-AlOOH) surface in suspension. They found two pH-dependent NMR peaks (referred to in their discussion A and B, d_A = -10 ppm to 1 ppm, d_B = 0 ppm to 3 ppm), of which they assigned peak A to an inner-sphere surface complex. Due to a lack of positive evidence, they were hesitant to decide whether peak B could be assigned to a surface complex or a surface precipitate. Both

species exhibit the expected pH-dependence, *i.e.* the chemical shift increases to more positive values with increasing pH value. Bleam and coworkers (1991) argued that the two species can not differ by the number of protons attached to the phosphate molecule, because proton exchange with water molecules and hydroxyl groups at the surface is rapid, and the lifetime of differently protonated species is short on the time scale of the NMR experiment. Surface-bound phosphate molecules differing in the number of protons attached therefore give rise to only one NMR signal.

Since the chemical shift of phosphorus decreases to more negative values with an increasing number of aluminum atoms bound to the phosphate unit (Cody et al., 2001), the two species observed by Bleam et al. (1991) are necessarily bound to different numbers of aluminum atoms. Peak A could therefore be assigned to a binuclear bidentate complex and peak B to a mononuclear, monodentate complex, but no positive evidence exists for this assignment. Under the assumption that this assignment is valid, however, peak 1 (d_1 = -3.5 to -6 ppm) in Figure 1 can be assigned to a bidentate, binuclear surface complex of phosphate on the gibbsite surface, because it appears in the same chemical shift region as peak A observed by Bleam et al. (1991). This also implies that no mononuclear monodentate surface complexes are formed on the gibbsite surface.

Boehmite (γ-AlOOH) and gibbsite ($Al(OH)_3$) both have a layered structure. In gibbsite, the layer surfaces contain exclusively double-coordinated hydroxyl-groups and the layer-edges single-coordinated hydroxyl-groups (Saalfeld and Wedde, 1974). Parfitt (1978) reports that only the layer edges of gibbsite are reactive toward phosphate, while the predominating (001) plane is unreactive. Investigation of the boehmite structure

(Christoph et al., 1979) reveals that, similar to gibbsite, singly-coordinated hydroxyl-groups are located exclusively at the layer-edges in the direction of the crystallographic a- and c-axis. Reactivity towards phosphate is therefore only expected for the layer-edges.

The formation of a monodentate surface complex requires only one singly-coordinated hydroxyl-group and is therefore expected to form readily at the layer-edges of boehmite and gibbsite. The formation of a bidentate, binuclear surface complex requires two singly-coordinated hydroxyl groups in the proper distance to each other. The apical hydroxyl-groups of two corner-sharing $Al(O,OH)_6$-octahedra in gibbsite and boehmite are located 298 pm and 288 pm from each other, respectively. Gibbsite furthermore has singly-coordinated hydroxyl-groups in neighboring layers at a distance of 302 pm. In the aluminum phosphate minerals variscite (Kniep et al., 1977) and wavellite (Araki and Zoltai, 1968), the phosphate tetrahedra are only slightly distorted with edge lengths of 248 – 253 pm. The formation of a bidentate, binuclear surface complex requires therefore the distortion of the phosphate tetrahedron and the widening of the O-P-O angle. The formation of a mononuclear bidentate surface complex is geometrically more favorable, because the aluminum octahedra in gibbsite and boehmite have edge-lengths in the range of 203 pm – 280 pm. An interconnection of aluminum octahedra and phosphate tetrahedra in this manner, however, is generally not observed in aluminum phosphate minerals (Hawthorne, 1998) because of the strong repulsion between the trivalent aluminum and the pentavalent phosphorus. Therefore binuclear bidentate rather than mononuclear bidentate complexes are expected to form. In gibbsite

they can also bridge adjacent layers, while in boehmite their formation is restricted to one layer.

Lookman and coworkers (1994) conducted a solid-state NMR-investigation of phosphate sorption to synthetic amorphous aluminum hydroxide dried at various temperatures. Unlike Bleam et al. (1991), they exclusively observed broad resonances with peak-widths at half-height of approximately 20 ppm. The peak maximum shifted with reaction time from -6 ppm after 3 days to -10 ppm after 120 days, but never reached that of the amorphous aluminum phosphate (d = -12 ppm) that they also investigated. They concluded that phosphate remains adsorbed to the surface with no bulk aluminum phosphate formed when it is sorbed to aluminum hydroxide dried at 200 °C. For sorption reactions with aluminum hydroxide dried at 70 °C and elevated phosphate concentrations, they proposed a phosphate-induced weathering of the aluminum hydroxide surface and the formation of an amorphous aluminum phosphate phase. They based this conclusion on the observation that the peak-maximum of the broad phosphate peak in the P-NMR spectrum shifted to -11 ppm. Interestingly, phosphate is known to inhibit the proton-promoted dissolution of mineral surfaces (Stumm, 1986, 1997) and is therefore very unlikely to promote the weathering of the gibbsite surface.

The NMR-studies by Bleam et al. (1991) and Lookman et al. (1994), and extensive FT-IR spectroscopic investigations of phosphate sorption to iron and aluminum oxy-hydroxides (Arai and Sparks, 2001; Laiti et al., 1996; Nanzyo, 1984, 1986; Nanzyo and Watanabe, 1982; Persson et al., 1996; Tejedor-Tejedor and Anderson, 1986, 1990) remained inconclusive as to the nature of the surface complexes formed. They agree,

however, that at elevated phosphate concentrations, over prolonged reaction times and at low pH values, a transformation of the surface complexes to a metal phosphate occurs (Laiti et al., 1996; Nanzyo, 1984, 1986; Nanzyo and Watanabe, 1982; Persson et al., 1996; Tejedor-Tejedor and Anderson, 1986, 1990). The nature of this surface precipitate in the samples investigated in this work is discussed in the following.

Chemical shifts of various aluminum phosphate solids are reported in the literature (Bleam et al., 1989a, b; Duffy and van Loon, 1995; Hinedi et al., 1989b). Depending on crystallinity, water content, and degree of condensation, the phosphorus nuclei in these solids resonate between -7 and -30 ppm. Duffy and vanLoon (1995) reported downfield shifts for aluminum phosphate precipitates that had been calcined and had therefore a higher degree of condensation. These findings are corroborated by simulations of NMR spectra of aluminum phosphate glasses (Cody et al., 2001), which indicate that phosphate peaks shift to more negative values with increasing number of aluminum atoms bound. Furthermore, phosphorus peaks shift to more negative values with decreasing pH. These two trends occur simultaneously and are very likely to be indistinguishable from each other. The minerals Wavellite ($Al_3OH_3(PO_4)_2 \cdot 5\ H_2O$, (Araki and Zoltai, 1968)) and Variscite ($AlPO_4 \cdot 2\ H_2O$, (Kniep et al., 1977)), which were included in this study, had chemical shifts of -11 ppm and -19 pm, respectively, in agreement with published values (Bleam et al., 1989b; Frossard et al., 1994). For Wavellite, a chemical shift range from -11 to -13 ppm has been reported (Frossard et al., 1994). The chemical shift of Berlinite ($AlPO_4$) has been reported at -25 ppm (Bleam et

al., 1989b). Bleam et al. (1989b) suggested that these three minerals form in the soil environment.

Comparing the chemical shift values found in this study with the literature values suggests that peak 2, which has a chemical shift of $d_2 = -13 \pm 1$ ppm, corresponds to a surface precipitate of wavellite on gibbsite. Wavellite ($Al_3(OH)_3(PO_4)_2 \cdot 5\ H_2O$) is an uncondensed aluminum phosphate phase, in which chains of corner-sharing aluminum hydroxide octahedra are cross-linked by phosphate molecules. Every phosphate molecule is bound to four aluminum cations (Araki and Zoltai, 1968).

The chemical shift of peak 3 suggests variscite (-19 ppm, (Bleam et al., 1989b)) or metavarsicite (-19.2 ppm, (Duffy and van Loon, 1995)). Variscite ($AlPO_4 \cdot 2\ H_2O$) consists of a three-dimensional network of phosphate tetrahedra and aluminum octahedra connected at the apices, with the two water molecules occupying two neighboring corners of the aluminum octahedra. Every phosphate molecule in variscite is bound to four aluminum cations, and every aluminum cation is bound to four phosphate molecules (Kniep et al., 1977).

The main difference between wavellite and variscite is the degree of condensation in the aluminum sub-lattice: In variscite, there are no connections between the aluminum octahedra, whereas in wavellite the aluminum octahedra form infinite chains. It is known that calcination transforms variscite under loss of two water molecules to the more condensed phase berlinite ($AlPO_4$) (Duffy and van Loon, 1995), the phosphorus nuclei of which resonate at -24 ppm (Bleam et al., 1989b; Duffy and van Loon, 1995). Berlinite has a quartz structure, with aluminum and phosphorus replacing silicon and both having

tetrahedral environments. The chemical shift varies by approximately 10 ppm from wavellite to berlinite although the phosphate groups of all these minerals remain coordinated to four aluminum cations. This indicates that the phosphorus chemical shift is very sensitive to the degree of condensation in the aluminum sub-lattice, with downfield shifts for phosphate tetrahedra bound to extended aluminum hydroxide clusters.

The broad resonance peaks, however, indicate that the samples contain no crystalline phosphate phases, but rather poorly ordered aluminum phosphate phases with a close range ordering similar to the crystalline phases. The P K-edge XANES spectra can be used to further investigate the crystallinity of the surface precipitates. The P K-edge XANES spectra of several sorption samples and the two aluminum phosphate minerals variscite and wavellite are compared in Figure 5. The differences between the sorption samples reacted for different times at different pH values are only subtle: They all contain a sharp peak at the absorption edge (ca. 2.156 keV), the "white line", and a broad, symmetric peak at ca. 2.175 keV, the so-called "oxygen-oscillation" (Peak et al., 2002). The long-term sorption samples further contain a weak shoulder on the low-energy side of the oxygen-oscillation. The mineral phases, however, show characteristic spectral features, generally more asymmetric oxygen-oscillations and an additional peak between the white line and the oxygen oscillation. The absence of these characteristic features indicates that no crystalline surface precipitates are formed on the gibbsite surface. Peak 2 and 3 are therefore amorphous phases with a close range ordering similar to wavellite and variscite, respectively.

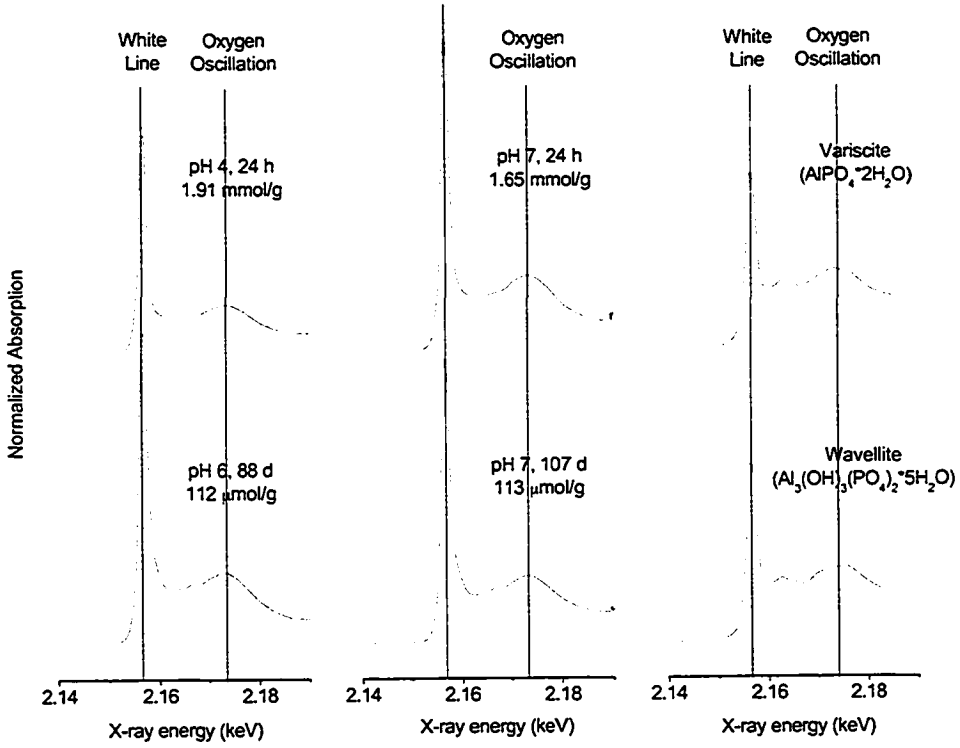

Figure 5. P K-edge XANES spectra of phosphate sorbed to gibbsite at pH 4 and pH 7 for 24 h, at pH 6 and pH 7 for 88 and 107 d, respectively, and the two minerals variscite and wavellite.

2.5.1.2. Time-Effects

Figure 6 illustrates the effect of reaction time on the CP-MAS NMR spectra of phosphate sorbed to gibbsite. The same three principal species are present, but no clear trend is visible. In the spectrum of the sample reacted at pH 4 for 10 days, the peak attributed to a wavellite-like surface precipitate (d_2 = -13 ppm) increases relative to peaks 1 and 3 (d_1 = -5 ppm, d_3 = -20 ppm), which were attributed to a surface complex and a more variscite-like surface precipitate, respectively. This agrees with the observation by Laiti et al. (1996, 1998) that the surface complexes transform to a surface precipitate with increasing reaction time. Interestingly, and contrary to these observations, the peak ascribed to surface complexes (d_1 = -5 ppm) in the spectrum of the sample reacted for 88 days at pH 6 increases in intensity relative to the peaks attributed to surface precipitates (d_2 = -13 ppm, d_3 = -20 ppm). Although the numerical values of the deconvolution remain ambiguous, this could be indicative of slow diffusion of phosphate into micro-pores of gibbsite or aggregates of gibbsite platelets with subsequent adsorption as a surface complex. Both diffusion and the formation of a surface precipitate are therefore important in the long-term reactions of phosphate with aluminum hydroxide.

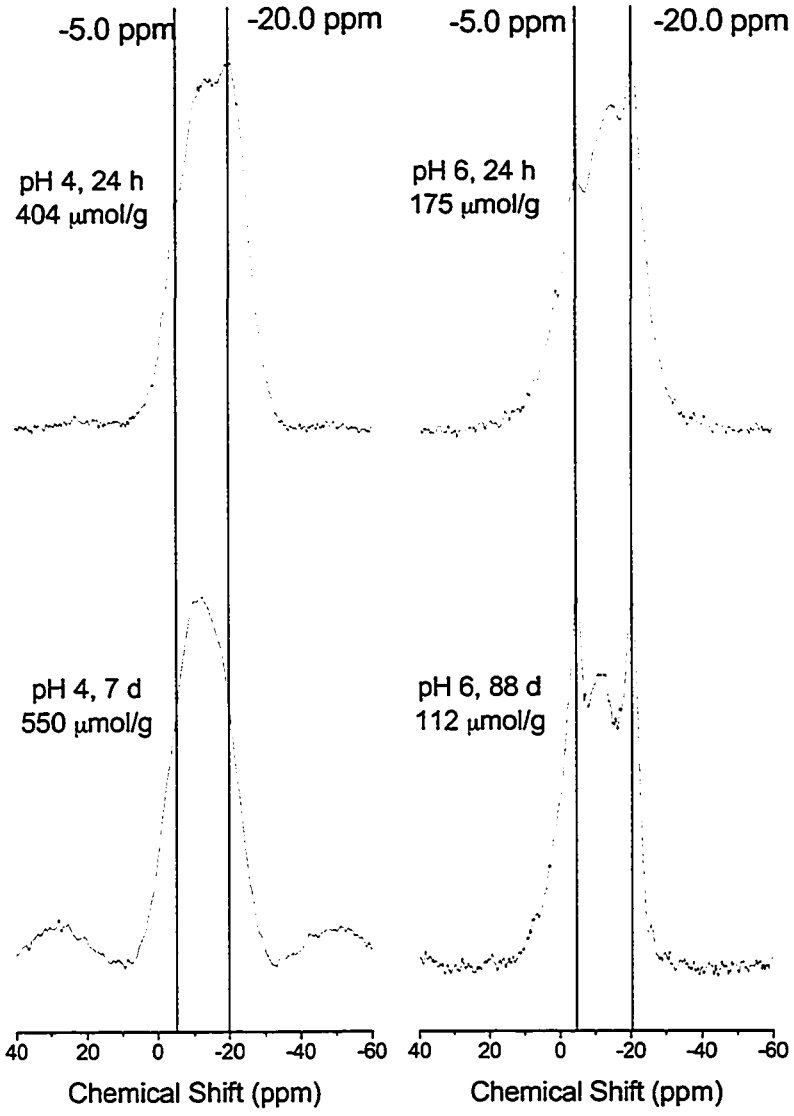

Figure 6. Effect of time on the CP-MAS NMR spectra of phosphate sorbed to gibbsite.

In a more recent solid-state P-NMR study of phosphate species in arable soils under long-time cultivation, McDowell et al. (2002) observed broad phosphate resonances that could be deconvoluted into a set of peaks. The peaks found were assigned to solid aluminum phosphate phases (wavellite, variscite, berlinite), amorphous aluminum phosphate and "other" phosphate species associated with aluminum. The fact that they observe similar species in soils demonstrates that they investigation of model systems can shed light on processes in natural systems.

Two different techniques were used to prepare the samples after conclusion of the sorption reaction. After separation by centrifugation, the solids were washed once with either deionized water or ethanol and then freeze-dried. Removal of entrained solution is important to avoid that non-adsorbed phosphate is forced to the surface during drying. The washing step with ethanol was intended to minimize desorption of both phosphate and the background electrolyte while efficiently removing entrained phosphate solution. The sorption samples presented so far were prepared involving a washing step with deionized water. Figure 7 and Figure 8 show the NMR spectra of sorption samples washed with ethanol. The samples in Figure 7 and Figure 8 were reacted at pH 4 and pH 7 for 10 minutes to 30 days, respectively. Although the resonances are broad and exhibit less detail than those in Figure 1 and Figure 6, they appear in the same chemical shift range. Deconvolution of the signal into single peaks is ambiguous at best due to the symmetric, Gaussian peak shape, and is therefore not performed. Symmetric, Gaussian peaks can be deconvoluted into an arbitrary number of Gaussian peaks, according to the

deconvolution software. The position of the peak maximum, however, can be used to investigate trends with reaction time and pH.

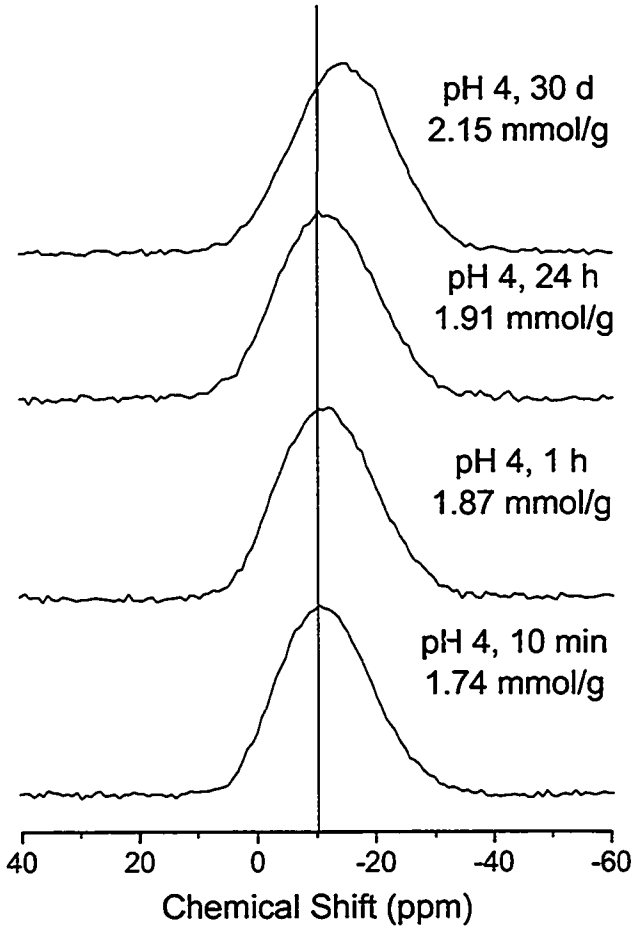

Figure 7. CP-MAS NMR spectra of phosphate reacted with gibbsite at pH 4 in a background electrolyte of 0.1 *M* NaCl for times up to 30 days.

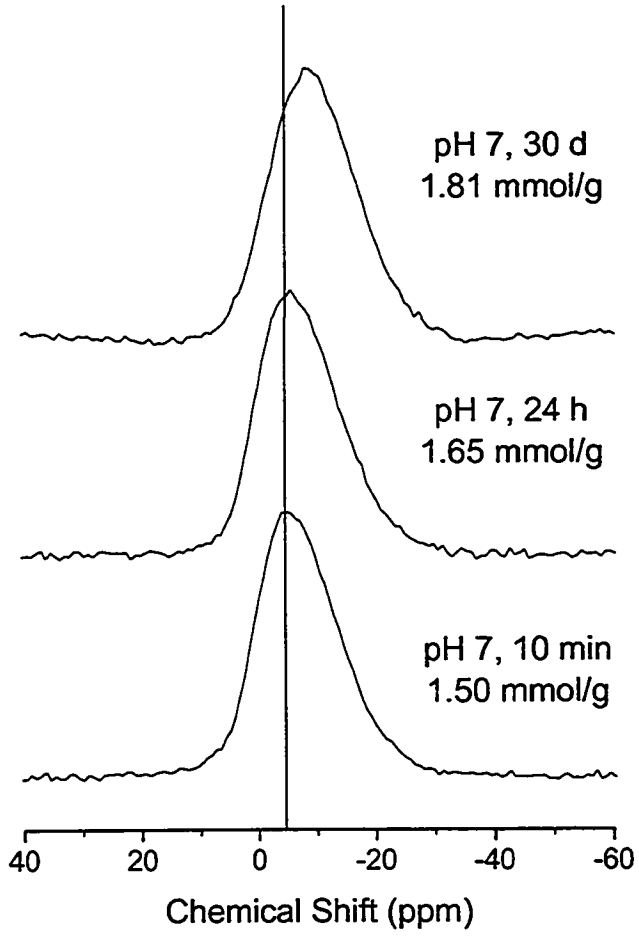

Figure 8. CP-MAS NMR spectra of phosphate reacted with gibbsite at pH 7 in a background electrolyte of 0.1 M NaCl for times up to 30 days.

Between 10 minutes and 24 hours, the resonance peak of the samples reacted at pH 4 remains centered at approximately -10 ppm (Figure 7). Over the next 29 days, the maximum shifts upfield to -15 ppm. The same trend to more negative chemical shifts is also observed for the samples reacted at pH 7 (Figure 8). The difference between the samples reacted at pH 4 and pH 7 is that the peak maximum has more positive chemical shifts, specifically d = -5 ppm after 10 minutes and d = -8 ppm after 30 days. These trends are similar to the trends observed earlier in Fig. 1 and 6: The intensity of the upfield peaks (d_2 = -13 ppm, d_3 = 20 ppm) increases with decreasing pH, while the spectrum at high pH is dominated by the downfield peak (d_1 = -5 ppm). The spectra of the samples reacted at pH 4 exhibit the same time-effect, with peak 2 dominating after long reaction times.

The spectra of the samples washed with ethanol have signals in the same chemical shift range and exhibit the same time and pH effects as the samples washed with deionized water. The main difference is that the sharp peaks of the latter are now much broader and indistinguishable from each other, which indicates a broader range of chemical environments. While the samples washed with water have generally better distinguishable species with some disorder in the aluminum phosphate phases (peaks 2 and 3), the samples washed with ethanol have a range of phosphate species that differ both in degree of condensation and in the number of aluminum atoms bound to the phosphate molecule.

Washing the samples with ethanol, and thereby reducing the dielectric constant of the suspension could have had two effects. It could have caused the phosphate remaining

in solution to adsorb to the surface, because phosphate is less soluble in ethanol and ethanol-water mixtures. Reducing the dielectric constant also reduces the thickness of the electrical double layer of the gibbsite particles in suspension (Sposito, 1984), causing the gibbsite particles to collapse and form cross-links during drying. The effect of changing the dielectric constant is however small compared with the effect that a change in the ionic strength has (Sposito, 1984; Stumm and Morgan, 1996). It is therefore more probable that forcing more phosphate molecules to adsorb to the surface caused the increased disorder in the surface species.

2.5.2. Influence of competing organic acids on the sorption reaction of phosphate to the gibbsite surface.

The effect of competing polycarboxylic organic acids on the sorption of phosphate to gibbsite was investigated using citric acid as a model compound. Organic acids are formed in soils during the decomposition of complex organic matter and are also exuded by plant roots or microorganisms. They play an important role in the mobilization and acquisition of nutrients (Fe, Mn, and P) and in the detoxification of aluminum (Jones, 1998; Jones and Darrah, 1994). Soils contain a wide variety of organic acids, of which citric acid is one of the more common representatives (Jones, 1998).

The sorption isotherms of phosphate on gibbsite in a background electrolyte of 0.1 *M* NaCl and suspension density of 1.0 g/L in the presence and absence of citric acid are shown in Figure 9. The amount of phosphate taken up from solution at pH 4 is significantly reduced in the presence of total concentrations of 0.45 and 0.9 m*M* citric acid in solution. Competition is less pronounced at pH 7. The phosphate sorption isotherms exhibit high affinity behavior at low solution concentrations at both pH values but no apparent sorption maximum is reached. Examination of the low concentration part of the sorption isotherm at pH 4 reveals that sorption inhibition is more pronounced at low solution concentrations of phosphate than at high solution concentrations.

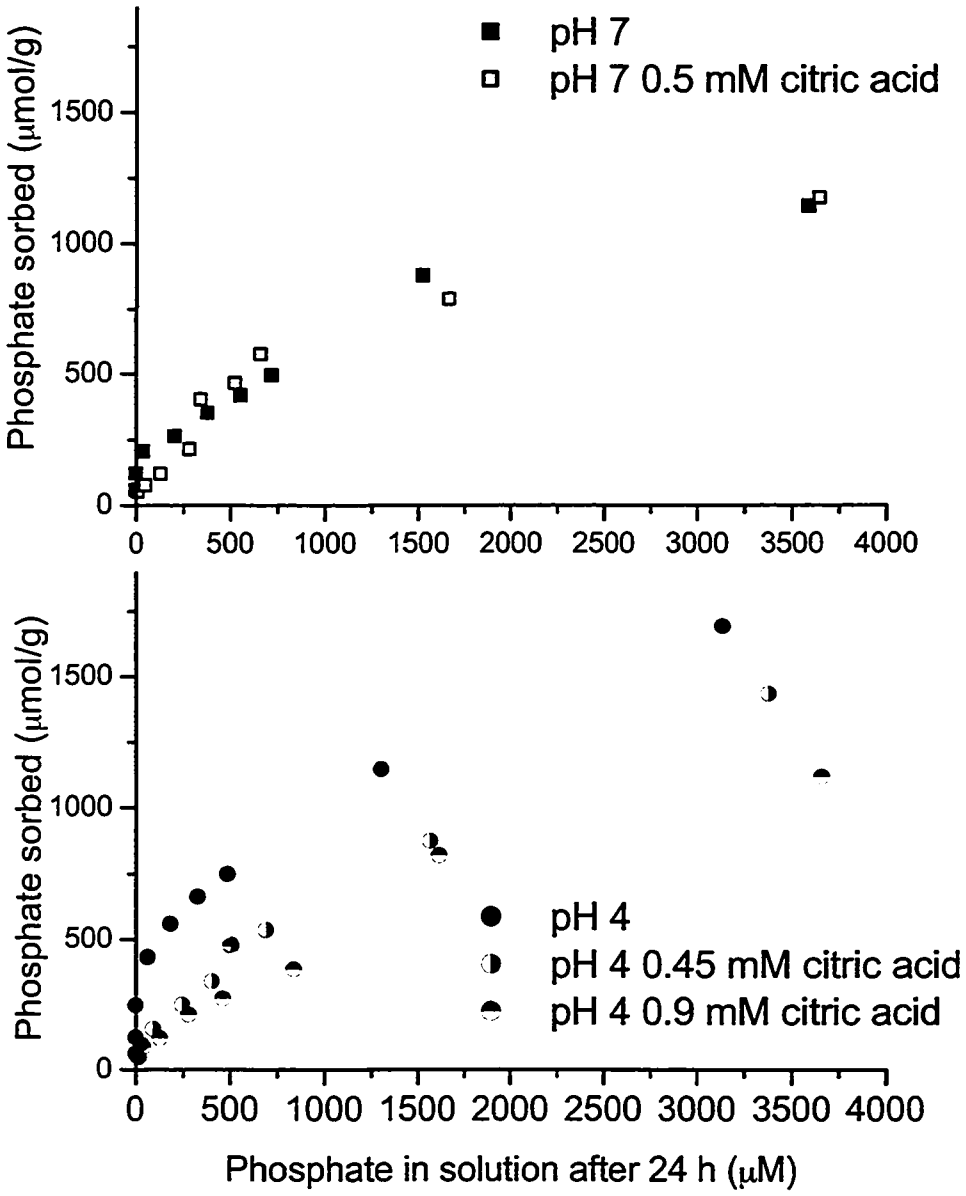

Figure 9. Sorption isotherms of phosphate on gibbsite (0.1 *M* NaCl, 1.0 g/L) at pH 4 and 7.

The effect of time on the sorption reaction in the presence and absence of citric acid was investigated at pH 4, 6 and 7. Figure 10 shows that at all pH values under investigation the initial fast sorption reaction was complete within the first hour in both the presence and the absence of citric acid. In the presence of the competing ligand, the sorption reaction proceeded much slower after the initial fast reaction and only at pH 4 were considerable amounts of phosphate taken up from solution. At pH 7, the amount sorbed leveled off after 10 days, whereas at pH 4 the reaction still continued. No comparison with the sorption reaction at pH 6 is possible because the data set included only the first three days.

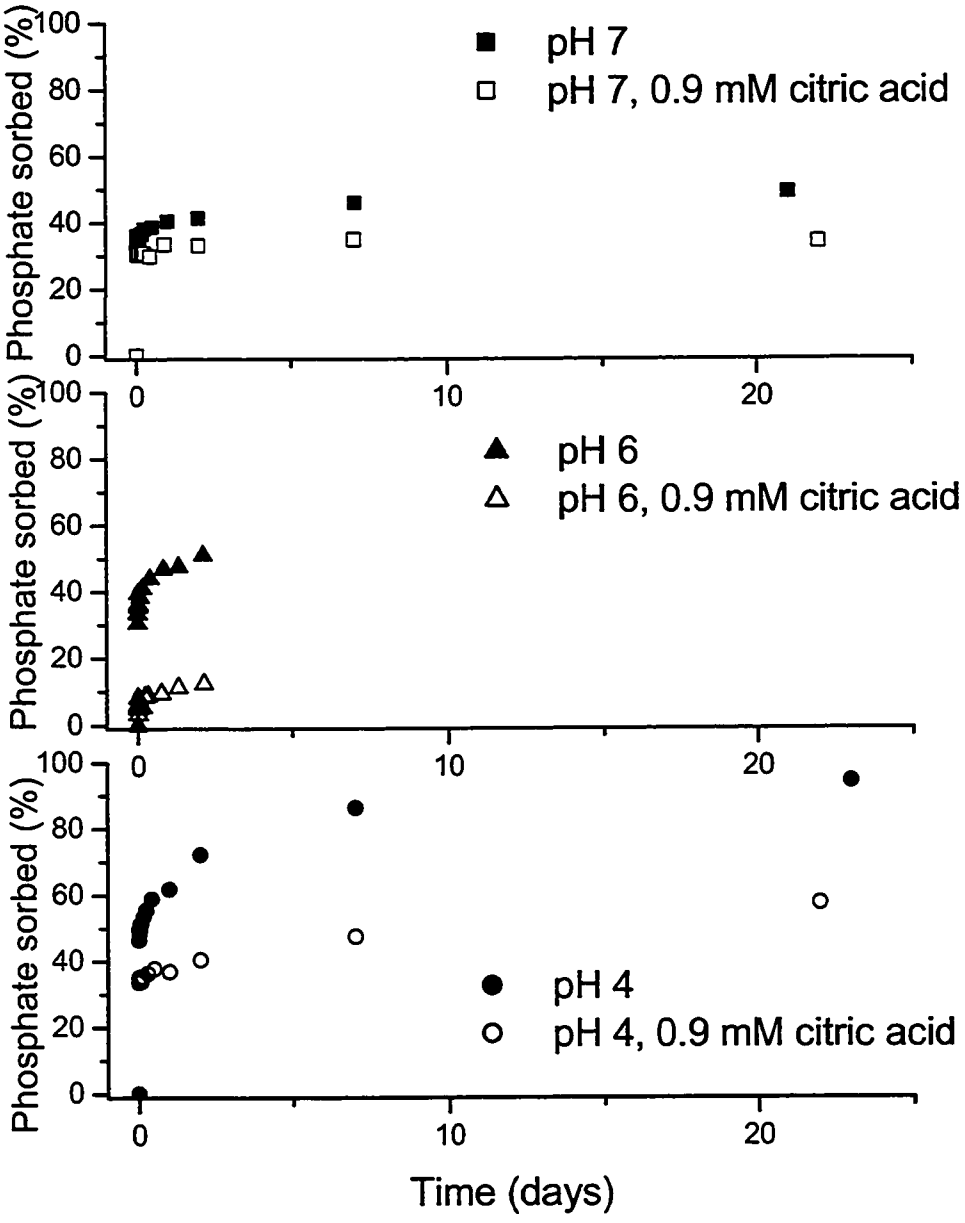

Figure 10. Sorption kinetics of phosphate on gibbsite at pH 4, 6 and 7, in a background electrolyte of 0.1 *M* NaCl with and without equal initial concentrations of citric acid. The data set at pH 6 ends after 3 days.

Interestingly, similar amounts of phosphate are taken up from solution at pH 4 and 7 during the first hour in the presence of citric acid, while at pH 6 much less is sorbed in the same time frame. Apparently, citric acid competes most efficiently in this pH range with phosphate surface sites. Geelhoed et al. (1998) observed a similar minimum of phosphate uptake by goethite at approximately pH 5. Although both anions show sorption maxima at and below pH 4 on gibbsite and goethite, the competition from citric acid is greater at pH 6 and 5, respectively. Geelhoed and coworkers (1998) were able to model this behavior using the CD-MUSIC model under the assumption that only inner-sphere surface complexes are formed. Changes of the phosphate species at the gibbsite surface in the presence of citric acid are examined in the following.

Figure 11 and Figure 12 compare the CP-MAS NMR spectra of phosphate on gibbsite at pH 4 and 6. Reaction times were 24 hours at both pH values (Figure 11), and 7 days and 88 days at pH 6 and pH 4, respectively (Figure 12). In the presence of citric acid, the intensities of peaks 1 and 3 (d_1 = - 4 ±1 ppm, d_3 = -20 ±1 ppm) are considerably reduced compared with their counterparts in the absence of citric acid, whereas peak 2 (d_2 = -13 ±1 ppm) is more prominent; this behavior can be seen at both pH values and after long and short reaction times. Deconvolution of the spectra further reveals an additional peak at d_4 = -10 ±1 ppm (Figure 13 a through d), which remains a minor species. Figure 13 also shows that peak 2 increases with time at both pH values.

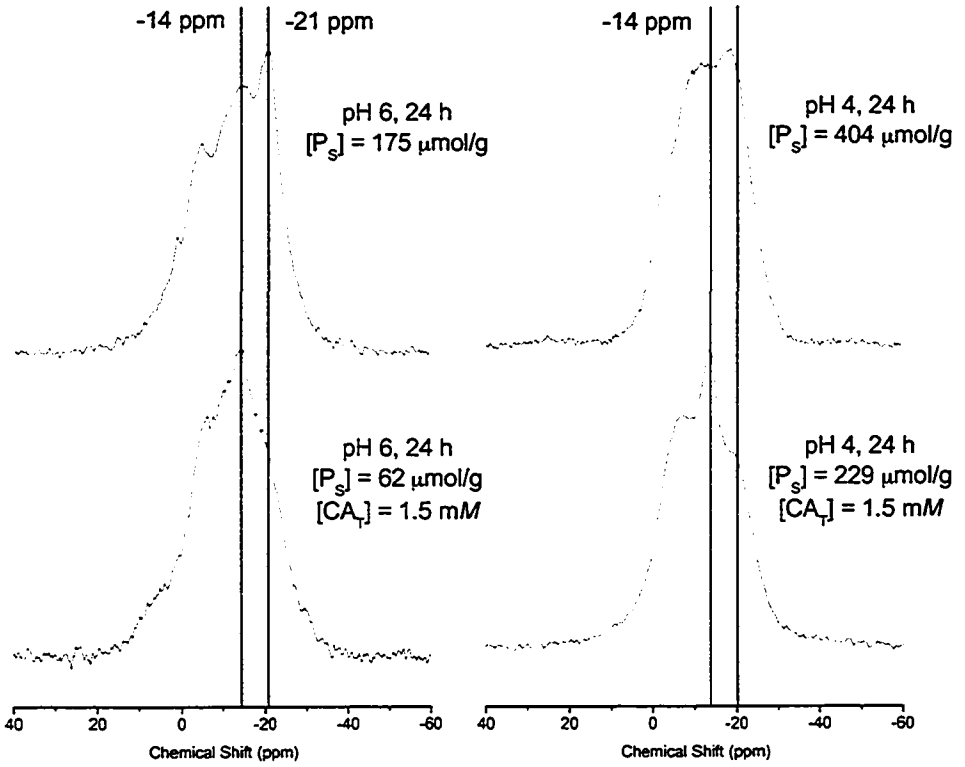

Figure 11. CP-MAS spectra of phosphate on gibbsite after a reaction time of 24 hours in the absence and presence of citric acid. Reaction conditions: pH 4, 0.1 *M* NaCl, 0.9 g/L gibbsite; pH 6, 0.01 *M* NaCl, 8.8 g/L gibbsite. [P_S]: concentration of phosphate sorbed to the surface, [CA_T]: total concentration of citric acid in solution.

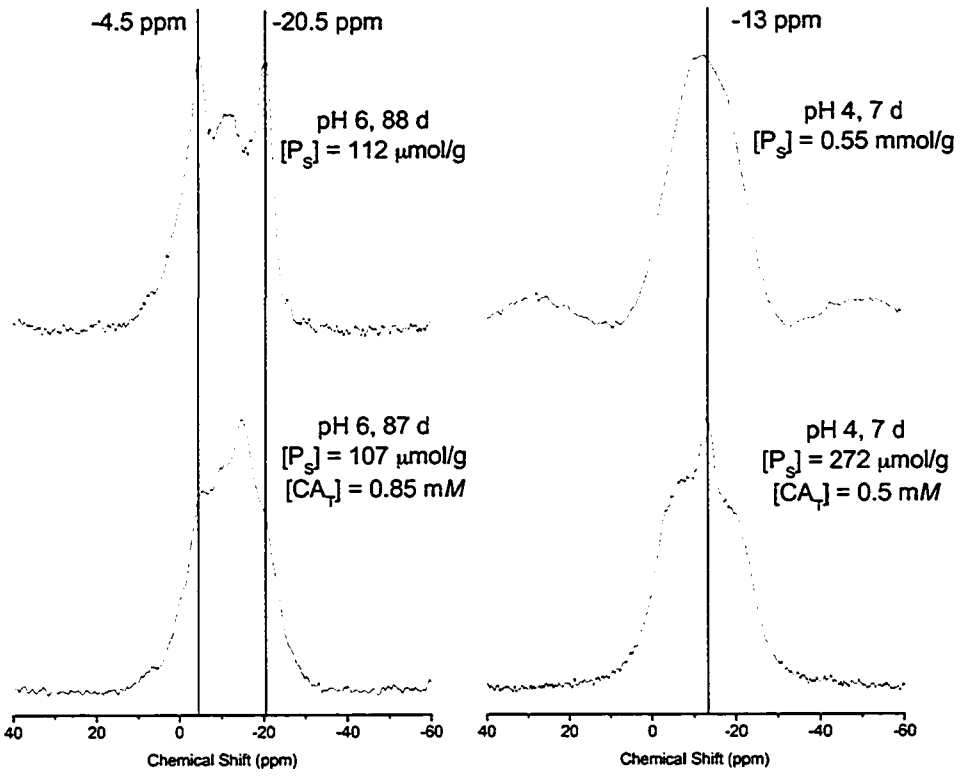

Figure 12. CP-MAS spectra of phosphate on gibbsite after a reaction time of 7 to 88 days in the absence and presence of citric acid. Reaction conditions: pH 4, 0.1 *M* NaCl, 0.9 g/L gibbsite; pH 6, 0.01 *M* NaCl, 8.0 g/L gibbsite. [P_S]: concentration of phosphate sorbed to the surface, [CA_T]: total concentration of citric acid in solution.

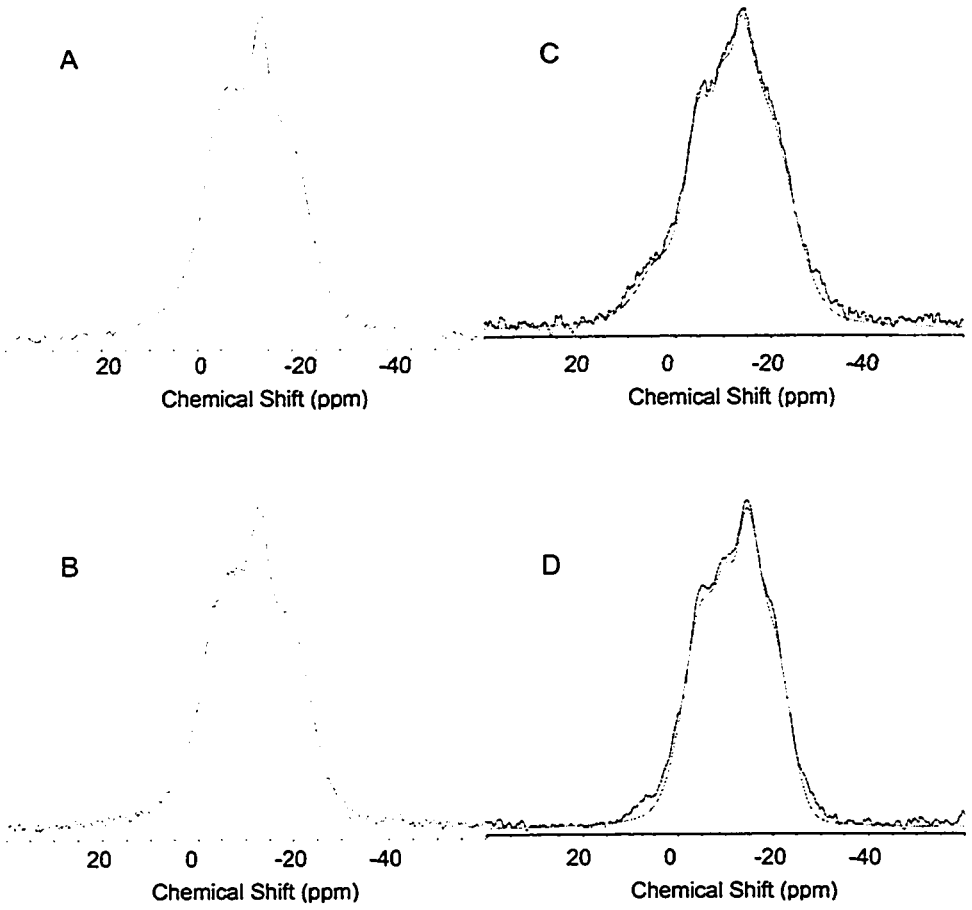

Figure 13. Deconvolution of the spectra in Fig. 11 and 12. A: pH 4, 24 h. B: pH 4, 10 d. C: pH 6, 24 h. D: pH 6, 87 d.

These spectroscopic results indicate that citric acid not only competes with phosphate for sorption sites to form inner-sphere surface complexes (Geelhoed et al., 1998; Hiemstra and van Riemsdijk, 1999; Nilsson et al., 1996), but also inhibits the formation of the surface precipitate with a poorly ordered variscite-type structure (d_3 = -20 ±1 ppm). Whether the formation of the surface precipitate with a structure similar to wavellite is also inhibited can not be determined from Figure 11 through Figure 13 alone.

The additional peak can not be attributed to any known phosphate species with certainty. The chemical shift indicates that the phosphate molecule is bound to several aluminum cations, and that the aluminum cations exhibit furthermore some degree of condensation. The fact that this species only forms in the presence of citric acid, indicates that the latter is also part of the structure. The narrow peak indicates, however, that this species is rather uniform with only little variation, a fact which is contradicted by the multitude of possible structures that satisfy the conditions listed above. A peak assignment is therefore not possible at this point.

2.5.3. Influence of calcium cations on the phosphate speciation at the gibbsite surface

Past research has shown that the sorption of metal cations and phosphate to variably charged soil minerals is enhanced when they are both present (Diaz-Barrientos et al., 1990; Kuo, 1986; Kuo and McNeal, 1984; Rietra et al., 2001; Venema et al., 1997). This interaction is important for the mobility and bioavailability of contaminants as well as nutrients not only in limed, acid soils that receive phosphate, but also in calcareous soils. Hamad and coworkers have shown that phosphate sorption in calcareous soils is

dominated by interactions with surface coatings of iron hydroxides on mineral grains (Hamad et al., 1992). However, no molecular information on the specific mechanisms of this interaction is available. The interaction of phosphate and calcium at the gibbsite surface was therefore investigated using ^{31}P-NMR and P K-edge XANES spectroscopy.

The sorption edges of phosphate and calcium at the gibbsite surface are shown in Figure 14. Because calcium adsorbs predominantly via an ion-exchange mechanism, it is only sorbed above the PZC of gibbsite (pH_{PZC} 10) in the absence of phosphate. The sorption edge of calcium in the absence of phosphate is therefore not shown. The quality of the calcium data suffers from the scattering of the solution concentrations, but it is evident that sorption occurs above pH 7.5 in the presence of 0.6 and 1.1 m*M* of phosphate in solution. The phosphate sorption envelope exhibits the shape expected for a tribasic oxyanion (Sparks, 1995), with declining sorption as the pH approaches the PZC. Phosphate sorption is enhanced in the presence of 0.65 m*M* calcium above pH 6.5.

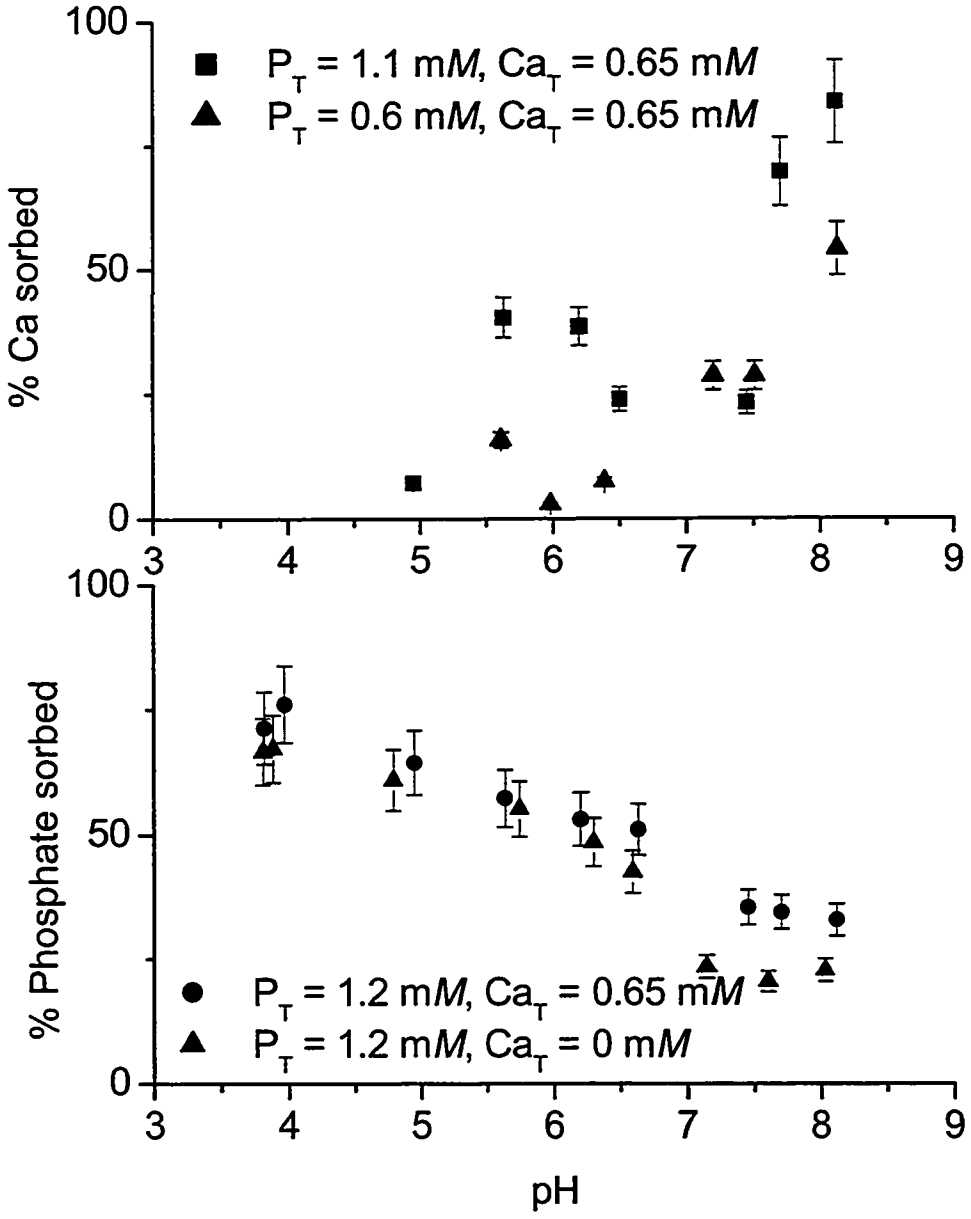

Figure 14. Sorption edges of Ca^{2+} and phosphate on gibbsite (2.5 g/L gibssite, 0.1 *M* NaCl background electrolyte, 24 h reaction time). P_T and Ca_T are total phosphate and Ca^{2+} concentrations, respectively.

A similar synergistic sorption enhancement has been found by Rietra and coworkers (2001) in their study of phosphate and calcium sorption to goethite. The CD-MUSIC model successfully predicted the sorption behavior of phosphate and calcium under the assumption of only electrostatic interactions, *i.e.* under the exclusion of ternary surface complexes or calcium phosphate surface precipitates. According to their model, the reduction of positive surface charge by the adsorption of phosphate anions is sufficient to explain the enhanced sorption of calcium below the PZC, while the reduction of negative surface charge due to the adsorption of calcium explains the enhanced phosphate adsorption. Similar results were obtained by Venema et al. (1997) in a study of the interaction of cadmium and phosphate at the goethite surface. No evidence on a molecular scale was provided by both studies to support this interpretation.

Several mechanisms of interaction of phosphate with metal cations at the surface of variably charged minerals are possible. 1) Indirect interaction via reduction or even reversion of the surface charge. 2) Formation of ternary complexes as observed by Elzinga et al. (2001) for the cooperative sorption of lead and sulfate to goethite. 3) Formation of a metal phosphate surface precipitate. Metal phosphate surface precipitates are easily detected by molecular spectroscopic techniques if present in sufficient amounts due to characteristic spectral features. Ternary complexes, however, are not as easily observed by mere fingerprinting techniques, such as NMR and XANES spectroscopy, because the influence exerted on the phosphorus atom by a single calcium cation is attenuated by the distance between the atoms and the oxygen atoms in the first coordination shell.

The MAS-NMR spectra of phosphate sorbed to gibbsite in the presence of two different calcium concentrations are shown in Figure 15 together with the spectrum of phosphate on gibbsite at pH 8 for comparison. The suspensions were undersaturated with respect to hydroxyl-apatite at both calcium concentrations. The NMR spectra of phosphate sorbed in the presence of calcium exhibit a slightly narrower line-width than the spectrum of phosphate on gibbsite at the same pH value. Whereas the spectrum of the binary system can be deconvoluted into the three peaks discussed earlier, the two spectra of the ternary system are dominated by peak 1 and 2 (d_1 = -4 ppm, d_2 = -13 ppm), with only a weak shoulder showing at -20 ppm. Peak 1 is stronger than peak 2 in the presence of calcium. No indication for the presence of amorphous calcium phosphate, apatite or octacalcium phosphate (d = 3.0 ppm, 3.05 ppm and 3.4 ppm, respectively (Elliott, 1994)) is detected.

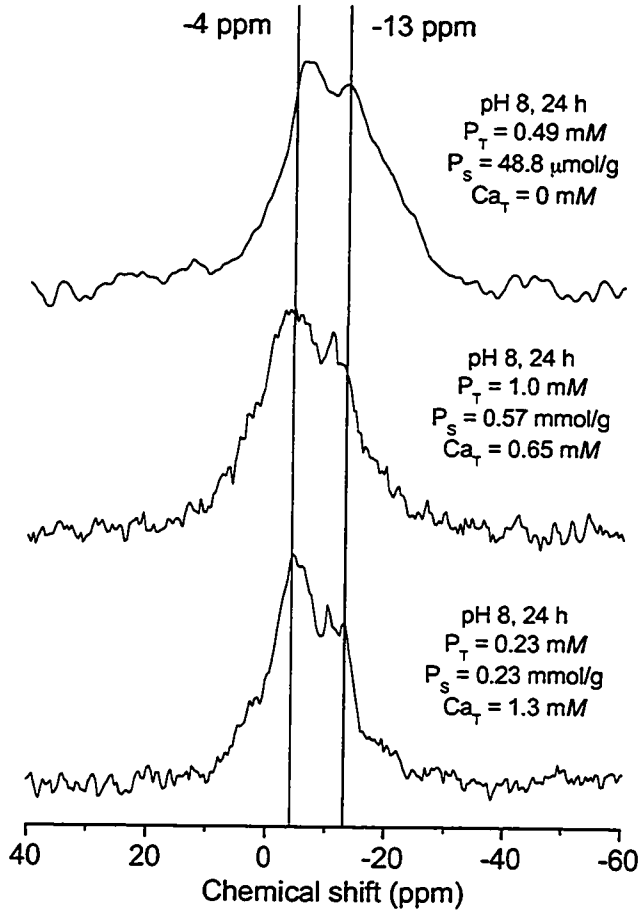

Figure 15. CP-MAS NMR spectra of phosphate sorbed to gibbsite in the presence of Ca^{2+} (2.5 g/L gibbsite, 0.1 *M* NaCl background electrolyte, pH 8, 24 h reaction time). P_S and Ca_T are the amount of phosphate sorbed and the total Ca^{2+} concentration, respectively.

The phosphate sorbed additionally in the presence of calcium is clearly adsorbed as inner-sphere surface complexes, possibly as binuclear, bidentate complexes. This agrees with the results of Rietra et al. (2001) and Venema et al. (1997). Furthermore, the

presence of calcium seems to stabilize the surface complexes and prevent them from transforming into an aluminum phosphate surface precipitate.

XANES spectra of phosphate sorbed to gibbsite in the presence of calcium were also collected. Figure 16 compares the XANES spectra of phosphate on gibbsite at two different ratios of total phosphate to calcium concentration with the spectra of phosphate on gibbsite alone and a calcium phosphate standard. None of the spectral features of calcium phosphate are detected in the spectra of the ternary systems, which closely resemble the spectrum of phosphate on gibbsite alone. Figure 17 compares the XANES spectra of phosphate sorbed to gibbsite in the presence of calcium at different orders of addition of the reagents. No differences are observed between the spectra, which again closely resemble those of phosphate on gibbsite alone. Clearly no calcium phosphate surface precipitates are formed.

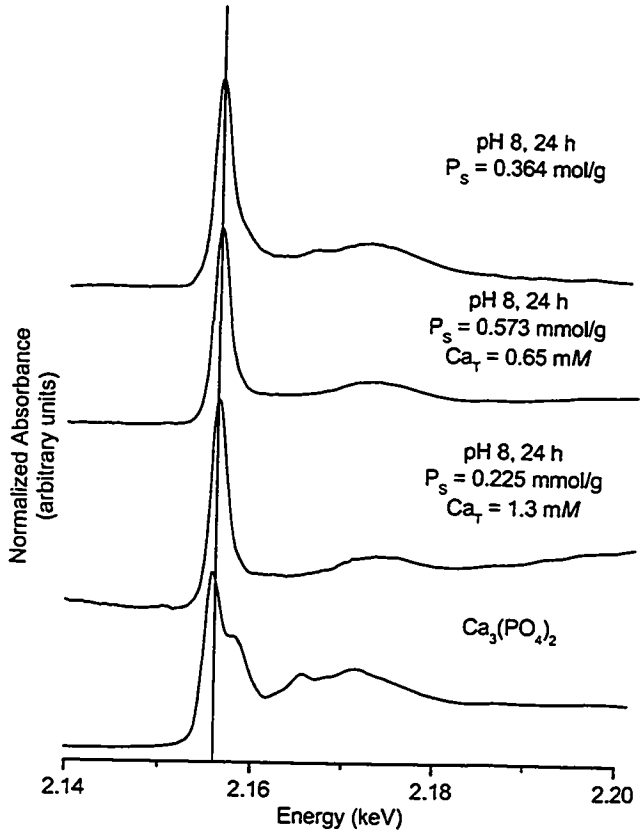

Figure 16. P K-edge XANES spectra of phosphate sorbed to gibbsite in the presence of Ca^{2+} (2.5 g/L gibbsite, 0.1 *M* NaCl background electrolyte, pH 8, 24 h reaction time). P_S and Ca_T are the amount of phosphate sorbed and the total Ca^{2+} concentration, respectively.

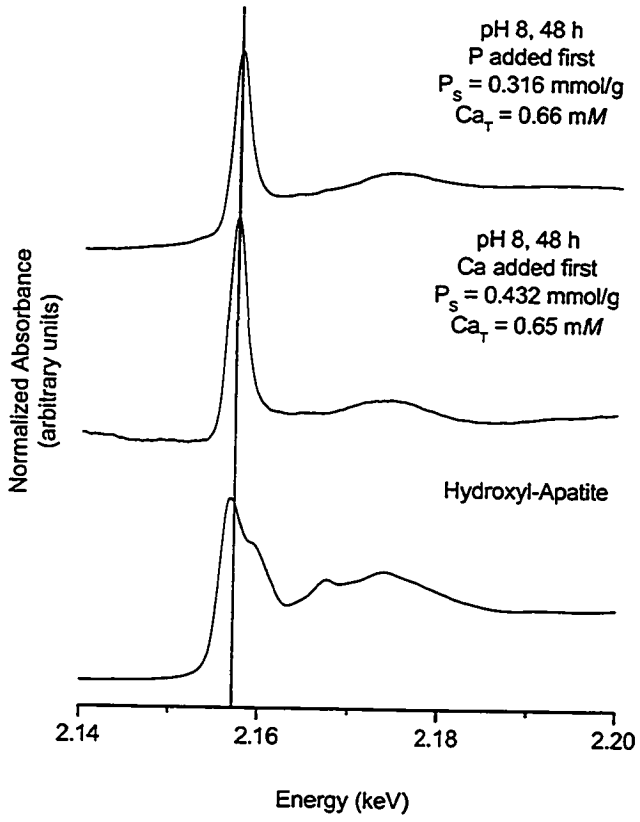

Figure 17. P K-edge XANES spectra of phosphate sorbed to gibbsite in the presence of Ca^{2+} (2.5 g/L gibbsite, 0.1 M NaCl background electrolyte, pH 8, 48 h reaction time) and the mineral standard hydroxyl-apatite. The order of addition of the reagents was varied as indicated. P_S and Ca_T are the amount of phosphate sorbed and the total Ca^{2+} concentration, respectively.

2.5.4. Investigation of the phosphate speciation in the ternary system phosphate/ gibbsite/ calcite

Because the sorption reaction of phosphate to calcite has been extensively investigated with macroscopic methods in the past (Griffin and Jurinak, 1973, 1974; Kuo and Lotse, 1972), this research focuses on the spectroscopic approach, starting with a complementary XANES investigation of phosphate sorption to calcite.

Figure 18 compares the P K-edge XANES spectra of phosphate sorbed to the calcite surface at pH 8 with tribasic calcium phosphate and hydroxyl-apatite. The spectra of the reaction product after 30 d at both surface loadings closely resemble tribasic calcium phosphate in the position of the white line and the shoulder at 2.158 keV and in the peak heights relative to the white line. The second peak that is common to all spectra (2.166 keV), however, is broader in the sorption samples than in both tribasic calcium phosphate and hydroxyl-apatite and located between the same peak in tribasic calcium phosphate (2.165 keV) and hydroxyl-apatite (2.167 keV). This indicates that the product is either rather amorphous or a mixture of both calcium phosphate phases.

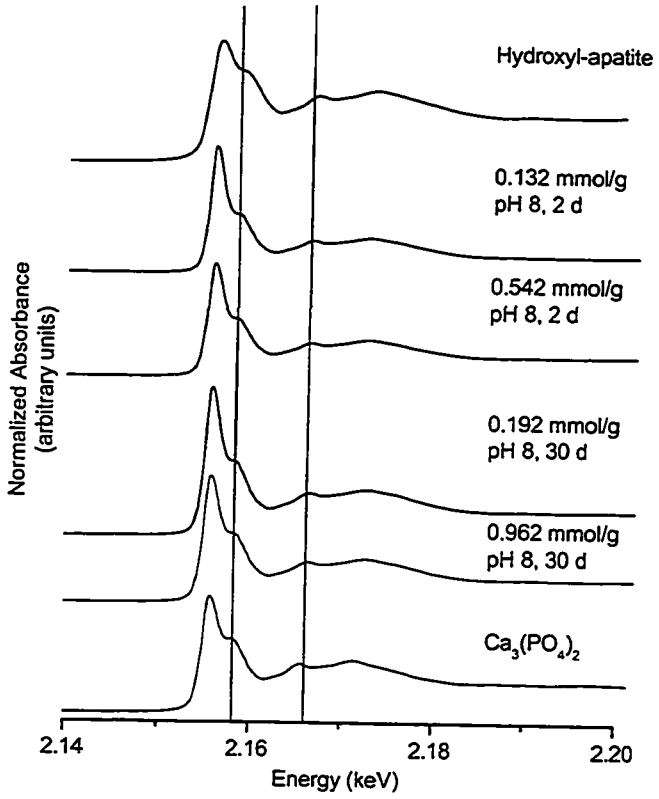

Figure 18. P K-edge XANES spectra of phosphate sorbed to calcite at pH 8 (5 g/L calcite, 0.1 *M* NaCl background electrolyte, 2 d and 30 d reaction times, two different surface loadings) and the standards hydroxyl-apatite and tribasic calcium phosphate.

In the spectra of the sorption samples after 48 h, the peaks appear at the same energies as in the long term sorption samples, but show a different intensity distribution. The white line in these spectra is sharper and more intense than in the long term sorption samples or in the mineral standards. Overall, the intensity of the white line decreases from the short over the long term sorption samples, to tribasic calcium phosphate, and finally hydroxyl apatite. Knowing that the initially forming sorption product is a surface

complex which slowly transforms to a surface precipitate of apatite (Griffin and Jurinak, 1973, 1974), it can be argued that the spectrum of the surface complex is dominated by the white line, similar to the surface complex formed on gibbsite. As the surface precipitate grows, the spectral features of the calcium phosphate phases increase in comparison to the white line. The spectral results indicate that even after 30 d and at high surface loadings of phosphate, a mixture of a surface complex, tribasic calcium phosphate, and hydroxyl-apatite still exists.

In comparison to the P-XANES spectra, the ^{31}P-NMR spectra of the phosphate sorption samples on calcite are rather poor in details. All exhibit a single sharp peak at δ = 3.0 ppm, which can be assigned to both amorphous calcium phosphate and hydroxyl-apatite (Elliott, 1994; Rothwell et al., 1980). The surface complex, which is present at short reaction time, does clearly not have a chemical shift different from the mineral standards. This has to be taken into account when examining the ^{31}P-NMR spectra of phosphate sorbed in the ternary system phosphate/ gibbsite/ calcite.

The ^{31}P-NMR spectra of phosphate sorbed in the competitive system gibbsite/ calcite at pH 7, 8, and 9 are presented in Figure 19, Figure 20, and Figure 21, respectively, together with the spectra of the sorption samples of phosphate on gibbsite and on calcite alone. Two different initial phosphate concentrations were employed, 0.48 m*M* and 1.2 m*M*. Furthermore the suspensions contain approximately 1 m*M* of free Ca^{2+} in equilibrium with calcite (Stumm and Morgan, 1996) and are therefore oversaturated with respect to apatite. The reaction time was 24 h for all samples except for the sorption sample of phosphate on calcite (48 h). Since calcium phosphate phases are suppressed in

CP-MAS spectra, both CP-MAS and single-pulse MAS spectra have been recorded. The latter are not available for the sorption samples of phosphate on gibbsite at all three pH values, and for the sorption sample of phosphate on gibbsite/ calcite at pH 9 due to low surface loading and thus unacceptable experiment times. The CP-MAS spectra of sorption samples of phosphate on gibbsite are however not different from the single-pulse MAS spectra and can therefore be used alone.

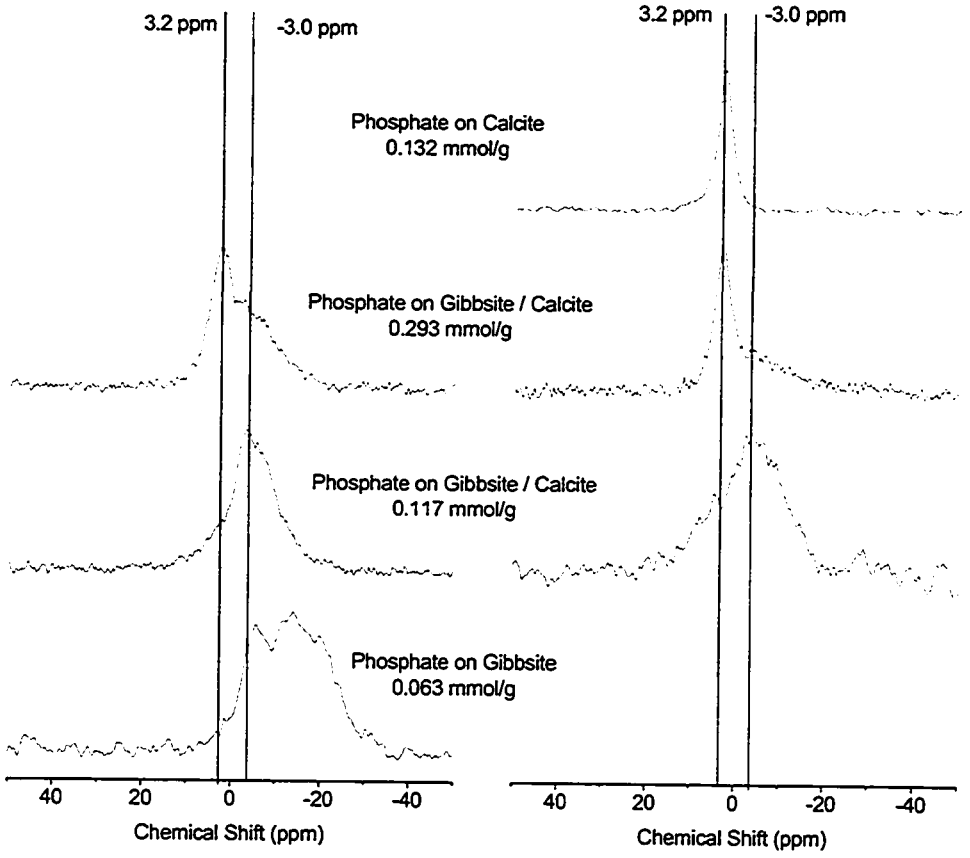

Figure 19. CP-MAS NMR spectra (left column) and single-pulse MAS NMR spectra (right column) of phosphate sorbed to calcite and gibbsite at pH 7 (2.5 g/L calcite and gibbsite, respectively, 0.1 *M* NaCl background electrolyte, 24 h reaction time).

The NMR spectra of the ternary system exhibit peaks in both the chemical shift range of calcium phosphate phases ($d > 0$ ppm) and in the chemical shift range of phosphate associated with aluminum ($d < 0$ ppm). At high surface loading levels, a sharp peak at $d = 3.0$ to 3.3 ppm dominates, indicating a mixture of tribasic calcium phosphate or apatite ($d = 3.0$ ppm) and octacalcium phosphate ($d = 3.4$ ppm). At low surface loading levels, however, the phosphate species at the gibbsite surface ($d < 0$ ppm) predominate, with the calcium phosphate phases present only as a weak shoulder. Interestingly, at both surface loading levels the peaks assigned to aluminum phosphate surface precipitates (d_2 = -13 ppm and d_3 = -20 ppm) are significantly reduced in intensity compared to the spectra of the binary sorption samples phosphate/ gibbsite.

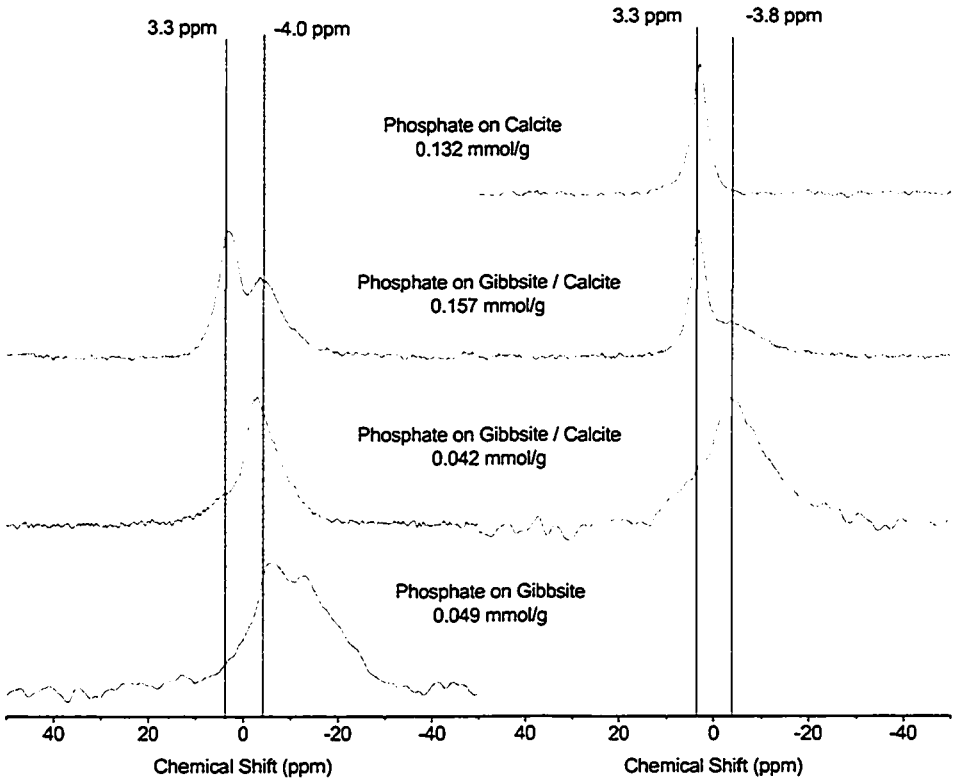

Figure 20. CP-MAS NMR spectra (left column) and single-pulse MAS NMR spectra (right column) of phosphate sorbed to calcite and gibbsite at pH 8 (2.5 g/L calcite and gibbsite, respectively, 0.1 M NaCl background electrolyte, 24 h reaction time).

The dominant peak in the ternary system at high surface loading levels has a chemical shift of d_1 = - 3.0 to - 4.0 ppm, slightly downfield from the peak assigned to a binuclear bidentate surface complex, and it is also narrower than the corresponding peak in the binary sorption systems. Comparison of the single-pulse MAS spectra with CP-MAS spectra shows that this peak is furthermore selectively enhanced by cross-polarization. This indicates that the phosphate species is either protonated or in close proximity to protons, such as in surface hydroxyl-groups. However, the fact that the chemical shift does not change significantly with pH rules out the direct protonation.

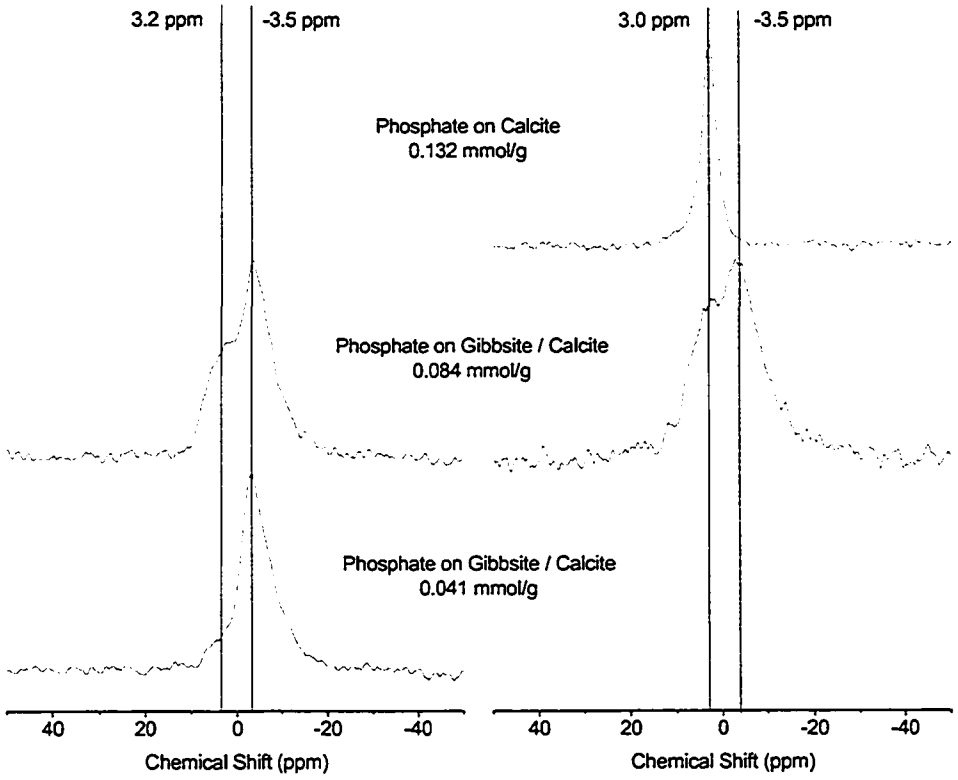

Figure 21. CP-MAS NMR spectra (left column) and single-pulse MAS NMR spectra (right column) of phosphate sorbed to calcite and gibbsite at pH 9 (2.5 g/L calcite and gibbsite, respectively, 0.1 M NaCl background electrolyte, 24 h reaction time).

The downfield shift of peak 1 in the ternary system can be explained with the formation of a ternary complex, *i.e.* the coordination of a calcium cation to a surface-bound phosphate anion. The effect of the cations in crystalline metal phosphate phases has been investigated by Turner and coworkers (1986). They found that the chemical shift of phosphate is influenced among others by the number and electronegativity of nearest-neighbor cations, with upfield shifts associated with more electronegative cations. The exchange of a proton with a calcium cation results therefore in a more positive chemical shift. To further corroborate the spectral assignments, a TRAPDOR experiment was conducted with the sample of phosphate reacted with gibbsite and calcite at pH 9. This sample has an acceptable surface loading (84 μmol/g) and the peaks assigned to a calcium phosphate phase and a surface complex on gibbsite are of comparable intensity. A clear TRAPDOR effect was however not observed and the data is therefore not presented.

A possible mechanism for phosphate sorption in the ternary system is subsequently outlined. During the initial, fast adsorption reaction, the gibbsite surface effectively competes with the calcite surface until saturation of the adsorption sites. During this phase, predominantly binuclear bidentate surface complexes and ternary complexes are formed. This is corroborated by the results of the spectroscopic investigation of the ternary system phosphate/ gibbsite/ calcium discussed in the previous chapter, which indicated that in the presence of free calcium the formation of aluminum phosphate precipitates is inhibited and the binuclear bidentate surface complex is stabilized. Phosphate remaining in solution reacts further with the calcite surface, leading

to the formation of the already discussed crystallization nuclei and growth of an apatitic surface precipitate. During this phase of the sorption reaction, the formation of an aluminum phosphate surface precipitate at the gibbsite surface is effectively inhibited, firstly due to competition from the calcite surface and secondly due to stabilization of the surface complexes by coordination of calcium.

These results have profound implications for phosphate reactions in calcareous soils and acid soils that are limed to attain an optimum pH for plant growth. Aluminum hydroxides and iron oxy(hydroxides) predominate in subtropical and tropical soils but also exist in many highly weathered, temperate soils (Sparks, 1995). Although trivalent iron is more commonly found than trivalent aluminum, the two cations tend to behave similarly, due to their similar radii and equal ionic charges. Anion sorption has been shown to proceed via similar mechanisms to iron oxy(hydroxides) and aluminum hydroxides (Parfitt, 1978) and aluminum and iron phosphate phases have similar pH ranges over which they are stable (Lindsay, 1979). Under the assumption that the sorption of phosphate to aluminum hydroxides is similar to the sorption to iron (oxy)hydroxides, it can be concluded that aluminum and/ or iron phosphate surface precipitates are not formed when calcite is present, but rather surface complexes on the variably charged minerals and calcium phosphate surface precipitates on the calcite surface.

Chapter 3

DIRECT SPECIATION OF PHOSPHORUS IN ALUM-AMENDED POULTRY LITTER

3.1. Abstract

Amending poultry litter (PL) with aluminum sulfate (alum) has proven effective in reducing water-soluble phosphorus (P) in the litter and in run-off from fields that have received PL applications, and it has therefore been suggested as a best management practice. Although its effectiveness has been demonstrated on a macroscopic scale in the field, little is known about P-speciation in either alum-amended or unamended litter. This knowledge is important for the evaluation of long-term stability and bioavailability of P, which is a necessary prerequisite for the assessment of the sustainability of intensive poultry operations.

Solid-state MAS and CP-MAS ^{31}P-NMR as well as ^{31}P{^{27}Al}TRAPDOR was used to investigate the P speciation in alum-amended and unamended PL. The results indicate the presence of a complex mixture of organic and inorganic orthophosphate phases. A calcium phosphate phase, probably a surface precipitate on calcium carbonate, could be identified in both unamended and alum-amended PL, as well as phosphate bound by hydrogen bonds to adsorbed water molecules or organic functional groups. Phosphate associated with Al was found in the alum-amended PL, present either as a poorly ordered Wavellite or as phosphate surface complexes on aluminum hydroxide that

had been formed by the hydrolysis of alum. However, a complex mixture of organic and inorganic phosphate species could not be resolved.

Preliminary data about the effects of storage of the samples indicated that more phosphate is present as calcium phosphate and in association with aluminum hydroxide after seven months of storage, while the quantity of the phosphate pool, which could not be resolved by solid-state NMR, decreased and the physical bound phosphate completely disappeared.

Combining solid-state NMR-spectroscopy with a chemical extraction sequence confirmed that calcium phosphate phases present in the litter are removed only by extraction with hydrochloric acid. However, phosphate associated with aluminum as surface complexes on aluminum hydroxide or in an uncondensed aluminum hydroxyphosphate, was not exclusively extracted by sodium hydroxide, as has been proposed in the literature, but also by hydrochloric acid.

3.2. Literature review

3.2.1. Phosphorus speciation in chemically amended poultry litter

Agriculture relies on the application of nutrients to soils to enhance food production. Animal manures have especially proven an inexpensive and effective way to improve soil quality and agricultural productivity. However, in areas with extensive animal operations, the quantities of animal manure that must be disposed of have led to the over-application of nutrients, especially P. Phosphorus can be lost from soils by erosion (particulate P) and by surface run-off and leaching (primarily soluble P).

To reduce the negative effects of over-application of animal manures in agriculture, efforts have been made to reduce the amount of water-soluble P in animal manures. A promising approach is the addition of chemical amendments, such as lime, ferric chloride or alum (aluminum sulfate hydrate) (Moore and Miller, 1994; Moore et al., 1995a). Alum has received particular interest in the treatment of poultry litter (PL) for its effectiveness in reducing the amount of water-soluble P while at the same time preventing loss of nitrogen (N) by ammonia-volatilization, which diminishes air quality as well as the quality of the litter as fertilizer (Moore et al., 2000; Shreve et al., 1995). Alum has also been shown effective in reducing water-soluble metal concentrations in PL (Moore et al., 1998; Sims and Luka-McCafferty, 2002).

Although the effectiveness of alum as an amendment for PL has been proven on a macroscopic scale in poultry houses and in the field, the reactions responsible for this effectiveness have been speculative. Initially, it was assumed that phosphate in animal

manures reacts with Al^{3+} to form solid aluminum phosphate ($AlPO_4$) (Moore and Miller, 1994), which is insoluble in the pH range typical for agricultural soils (Lindsay, 1979). Although this assumption has been recognized as oversimplified (e.g. (Duffy and van Loon, 1995)), little, if any, information about the mechanisms of P fixation in PL is available, mainly due to the lack of methods sufficiently sensitive to directly determine the species, or form of P, in heterogeneous materials such as PL and soil. Recently, an X-ray Absorption Near Edge Structure (XANES) spectroscopic study of PL showed the presence of a calcium phosphate phase in the unamended PL samples, whereas features in the XANES spectra of the alum-amended PL samples indicated the formation of a P-species similar to phosphate adsorbed to aluminum hydroxide (Peak et al., 2002).

3.2.2. ^{31}P-NMR spectroscopy of manure and biosolids

Recent advances in nuclear magnetic resonance (NMR) spectroscopy have made it a versatile technique in soil and environmental sciences research (Nanny et al., 1997; Wilson, 1987). NMR spectroscopy is sensitive to the direct chemical environment of the investigated nucleus and does not require crystalline samples, which makes it an ideal technique to study molecular species in heterogeneous and amorphous matrices.

Liquid-state NMR has been used to characterize P species in extracts of soils (Amelung et al., 2001; Cade-Menun et al., 2002; Cade-Menun and Preston, 1996; Condron et al., 1985; Mahieu et al., 2000; Newman and Tate, 1980; Pant et al., 1999; Robinson et al., 1998; Zhang et al., 1999), wastewater sludge (biosolids) (Hinedi et al., 1988, 1989a), and animal manures (Crouse et al., 2000; Leinweber et al., 1997). While this method advanced our understanding of transformation and mineralization of organic

phosphates in soils, animal manures and biosolids, the possibility of the creation of artifacts by hydrolysis during the extraction steps makes a less invasive technique desirable.

High-resolution solid-state NMR spectroscopy is an important non-invasive tool to provide specific information about elemental speciation in amorphous and/or heterogeneous matrices. Using ^{31}P magic angle spinning (MAS) NMR, Hinedi (Hinedi and Chang, 1989; Hinedi et al., 1989b) identified calcium phosphate, aluminum phosphate, and pyrophosphate solid phases in anaerobically digested sewage sludge and soils amended with these biosolids. They also observed however, that phosphate species in close contact with paramagnetic cations could not be accounted for due to the broadening of the NMR-signals, a commonly encountered problem in NMR spectroscopy of soils (Blumberg, 1960; Smernik and Oades, 2002).

Frossard and coworkers (1994) characterized urban sewage sludge by sequential chemical fractionation with consecutive solid-state ^{31}P-NMR analysis of the residual solids. They found that a complex mixture of phosphate solids was present in the sludge, including several calcium phosphates and aluminum phosphate.

Duffy and vanLoon (1995) investigated the Al and P speciation in sewage sludge by comparing it with aluminum hydroxyl-phosphates aged for different times using solid-state ^{31}P- and ^{27}Al-NMR spectroscopy. They found that phosphate species associated with aluminum generally have ^{31}P -chemical shifts in the range from -7 to -30 ppm, with the less condensed aluminum phosphate polymers appearing at the higher end of this range. This broad range of reported chemical shifts requires a technique sensitive for

dipolar coupling between P nuclei and Al nuclei to unambiguously assign peaks arising from the interaction between these spin pairs.

3.2.3. ^{31}P {^{27}Al} TRAPDOR experiments

$^{31}P\{X\}$ TRAPDOR (TRAnsfer of Polarization during DOuble Resonance) has been used to directly probe the P-X connectivities (where X is a quadrupolar nucleus, e.g. ^{27}Al, ^{23}Na or ^{11}B) in amorphous or microcrystalline materials, such as glasses and catalyst precursors. Using $^{31}P\{^{27}Al\}$ TRAPDOR, van Eck and coworkers (1995) were able to show that a surface layer of $AlPO_4$ rather than one of phosphate polymers is formed on γ-Al_2O_3 during impregnation with phosphate. The complex ^{31}P-NMR spectra of sodium aluminophosphate glasses (Lang et al., 2001), phosphate-containing aluminosilicate (Schaller et al., 1999) and aluminoborosilicate glasses (Rong et al., 1998) could be conclusively interpreted by identifying phosphate species directly bound to Al, Na or B.

Because of the specificity for P-species that are in close contact with Al, ^{31}P {^{27}Al} TRAPDOR experiments were used to probe the P-Al connectivity in alum-amended PL and to help unambiguously identify aluminum phosphate phases.

3.2.4. Investigation of phosphorus speciation by sequential chemical extraction of poultry litter

Chemical extraction sequences have been used in the past to investigate changes in soil phosphorus fractions with different management practices (Hedley et al., 1982) and as a means to characterize phosphorus species in animal manures (Dou et al., 2000). The multitude of inorganic and organic phosphorus species in soils and manures makes it

impossible to measure their contributions individually and sequential extraction offers the possibility to divide the species present in broad categories based on their solubility in neutral, acid or alkaline media (Hedley et al., 1982). In using this technique, however, one has to be aware of its limitations.

A very popular extraction sequence employs first deionized water alone or in combination with an anion exchange resin as a sink for phosphate, followed by dilute $NaHCO_3$, sodium hydroxide, and hydrochloric acid. The residual phosphorus is dissolved using strongly acidic and oxidizing agents, such as sulfuric acid or nitric acid in combination with hydrogen peroxide (Dou et al., 2000; Hedley et al., 1982). The sum of the first two extraction steps is usually assigned to plant-available phosphorus (Dou et al., 2000), while amorphous and some crystalline aluminum or iron phosphate species are expected to dissolve during the treatment with sodium hydroxide, and calcium phosphate phases during the treatment with dilute acid (Dou et al., 2000; Hedley et al., 1982). Larger amounts of organic phosphorus compounds are reported to be released during the extraction steps with $NaHCO_3$ and sodium hydroxide (Hedley et al., 1982).

These assignments are, however, operationally defined and no information on a molecular level is available from a sequential extraction. A very promising approach is the combination of either extraction or desorption techniques with spectroscopic techniques and thus verify molecular assignments made from the macroscopic information. As mentioned at the beginning, Frossard et al. (1994) characterized urban sewage sludge by sequential chemical fractionation with consecutive solid-state ^{31}P-NMR analysis of the residual solids. They found that a complex mixture of phosphate

solids was present in the sludge, including several calcium phosphates and aluminum phosphate. Corresponding to the proposed sequence of dissolution, the calcium phosphate phases were dissolved during extraction with hydrochloric acid. The aluminum phosphate phase, which was tentatively assigned to a poorly ordered wavellite, was however present in the residual phosphate fraction, although it was expected to dissolve during extraction with sodium hydroxide. It was reasoned that the poorly ordered wavellite re-precipitated during the extraction.

Relevant research has also been done in the field of metal sorption in soils. Guest and coworkers (2002) used Mn K-edge XANES to investigate the manganese species extracted from soils in a chemical extraction sequence. Voegelin and coworkers (2002) combined column adsorption and desorption with EXAFS spectroscopy to investigate the formation of zinc surface precipitates in soil. These two studies demonstrate that a combination of extraction and desorption, respectively, with molecular spectroscopy allows for a better insight into element speciation in soils.

In this research, a chemical extraction sequence adapted from Hedley et al. (1982) is combined with solid-state ^{31}P-NMR spectroscopy to verify the assignments made according to the sequential extraction.

3.3. Objectives

The objectives of the research presented in this chapter were to investigate the phosphate speciation in unamended and alum-amended poultry litter using an array of methods and techniques. In particular, it was planned to:

a. Employ single-pulse MAS, CP-MAS ^{31}P-NMR spectroscopy and TRAPDOR to identify phosphate species in PL;

b. Combine sequential chemical extraction and ^{31}P-NMR spectroscopy to verify assignments made in the literature according to the sequential extraction.

3.4. Materials and Methods

3.4.1. Sample Preparation

Samples of PL were obtained from an on-farm evaluation of the effectiveness of alum as an amendment for PL. The details of this study are reported elsewhere (Sims and Luka-McCafferty, 2002). In brief, 194 poultry houses were chosen, of which 97 received alum and 97 served as a control group. The alum was applied and incorporated at an average rate of 90 g alum per bird shortly after the previous flock and the upper crust of litter had been removed (approximately every 5-6 weeks). Samples were collected from the entire depth of the litter layer after the removal of the last flock in the study and then homogenized. Subsamples were dried at 65 °C and ground to pass a 0.8 mm screen.

One sample (PL 181) was freeze-dried after two years of storage at 4°C, ground using mortar and pestle, und separated using standard mesh sieves into three size fractions (841 – 420 μm, 420 – 125 μm, and < 125 μm). The fine fraction (<125 μm) contained the highest Al and P concentrations, and was used for the TRAPDOR experiments. The fine fraction and the next coarser fraction (420 – 125 μm), were sequentially extracted and analyzed by both CP-MAS and single-pulse MAS NMR spectroscopy.

Total Al and P concentrations were determined after microwave-assisted digestion with concentrated HNO_3 and 30 % H_2O_2 (EPA 3051); water-soluble Al and P were determined after extracting the fresh litter sample with de-ionized (DI) water (1 : 10 (w : v)) and filtering the extract through a 0.45 mm Supor® filter (Gelman Laboratories, Ann Arbor, MI). Some of the extracted samples were freeze-dried and also used for

NMR-analysis. Phosphorous concentrations were measured by inductively coupled plasma atomic emission spectroscopy (ICP-AES) and using the colorimetric method described by Murphy and Riley (1962). Aluminum concentrations were determined using ICP-AES. Sample pH was determined in suspension in DI water, using a 1 : 4 PL to water ratio. Selected properties of the samples are listed in Table 2.

Table 2: Selected properties of the poultry litter samples used in the NMR studies

Poultry litter sample number[a]	pH[b]	Total P %[c]	Total Al %	Water Soluble	
				P[d] [mg kg^{-1}]	Al[d] [mg kg^{-1}]
PL 125	7.23	1.97	1.77	322	18.9
PL 134	7.37	2.32	1.09	783	23.1
PL 181 (<125μm)	ND[e]	2.31	3.30	1050	0
PL 182	7.03	1.94	1.63	1167	19.5
PL 191	6.89	1.91	2.16	542	18.8
PL 197	7.32	2.09	1.54	355	18.7
PL 502	7.82	1.94	0.08	1635	2.5
PL 511	7.6	1.99	0.12	1754	1.6
PL 541	8.23	1.96	0.10	1308	6.1
PL 559	8.21	2.08	0.10	1570	7.9
PL 597	7.73	2.14	0.09	2534	2.7

[a] Samples 125 through 197 are alum-amended, samples 502 through 597 are unamended;
[b] determined as a suspension in DI water (litter to water ratio 1 : 4);
[c] total P and Al are given in weight-% of the dry samples, determined by ICP-AES after digestion;
[d] water-soluble P and Al were determined by ICP-AES after extraction with DI water (fresh litter to water ratio 1 : 10);
[e] ND: not determined.

Reference phosphate compounds were purchased and analyzed for comparison. $CaHPO_4$ and $Ca_5(PO_4)_3OH$ were purchased from Fisher Scientific (Fair Lawn, NJ). Calcium phytate, and sodium phytate were purchased from Aldrich. Mineral samples of Wavellite ($Al_3OH_3(PO_4)2 \cdot H_2O$) and Variscite ($AlPO_4 \cdot 2H_2O$) were provided by the Excalibur Mineral Company.

3.4.2. Sequential chemical extraction of sample PL 181

A chemical extraction sequence was adapted from Hedley et al. (1982). The extractants were in their order of application deionized water, 0.5 *M* $NaHCO_3$, 0.1 *N* NaOH, and 1.0 *N* HCl. A standard extraction procedure was established as follows: 0.6 g of freeze-dried sample was shaken with 30 ml of extractant for 20 h (solid to solution ratio 1 : 50). The solids were separated from the supernatant by centrifugation (15 min, 15000 rpm) and decanting. The supernatant was passed through 0.2 μm Supor® filter paper (Gelman Laboratories, Ann Arbor, MI) and stored at 4°C until analysis. The solid to solution ratio employed in this work was higher than that published by Hedley et al. (1982) (1 : 60), Dou et al. (2000) (1 : 100) , or Frossard et al. (1994) (1 : 200). This ratio was chosen to allow for the larger sample amount required for solid-state NMR analysis.

Concentrations of P, Al, Ca and Fe in the extracts were determined by Inductively Coupled Plasma Atomic Emission Spectroscopy (ICP-AES). The total elemental concentrations were measured after digestion with concentrated HNO_3 and 30 % H_2O_2 for 24 h at 50 °C. A total number of four subsamples of each of the coarse and fine fraction of sample PL 181 were extracted. After each extraction step, one of the four

samples was freeze-dried and subsequently used for ^{31}P NMR analysis. Elemental concentrations are therefore average values of four samples for the first (deionized water), three for the second (0.5 *M* $NaHCO_3$), and two for the third extraction step (1.0 *N* HCl). Total concentrations of P, Ca, Al, and Fe, and the pH of sample PL 181 are presented in **Error! Reference source not found.**. All concentrations are calculated as mg/g (mg/kg in the case of Fe) of dried litter.

3.4.3. Single-pulse MAS and CP-MAS NMR experiments

Solid-state ^{31}P-NMR spectra were recorded on a Chemagnetics CMX Infinity spectrometer with an Oxford 300 MHz wide-bore magnet operating at a magnetic field of 7.04 Tesla, corresponding to resonance frequencies of 121.4 MHz for ^{31}P and 299.9 MHz for ^{1}H. To afford uniform distribution and homogeneous spinning of the rotor in the MAS probe, dried and ground samples were used. Spinning speeds were maintained constant at values from 7 to 10 kHz ± 5 Hz.

CP-MAS experiments used a proton p/2-pulse of 3.5 μs, a contact time of 1.3 ms and a pulse delay of 2 s. Depending on the P concentration, 2000 to 4000 scans were accumulated to give a signal to noise ratio of at least 30 : 1. Single-pulse, proton-decoupled spectra were recorded using a ^{31}P p/2-pulse of 3.7 μs and a relaxation delay of 60 s. For these experiments up to 512 scans were accumulated.

The spectra were processed using the NUTS NMR utility transform software by Acorn NMR. A line broadening of 50 – 100 Hz was applied prior to Fourier Transformation and phase correction. The complex signals were deconvoluted using a

minimal set of peaks. The quality of the fit increased when Lorentzian peaks for narrow peaks and Gaussian peaks for broad peaks were used. No other constraints were employed. Isotropic chemical shifts are all reported in parts per million (ppm) relative to the signal of 85% H_3PO_4 as an external reference; positive values correspond to low-field or high-frequency shifts.

3.4.4. TRAPDOR experiments

The TRAPDOR experiment is a rotor-synchronized solid-state NMR double resonance experiment which reintroduces the heteronuclear dipolar coupling in a spin system, from which it is largely removed under magic angle spinning (MAS) conditions (Grey et al., 1993). Two echo-sequences are applied to the nucleus of interest (in our case ^{31}P) and observed. The first echo-spectrum serves as a reference (Figure 22). During the evolution of the second echo, a radio frequency is applied to the channel of the quadrupolar nucleus (Figure 23), which induces transitions of the spins between the different energy levels. These transitions accelerate the dephasing of the magnetic momentum of the ^{31}P nuclei which are dipolar coupled to the quadrupolar nuclei. This TRAPDOR effect can be observed as a signal loss in the ^{31}P echo-spectrum and as a positive peak in the difference of the reference and the dephased spectra.

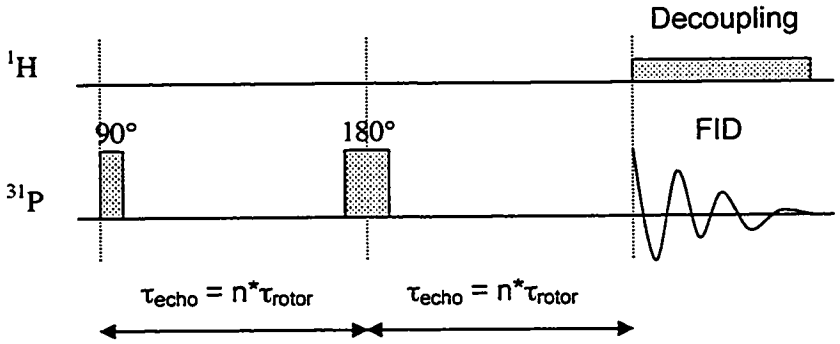

Figure 22. Schematic depiction of the echo pulse sequence.

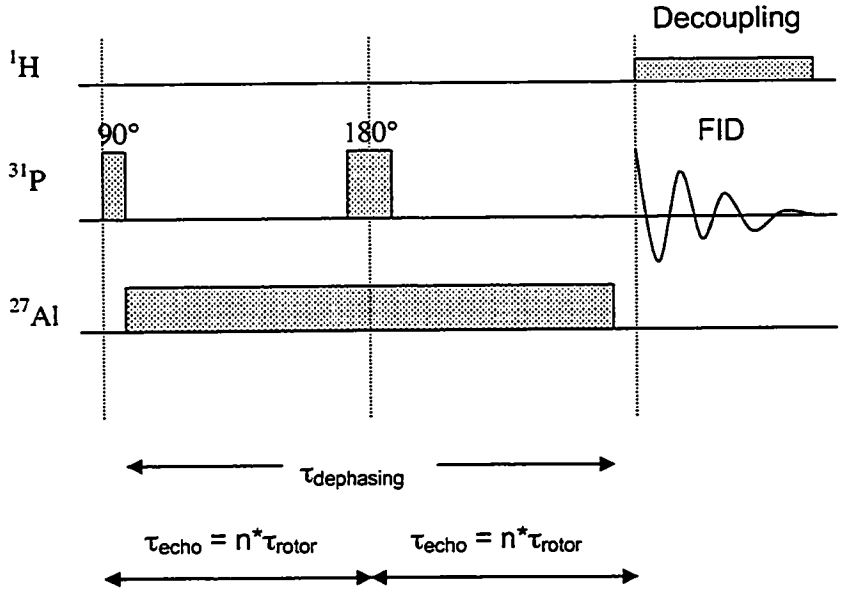

Figure 23. TRAPDOR pulse sequence

The TRAPDOR effect increases with increasing dephasing time $\tau_{dephasing}$ and increasing heteronuclear dipolar coupling between the nuclei. The latter is proportional to r^{-3} (with r being the inter-nuclear distance) because it is an interaction between two

permanent dipoles. The TRAPDOR effect will therefore decrease rapidly with increasing distance between the nuclei (Schaller et al., 1999).

Different P-species have different transversal relaxation times T_2 and will therefore lose signal intensity at different rates (Drago, 1992). This effect is superimposed by the TRAPDOR effect and the echo time has to be adjusted in order to retain maximum signal intensity.

At a static magnetic field-strength of 7.04 T, the resonance frequency for ^{1}H, ^{27}Al and ^{31}P were 299.99 MHz, 78.16 MHz and 121.44 MHz, respectively. Samples were spun in an HMX triple-resonance probe at a spinning speed of 10 kHz ± 5 Hz ($\tau_{rotor} = 0.1$ ms) about the so-called magic angle (54.7°). The echo and dephasing times were determined in a set of preliminary TRAPDOR experiments with a mixture of apatite and variscite (1:1 w/w). Echo times were varied between $\tau_{echo} = 2\tau_{rotor}$ and $16\tau_{rotor}$ and dephasing times were set to $\tau_{dephasing} = 2\tau_{echo} - 4$ μs. The p/2-pulse and p-pulse were 3.7 and 7.4 ms, respectively, and the pulse-delay was 10 s. For the standard compounds, an acquisition of 16 scans was sufficient, while the PL samples and sorption samples required more than 1000 scans and the experimental times exceeded 24 hrs. Therefore, TRAPDOR experiments were only performed with a narrow selection of samples.

Data analysis was performed using the 1D NUTS NMR utility transform software package (Acorn NMR). The reference spectrum was subtracted from the dephased spectrum in the time domain prior to Fourier Transformation and phase correction. A line-broadening of 100 Hz was applied to the echo spectra of the litter sample, while a

line-broadening of 300 Hz was applied to the difference spectrum. No line-broadening was applied to the spectra of the standard sample. After Fourier-Transformation of the time domain and phase correction, the spectra of the standards were normalized to the apatite peak, whereas the spectra of the PL and sorption samples were normalized to the highest peak. Chemical shifts are expressed in ppm relative to the signal of 85% H_3PO_4.

3.5. Results and Discussion

3.5.1. ^{31}P-NMR spectroscopic investigation of alum-amended and unamended poultry litter

Poultry feed contains dicalcium phosphate (DCP) and calcium carbonate, which dissolve during digestion; both calcium and phosphate ions will be partially excreted in some form. Since poultry is lacking the enzymes necessary to hydrolyze the phytic acid contained in the grain that makes up most of its diet, poultry manure and litter have long been known to contain phytic acid (Taylor, 1965). The PL consists of the feces and the bedding material, mainly wood chips and sawdust, and has neutral to slightly basic pH values (Table 2). In the alum-amended litter (Table 2, samples PL 125 through 197), the pH initially dropped to pH 5 – 5.5 after addition of alum and slowly increased over time as more feces were added, reaching slightly lower values than the unamended litter (Table 1, samples PL 502 through 597) (Sims and Luka-McCafferty, 2002).

Considering the elemental composition and the pH of PL (Moore et al., 1995b, 2000; Sims and Luka-McCafferty, 2002), P chemistry was expected to be dominated by interactions with Al (in the amended samples), Ca and Mg, and by organic phosphate (e.g. undigested phytic acid and compounds derived from metabolic processes). Other

components in PL that are expected to form stable compounds with P are Fe, Mn and Zn. In solid-state ^{31}P NMR spectroscopy, Ca, Mg and Al phosphate compounds have characteristic isotropic chemical shifts (Aramendía et al., 1998a, b; Bleam et al., 1989b; Elliott, 1994). Iron and manganese phosphate compounds are not expected to show in the spectra because of paramagnetic line-broadening (Blumberg, 1960; Hinedi et al., 1989b; Sutter et al., 2002). The chemical shifts of the more soluble phosphate salts with various cations (Na, K, NH_4, etc.) are also reported (Hartmann et al., 1994; Turner et al., 1986), but those are not expected to form as crystalline phases at high humidity and in the presence of cations forming less soluble compounds. The various cations present are nevertheless expected to influence the chemical shift of organic phosphate compounds and inorganic phosphate anions they are complexed with, by changing the electron density of the phosphate anion (Turner et al., 1986).

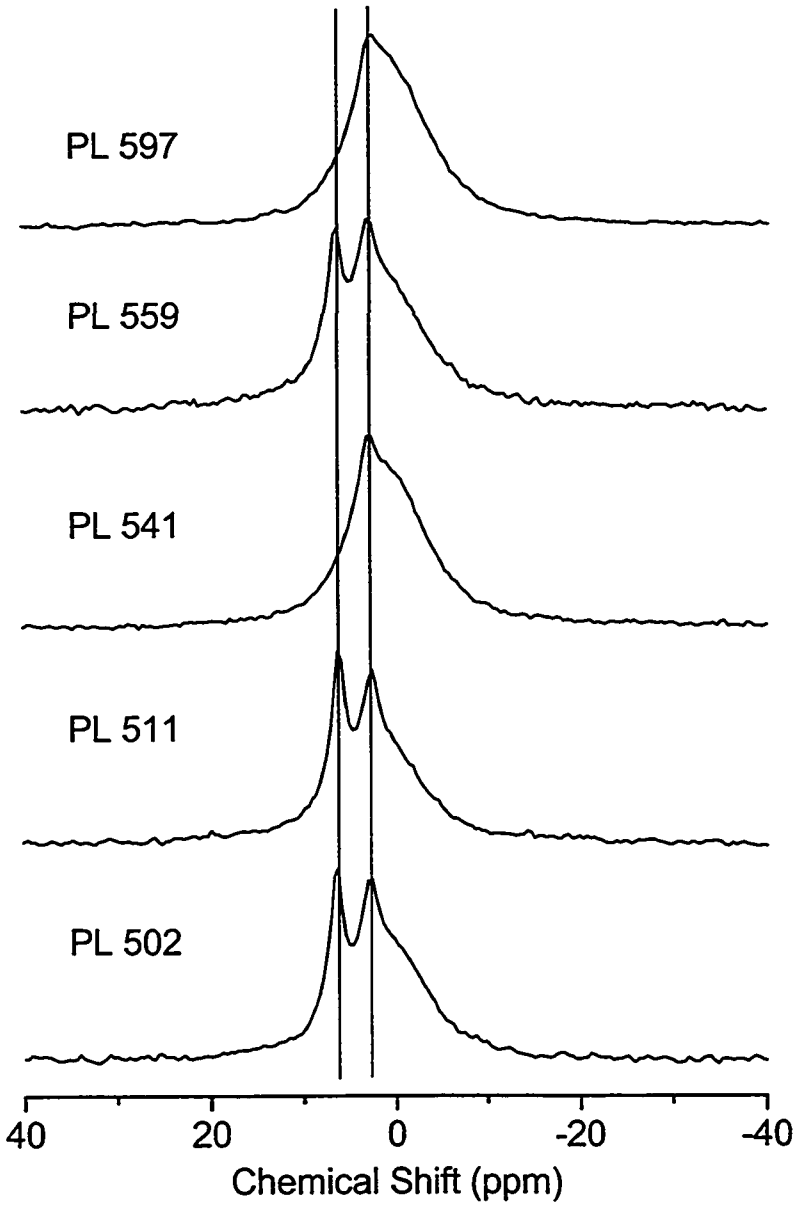

Figure 24. Single-pulse, proton decoupled 31P-MAS-NMR spectra of unamended PL samples; the chemical shifts of the marked peaks are d = 6.4 ppm and 2.8 ppm; for discussion see text.

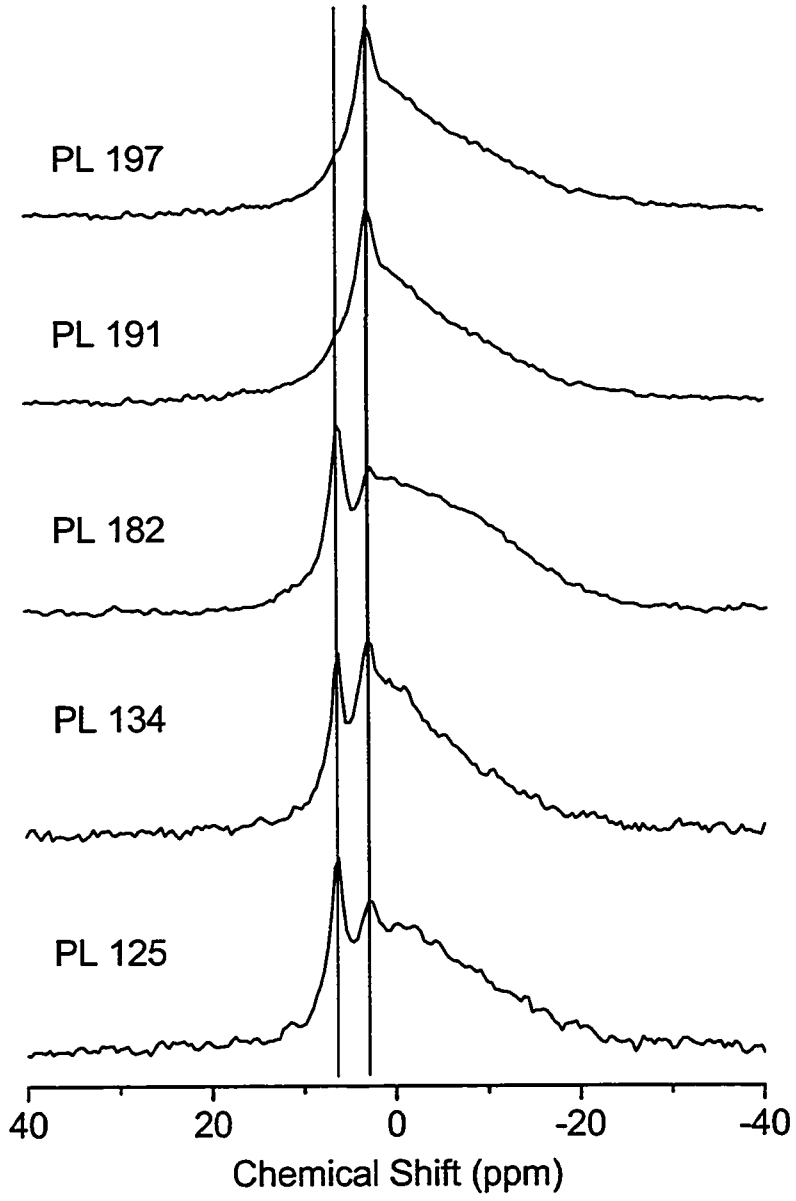

Figure 25. Single-pulse, proton decoupled ^{31}P-MAS-NMR spectra of alum-amended PL samples; the chemical shifts of the marked peaks are d = 6.4 ppm and 2.8 ppm; for discussion see text.

The single pulse spectra of both the unamended (Figure 24) and alum-amended samples (Figure 25) show broad, complex resonances centered at 0 ppm. The range of chemical shifts observed in these spectra confirms a predominant oxidation state of P(V) in the PL, which has also been shown by Peak et al. (2002). One or two relatively sharp peaks can be distinguished. Deconvolution of the signals is illustrated for sample PL 125 (alum-amended sample) in Figure 26. The complete deconvolution results are shown in Table 3. Deconvolution of the spectra reveals a set of up to four peaks, all of which are present in some of the alum-amended samples (samples PL 182, PL 134 and PL 125 in Figure 25), whereas in some unamended samples only two peaks are found (samples PL 541 and PL 597 in Figure 24). One sharp peak with a chemical shift of 2.6 to 3.1 ppm and varying intensity and a broad peak centered between -1 and 1 ppm are present in all of the samples investigated. Another sharp peak at 6.4 ppm can be found in most of the samples. The spectra of the alum-amended samples (Figure 25) are dominated by one very broad resonance of Gaussian line-shape centered between -4 and -10 ppm, which appears as a tailing on the negative side of the composite signal.

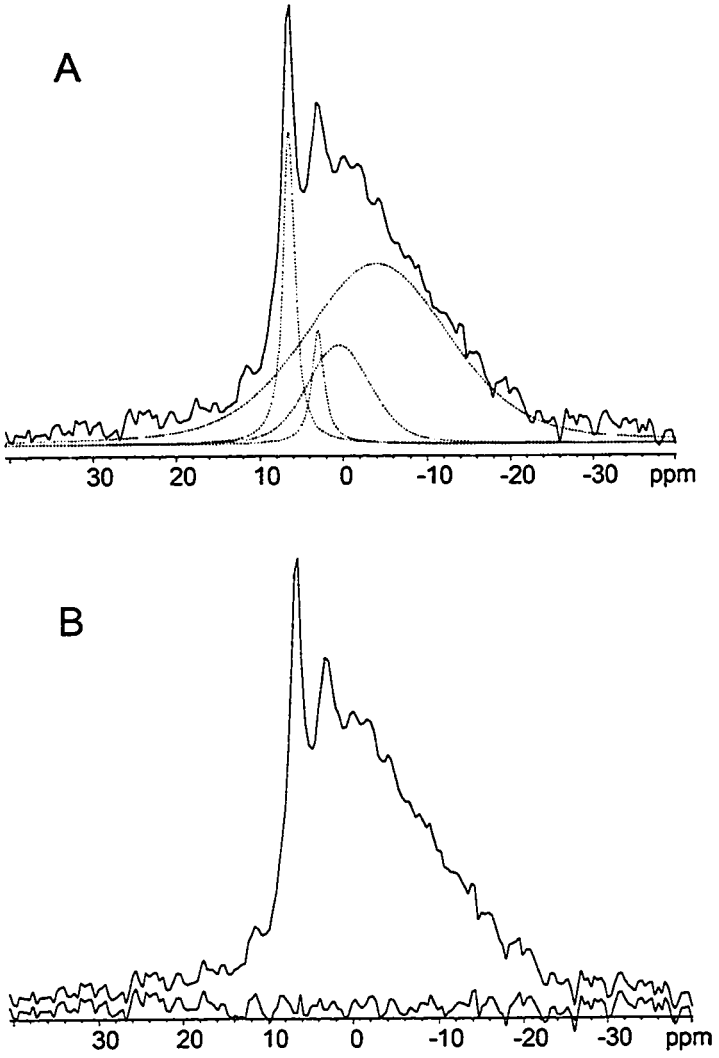

Figure 26. Deconvoluted single-pulse, proton decoupled ^{31}P-MAS-NMR spectrum of sample PL 125. A) The dashed lines are the fitted peaks at δ = 6.4 ppm, 2.9 ppm, -0.3 ppm, -4.4 ppm; the solid line represents the original data. B) The original data (top) and the difference spectrum (bottom).

Table 3: Deconvolution results of the single-pulse, proton decoupled ^{31}P-MAS-NMR spectra

Sample	Peak number	Chemical shift (ppm)	Relative height (% of peak 3)	Width (Hz)	Relative peak area (%)
PL 125	1	6.44	284	356	10.69
	2	2.98	110	302	5.34
	3	-0.68	100	1517	58.72
	4	-10.53	157	1726	25.25
PL 134	1	6.47	150	213	5.77
	2	3.09	98.4	235	3.99
	3	1.35	100	1378	62.89
	4	-7.73	114	1891	27.36
PL 182	1	6.27	374	221	6.75
	2	2.55	114	190	1.27
	3	2	100	1358	28.13
	4	-6.42	260	2228	63.85
PL 191	2	2.79	119	346	12.76
	3	0.79	100	1080	40.77
	4	-7.19	68.8	1780	46.47
PL 197	2	3.1	180	277	10.39
	3	1.07	100	1381	53.02
	4	-8.52	138	2020	36.59
PL 502	1	6.51	136	191	13.49
	2	2.8	77.7	207	8.08
	3	1.2	100	1348	78.43
PL 511	1	6.16	209	209	17.39
	2	2.67	142	224	10.14
	3	1.27	100	1224	72.46
PL 541	2	2.98	51.9	407	18.03
	3	-0.11	100	1209	81.97
PL 559	1	6.44	77.3	230	11.1
	2	2.97	46.6	252	7.27
	3	1.49	100	1311	81.63
PL 597	2	2.6	63	446	18.7
	3	-0.3	100	1224	81.3

Comparison of the single pulse (Figure 24 and Figure 25) and CP-MAS spectra (Figure 27 and Figure 28) shows that the peak at 6.4 ppm is selectively enhanced by cross-polarization and that it is present in all samples but sample PL 541 (Figure 27). The peak at 2.6 - 3.1 ppm, on the other hand, is suppressed in the CP spectra. The broad resonances are not affected by cross-polarization but appear to be of low intensity in comparison to the intense peak at 6.4 ppm. Additionally, a weak resonance at -20 ppm can be detected in the cross-polarized spectra of two of the unamended samples (sample PL 511 and PL 541, see enlarged spectra in Figure 27) and of two of the alum-amended samples (samples PL 125 and PL 182, see enlarged spectra in Figure 28). This peak is an artifact that can be traced to a contamination of the rotor with a small amount of variscite ($AlPO_4 \cdot 2H_2O$).

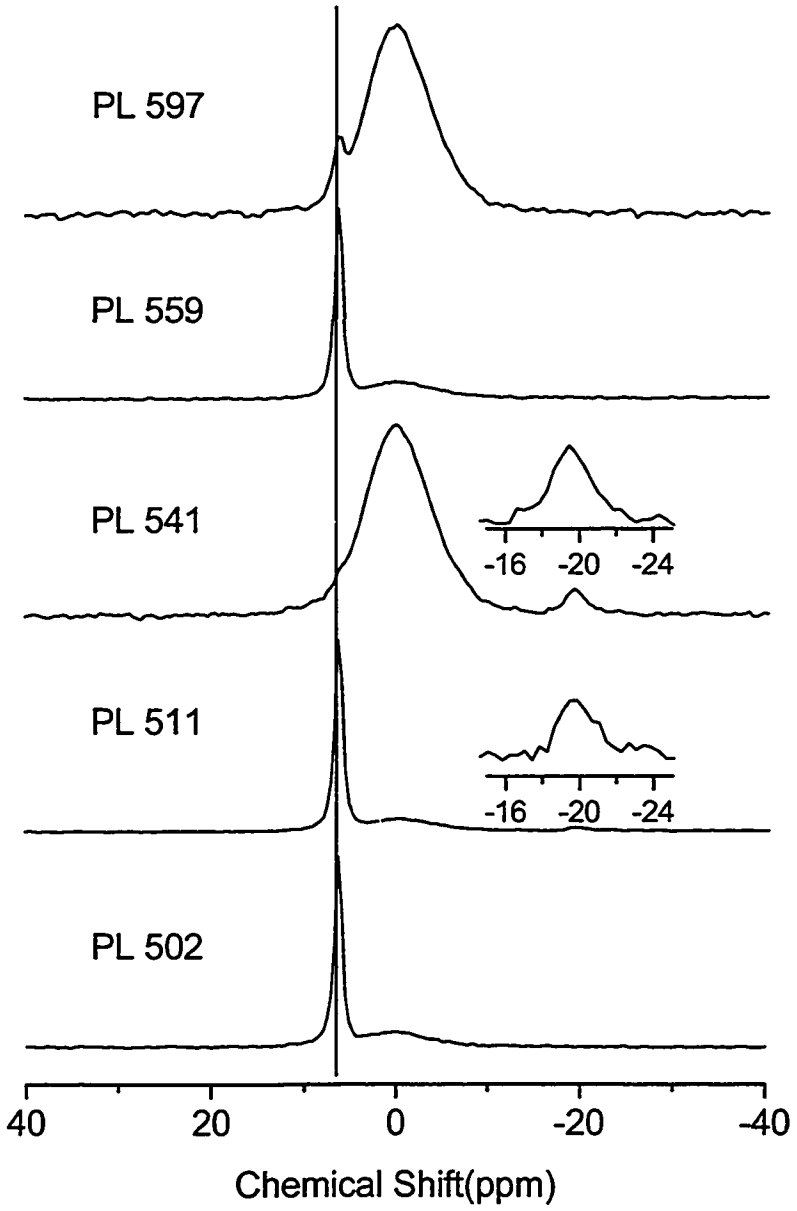

Figure 27. CP-MAS ^{31}P-NMR spectra of unamended PL samples; the insets show enlargements of the chemical shift region indicated; the chemical shift of the marked peak is d = 6.4 ppm; for discussion see text.

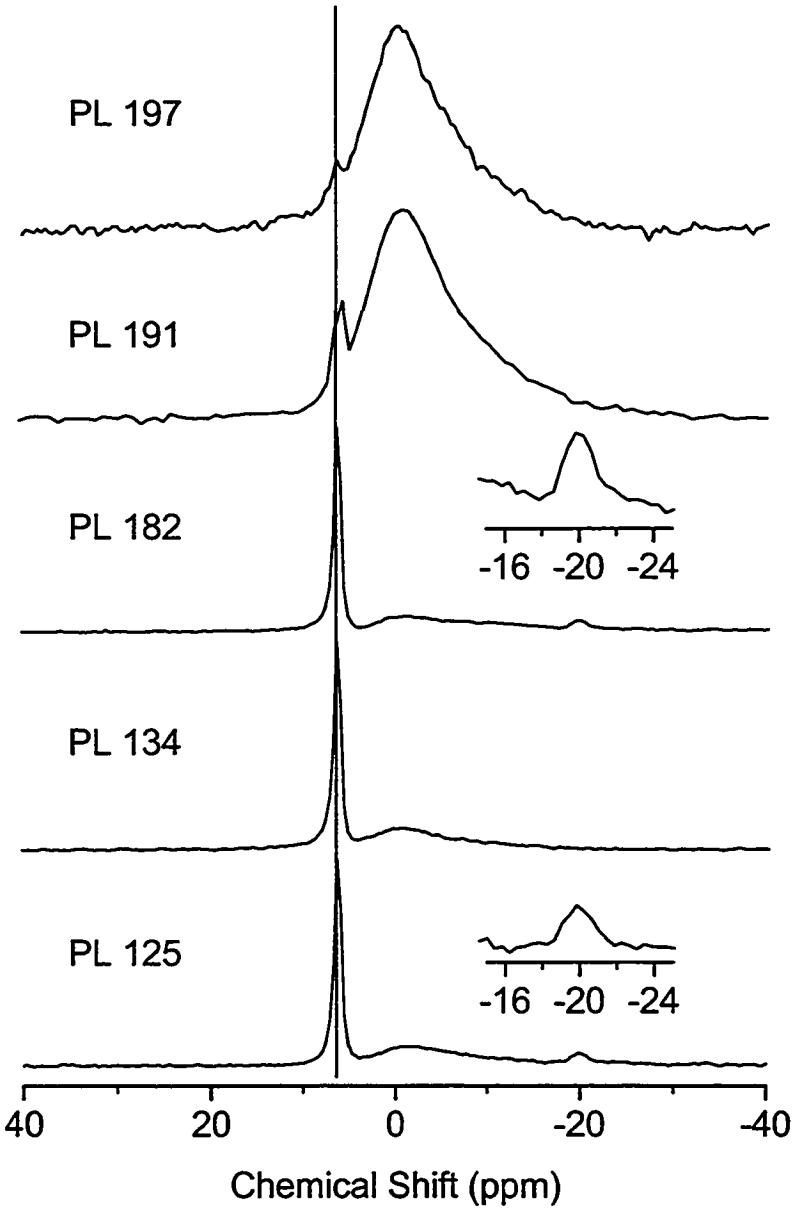

Figure 28. CP-MAS 31P-NMR spectra of alum-amended PL samples; the insets show enlargements of the chemical shift region indicated; the chemical shift of the marked peak is d = 6.4 ppm; for discussion see text.

The CP-MAS pulse sequence transfers magnetization from protons to the investigated nucleus in close proximity, in this case P, selectively enhancing the resonance signal (Hartmann and Hahn, 1962; Pines et al., 1973). The selective enhancement of the peak at 6.4 ppm in the CP-MAS spectra indicates that it is either a protonated or hydrogen-bonded phosphate species or a solid phosphate phase with protons in fixed crystallographic positions in close proximity to phosphate. This species further has a very uniform chemical environment, as indicated by the narrow line-width. A chemical shift of 6.6 ppm has been reported for crystalline Na_2HPO_4 by Turner and coworkers (Turner et al., 1986). Although sodium is present in PL (Moore et al., 1995b, 2000), the formation of a solid sodium phosphate of sufficient crystallinity to give a signal as narrow as the one observed in the spectra is very unlikely due to the heterogeneity of the material. Sodium phosphate is quite soluble, and it is not expected to precipitate in the presence of Ca, Mg and Fe, which are usually found in PL (Moore et al., 2000) and form less soluble solids with phosphate.

In alkaline extracts of soils and manures, the chemical shift of inorganic orthophosphate has been reported to be 6.3 - 6.5 ppm (e.g. (Cade-Menun et al., 2002; Cade-Menun and Preston, 1996; Leinweber et al., 1997)). The chemical shift of phosphate in aqueous solutions is sensitive to the pH and ranges from 0 ppm for H_3PO_4 through 8 ppm for PO_4^{3-} (Mortlock et al., 1993; Yoza et al., 1994), with HPO_4^{2-} appearing at about 6 ppm. Although the absolute water content of the samples used for the NMR experiments was considerably less in comparison with the PL *in situ* (30 – 35 %) due to drying at 65 °C, the water content of the samples (10 %) is sufficient for the physically

adsorbed phosphate to form hydrogen bonds with water bound to the surface of the organic material or inside the organic matrix. Unfortunately, no reference data exist for these phosphate species. Although it has not been established whether chemical shifts in solids can be directly compared to those in the liquid state, results from solution NMR experiments can be helpful in identifying species in PL. While P chemical shifts in crystalline and amorphous solid phases are influenced by the cations present for charge balance (Turner et al., 1986), this effect will be less pronounced for phosphate species in an organic matrix, due to complexation of the cations with the organic material and a considerably less uniform complexation environment for phosphate.

Based on the narrow line-width despite the complexity of the material, and on the chemical shift, it is therefore concluded that the signal at δ = 6.4 ppm corresponds to inorganic phosphate bound by hydrogen bonds to functional groups of the organic material or to physically adsorbed water. This interpretation is supported by the fact that the peak disappears upon extraction with water, which indicates that the species is readily water-soluble (compare Figure 29). In the following discussion, this phosphate fraction is referred to as being physically adsorbed.

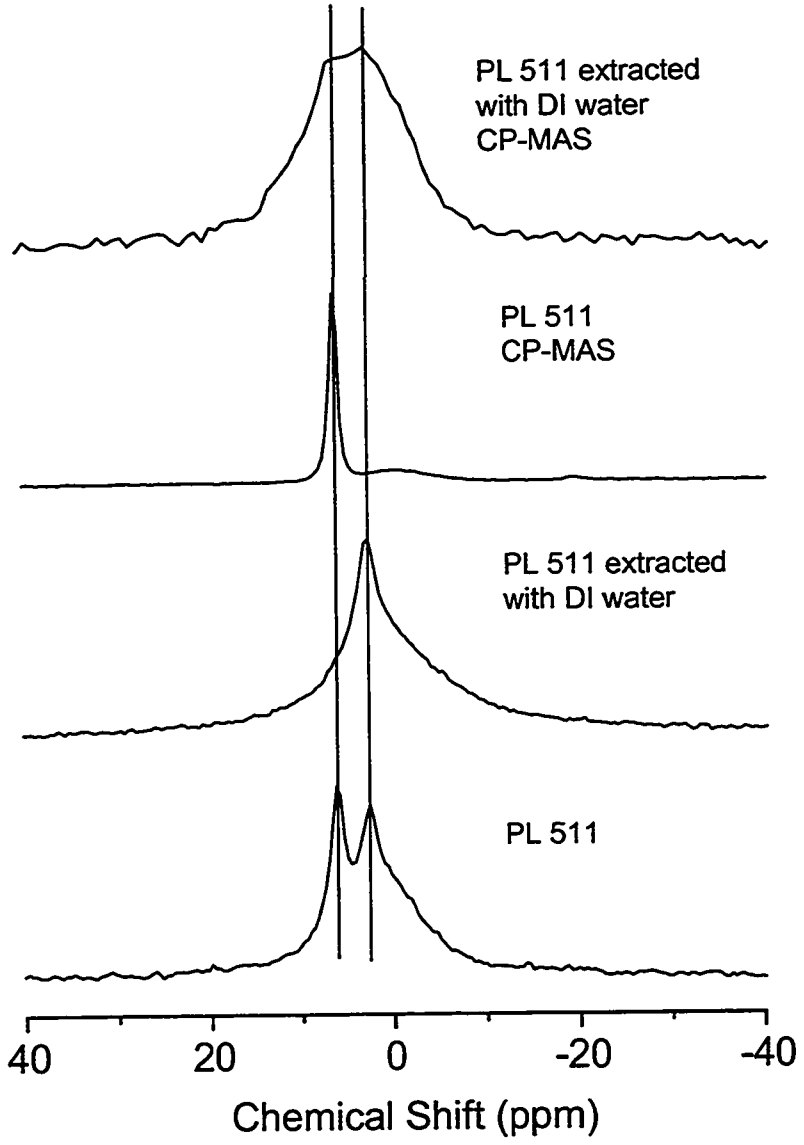

Figure 29. MAS NMR spectra of the unamended sample 511, before and after extraction with DI water; the chemical shifts of the marked peaks are: d = 6.4 ppm and 2.8 ppm; for discussion see text.

A phosphorus x-ray absorption near edge structure (XANES) spectroscopic study of the PL samples used in our study without prior drying indicated the presence of a calcium phosphate phase characterized as dicalcium phosphate (Peak et al., 2002). Similar to ^{31}P-NMR spectroscopy, P-XANES spectroscopy is element-specific and sensitive to the direct chemical environment of the investigated nucleus and can be used to analyze amorphous samples. As has been shown in chapter 2.5.1, both methods complement each other.

Chemical shifts for several crystalline calcium phosphate phases have been reported, ranging from -1.5 ppm and 0 ppm in anhydrous dicalcium phosphate (DCPA, monetite); 1.7 ppm in dicalcium phosphate dihydrate (DCPD, brushite); -0.2 ppm and 3.4 ppm in octacalcium phosphate (OCP); to 2.8 to 3.0 ppm in hydroxyl apatite (HAP) (Elliott, 1994; Rothwell et al., 1980) as well as in tribasic calcium phosphate (Turner et al., 1986). The chemical shift of a calcium phosphate phase formed at the surface of calcite in aqueous suspension was also reported at 3.0 ppm (Hinedi et al., 1992).

In general, the phosphate peaks shifted to more negative values are attributed to protonated phosphate anions, whereas the peaks shifted to more positive values are attributed to deprotonated species (Elliott, 1994), which corresponds to the trend of phosphate chemical shifts in aqueous solution. Phosphate species in calcium phosphate phases, which are characterized by chemical shifts of 2.8 ppm to 3.4 ppm, are referred to as being located in "apatitic" layers (Elliott, 1994), *i.e.* showing a local chemical environment similar to HAP. The signal of phosphate sorbed to calcite also appears at 2.8 ppm, which has been attributed to a carbonate apatite (Hinedi et al., 1992).

The less stable compounds DCP and OCP typically hydrolyze to eventually form HAP (Lindsay, 1979). Inskeep and Silvertooth (1988) and Grossl and Inskeep (1991), however, found that this process is retarded in the presence of various organic acids, such as citric acid, tannic acid or humic and fulvic acids. They suggested that organic acids adsorb to growth sites of the DCP and OCP crystals, efficiently inhibiting the transformation to HAP. Since PL contains a wide array of organic acids, the formation of a crystalline apatite is very unlikely.

Calcium carbonate forms under open atmosphere conditions when the pH of the litter increases after the initial decrease with addition of alum to the litter. Its recrystallization to calcite is, however, inhibited in the presence of organic acids (Hoch et al., 2000; Inskeep and Bloom, 1986), similar to the inhibition of HAP-crystallization. Any calcium carbonate phase in the litter is therefore expected to be amorphous, supplying a large surface area for phosphate sorption.

Since formation of crystalline HAP is not expected in the litter, the most likely calcium phosphate phases would therefore be a tribasic calcium phosphate ($Ca_3(PO_4)_2$) or a calcium phosphate surface precipitate on calcium carbonate (Hinedi et al., 1992).

Chemical shift values for magnesium phosphate phases have been published. The naturally occurring crystalline compounds Bobierrite ($Mg_3(PO_4)_2 \cdot 8H_2O$) and Newberyite ($MgHPO_4 \cdot 3\ H_2O$) have chemical shifts of d = 4.6 ppm and d = -7.2 ppm, respectively, and the amorphous compounds $Mg_3(PO_4)_2$ and $MgHPO_4$ have chemical shifts of d = 0.5 ppm and d = -2.4 ppm, respectively (Aramendía et al., 1998a, b). The crystalline magnesium phosphate phases and amorphous $MgHPO_4$ can be eliminated

because of the absence of resonance signals in the appropriate chemical shift range. Although amorphous $Mg_3(PO_4)_2$ can not be excluded, and is even likely to form, positive evidence can not be presented from the NMR spectra alone, because its NMR peak (d = 0.5 ppm) would be masked by the broad resonance at approximately 0 ppm.

Chemical shifts of various aluminum phosphate solids are reported in the literature (Bleam et al., 1989a, b; Duffy and van Loon, 1995; Hinedi et al., 1989b). Depending on crystallinity, water content, and degree of condensation, the phosphorus nuclei in these solids resonate between -7 and -30 ppm. Duffy and vanLoon (1995) reported downfield shifts for aluminum phosphate precipitates that had been calcined and had therefore a higher degree of condensation. These findings are corroborated by simulations of NMR spectra of aluminum phosphate glasses (Cody et al., 2001), which indicate that phosphate peaks shift to more negative values with increasing number of aluminum atoms bound. Furthermore, phosphorus peaks shift to more negative values with decreasing pH. These two trends occur simultaneously and are very likely to be indistinguishable from each other. The minerals wavellite ($Al_3(OH)_3(PO_4)_2 \cdot 5\ H_2O$) (Araki and Zoltai, 1968) and variscite ($AlPO_4 \cdot 2\ H_2O$) (Kniep et al., 1977), which were included in our study, had chemical shifts of d = -11 ppm and d = -19 ppm, respectively, in agreement with published values (Bleam et al., 1989b; Frossard et al., 1994). The chemical shift of Berlinite ($AlPO_4$) has been reported at -25 ppm (Bleam et al., 1989b).

Lacking any sharp peaks at chemical shifts below 0 ppm, the alum-amended PL samples clearly do not contain any crystalline aluminum phosphate species. The main difference between the spectra of the alum-amended and the unamended samples is an

additional broad peak centered between -4 and -10 ppm in the spectra of the former, which appears as a tailing on the negative side of the composite NMR signals. The broad line-width indicates that phosphate exists in this species in a distribution of chemical environments. The fact that this species is only present in the alum-amended samples indicates that it is probably an aluminum phosphate phase. Comparison with the model systems presented in the previous chapter indicates that this phase is probably phosphate adsorbed to aluminum hydroxide or an uncondensed aluminum phosphate phase such as a poorly ordered wavellite. This hypothesis was corroborated by a TRAPDOR experiment (see chapter 3.5.2).

At this point it is not yet possible to resolve the remaining complex resonances centered at about 0 ppm. They are possibly due to organic orthophosphate species with a range of chemical environments and molecular conformations, which cause the broadening of the signal. Furthermore, as mentioned before, the chemical shift of inorganic orthophosphate is influenced by the cations it is complexed with. Turner and coworkers (1986) found a linear correlation between chemical shift and the electronegativity of the cations in several metal phosphates, with the less electronegative metals shifting the phosphate peaks to more positive values. The same trend can be seen for an organic phosphate species in the spectra of sodium and calcium phytate (Figure 30). Those two compounds were included in our study because phytic acid is known to be contained in poultry litter (Taylor, 1965). Calcium phytate forms a crystalline phase with four magnetically non-equivalent phosphate groups and its NMR spectrum can accordingly be resolved into four different peaks. Although sodium phytate is a

crystalline phase as well, its phosphate groups are magnetically equivalent and can not be deconvoluted. The change of the cation from calcium to sodium also caused the peaks to shift to more positive values.

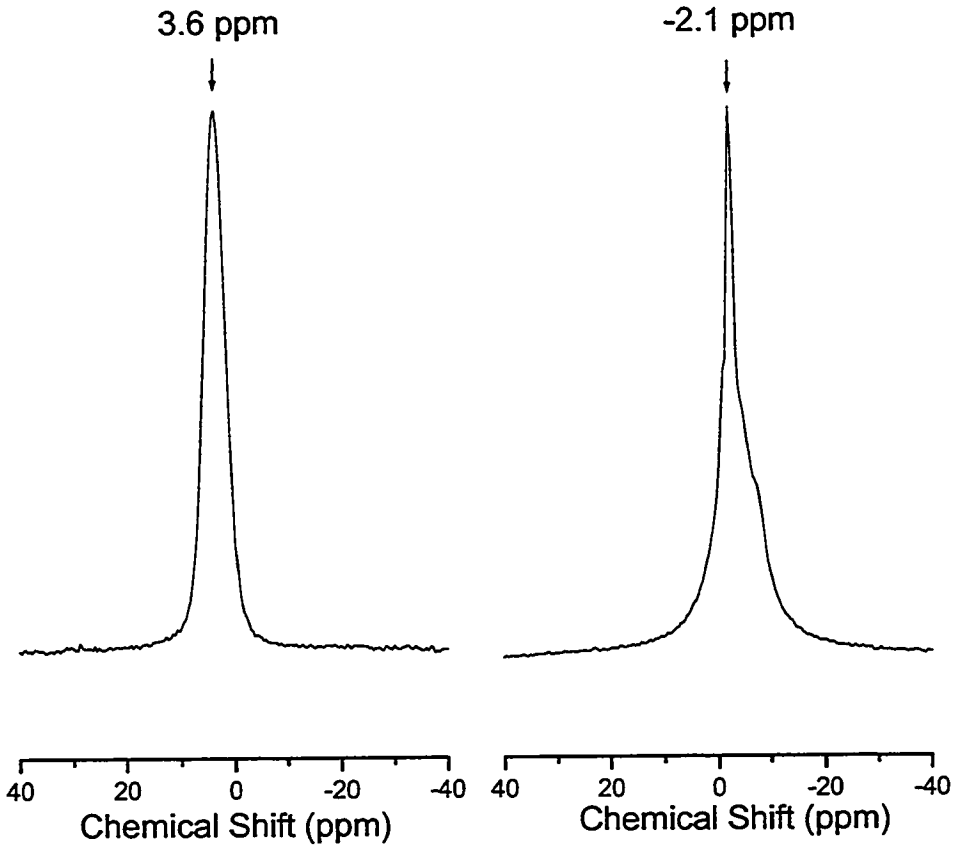

Figure 30. Single-pulse, proton-decoupled MAS NMR spectra of (left) sodium phytate and (right) calcium phytate.

The conclusions that can be drawn from these data are twofold: In the presence of a variety of cations, the organic orthophosphate species show broad, unresolved peaks. Furthermore, the presence of inorganic orthophosphate, which does not have a uniform

environment like the hydrogen-bonded species, but rather forms complexes with a wide variety of cations, can not be excluded.

In the single-pulse, proton decoupled ^{31}P-NMR spectra, the signal intensities, which are measured as the peak areas, are approximately proportional to the relative concentrations. For minor peaks, however, deconvolution is not as exact as for the major peaks in a spectrum, and care must therefore be taken when interpreting signal intensities of peaks of low intensity. In general, an error margin of ± 5 % of the combined signal intensity of all signals is assumed for the peak areas of the deconvoluted spectra.

In the spectra of the alum-amended PL samples (Figure 25), the peak attributed to phosphate adsorbed to aluminum hydroxide or to an uncondensed aluminum phosphate (-4 to -10 ppm) contributes between 25 % and 64 % to the overall peak intensities. This clearly shows that on average 40 ± 14 % of the total phosphate in the samples is bound in this manner and because of the strong covalent bond scarcely water-soluble.

The calcium phosphate phase, which is similarly insoluble in water, comprises on average 10 ± 5 % of the total P in both alum-amended and unamended PL. Significantly less of the calcium phosphate phase is present in alum-amended PL (7 ± 4 %) than in the unamended PL (14 ± 5 %).

Only a minor proportion can be clearly identified as weakly bound inorganic orthophosphate and is expected to be readily water-soluble. However, some of the unresolved organic and inorganic orthophosphate species are soluble as well. Since it is

impossible to deduce the exact proportion of these species, the quantitative solid-state NMR results can not be used to predict the soluble phosphate proportion.

The NMR spectra of the alum-amended PL samples indicate that most of the phosphate is distributed between a calcium phosphate phase and a combination of aluminum-bound phosphate species. A comparison with the phosphate speciation in the model system of phosphate sorbed to gibbsite and calcite, which was discussed in the previous chapter (see chapter 2.5.4), is therefore particularly informative. It was shown that phosphate in the competitive system gibbsite/ calcite is sorbed at low phosphate loadings and pH values comparable to PL predominantly as a binuclear, bidentate complex, possibly with calcium bound as a ternary complex. At elevated phosphate levels, a calcium phosphate surface precipitate on calcite rather than an aluminum phosphate surface precipitate is formed. This disagreement between the model system and the natural sample can be explained with the complexity of the litter: Precipitation of the aluminum hydroxide and the uncondensed aluminum phosphate, and sorption of phosphate to aluminum hydroxide and calcium carbonate occurs at the same time, as opposed to phosphate sorbing to crystalline materials.

These results show that solid-state ^{31}P NMR spectroscopy can be a valuable tool to identify some inorganic phosphate species in a heterogeneous material such as poultry litter. The resolution of organic phosphate species, on the other hand, is not possible. A combination of solid-state and liquid-state ^{31}P NMR spectroscopy seems therefore most promising for a more complete analysis of poultry litter that includes the organic species.

However accurate the P speciation of the PL samples by ^{31}P-NMR might be, it only shows a picture representative of the P transformations in alum-amended or unamended PL over a short time. These transformations are likely to continue during storage of the material and in PL-amended soils over a longer time scale than considered here. Depending on the properties of the soils where alum-amended PL is applied, the climate, the management practices, and whether the PL is incorporated or applied to the surface, the P species found will transform at different rates. Preliminary results from a study of the aging of PL are presented in chapter 3.5.3.

3.5.2. ^{31}P {^{27}Al} TRAPDOR experiments

Figure 31 shows the effect of the echo time on the signal intensities in the spectra of the standard sample. Clearly the relaxation time T_2 is shorter for variscite than it is for apatite, causing a faster signal loss. Figure 32 illustrates the increasing TRAPDOR effect with increasing dephasing time. However, signal intensity is lost due to both short T_2 and long $t_{dephasing}$. T_2 depends on a variety of parameters, e.g. temperature and crystallinity (Drago, 1992), and shorter relaxation times are expected for the more amorphous PL and sorption samples. In order to see a strong TRAPDOR effect while retaining signal intensity of the less ordered species, an echo time of t_{echo} = 0.8 ms and accordingly a dephasing time of $t_{dephasing}$ = 1.596 ms was chosen for subsequent TRAPDOR experiments.

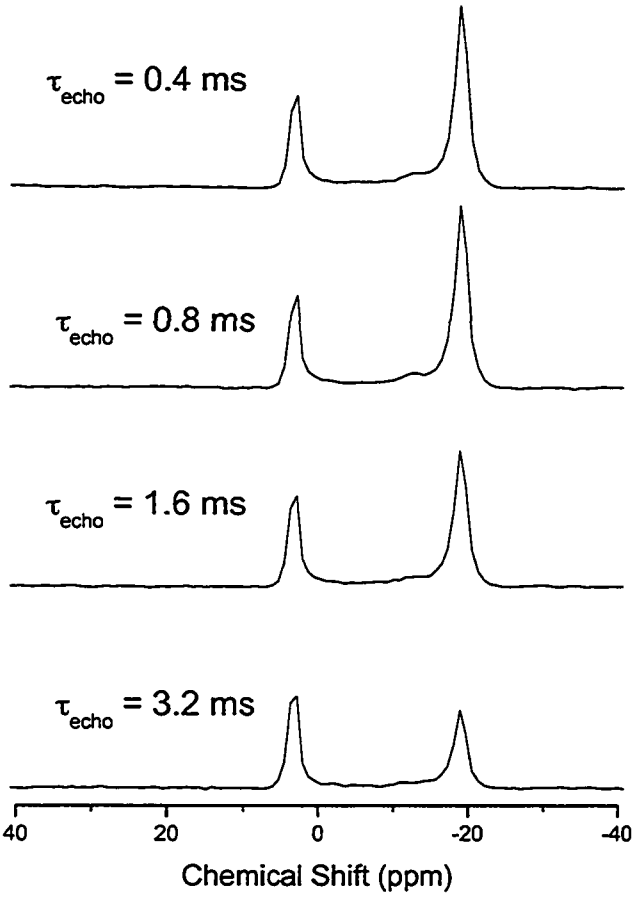

Figure 31. Effect of varying the echo time $t_{dephasing}$ from 0.4 to 3.2 ms. The species are hydroxyl-apatite (3.0 ppm) and variscite (-19.0 ppm); Parameters: 16 FIDs, 10 s relaxation delay, 3.7μs p/2-pulse, 7.4 μs p-pulse; the spectra are normalized with respect to the apatite peak.

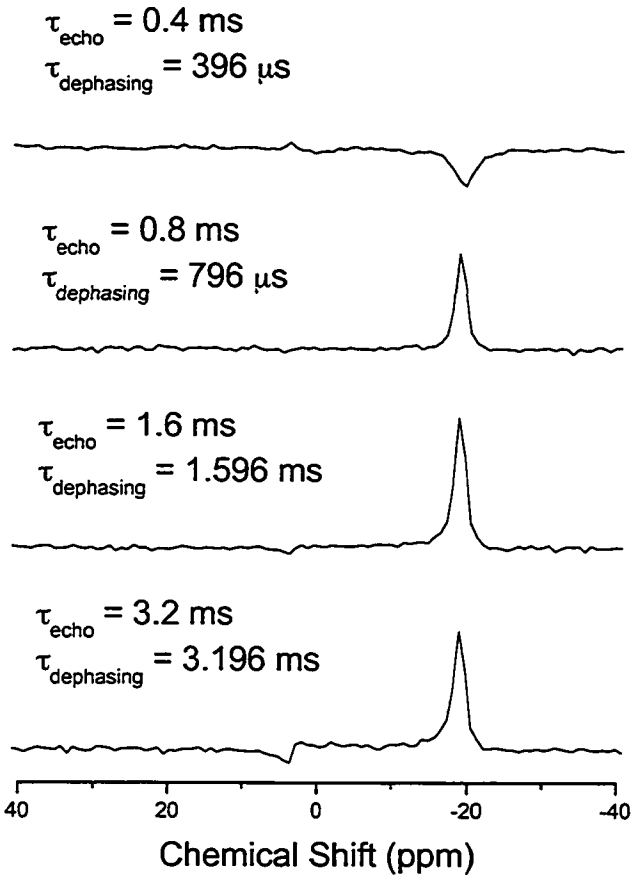

Figure 32. Difference spectra with various t_{echo} and $t_{dephasing}$. The species are hydroxylapatite (3.0 ppm) and variscite (-19.0 ppm). Parameters: 16 FIDs, 10 s relaxation delay, 3.7μs p/2-pulse, 7.4 μs p-pulse.

The fine fraction of PL sample 181 (<125 μm) was chosen for the TRAPDOR experiments because unlike the PL samples analyzed so far it had been stored at 4 °C and dried under mild conditions, and was therefore expected to retain the original speciation. As will be discussed in more detail in chapter 3.5.3, the P-species of PL samples stored at room temperature for over 6 months had changed toward more stable forms; particularly the fractions of the calcium phosphate phase and phosphate adsorbed to aluminum hydroxide had increased considerably.

The relevant NMR spectra are presented in Figure 33. The top-most spectrum shows the quantitative single-pulse, proton-decoupled spectrum. The peak at 3.4 ppm has been identified as a calcium phosphate phase, most probably an octacalcium phosphate surface precipitate on calcite. A detailed assignment of the peaks convoluted in the broad signal is not possible without further identification of, for example, Al-P connectivities.

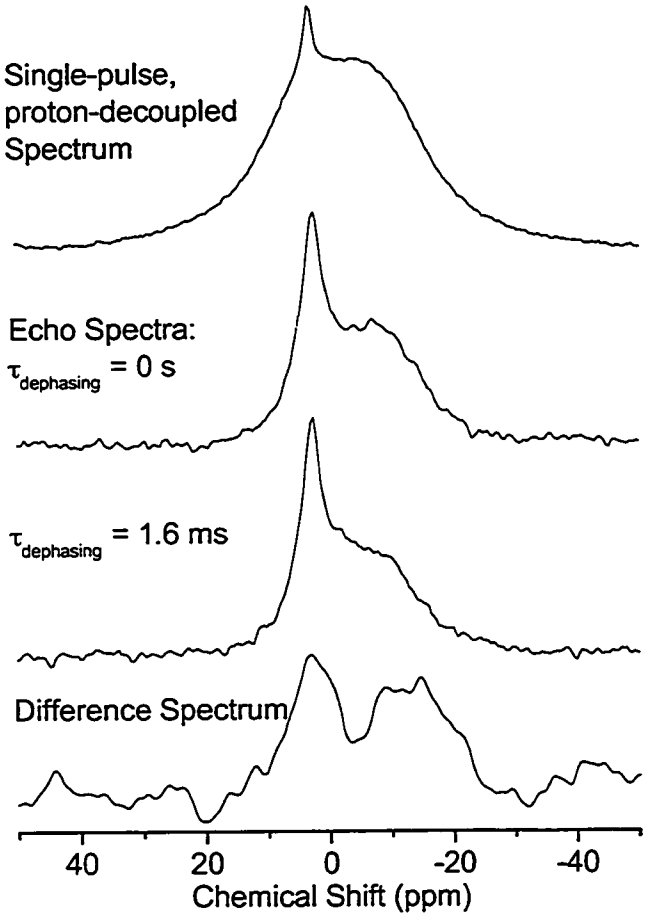

Figure 33. MAS-NMR spectra of PL sample 181 (fraction <125 μm, 2.0 % P). Top: Single-pulse, proton-decoupled spectrum (7.0 kHz ± 2 Hz spinning speed, 512 FIDs, 5.5 μs p/2-pulse, 60 s relaxation delay). Middle: Echo spectra (10. 0 kHz ± 5 Hz spinning speed, 1024 FIDs, 3.45 μs p/2-pulse, 6.9 μs p-pulse, and 30 s relaxation delay). Bottom: Difference of the echo spectra.

The echo-spectra with t_{echo} = 0.8 ms are shown in the middle. Comparison with the single-pulse spectrum shows that the broad, unresolved peak has lost intensity in relation to the calcium phosphate peak, which indicates a much shorter transversal relaxation time T_2. Furthermore, the convoluted peaks with d > 0 ppm have a shorter T_2 compared with the peaks with d < 0 ppm. Comparison of the echo spectrum without dephasing with the one with $t_{dephasing}$ = 1.596 ms reveals a reduction in peak height upon dephasing, which is shown more clearly in the difference spectrum. The broad peak is centered at d = -14 ppm, which indicates a heterogeneous chemical environment of the phosphate anions associated with aluminum. The chemical shift region is characteristic for phosphate species bound to one or two aluminum cations via oxygen bridges and the mineral wavellite. Possible structures are mononuclear and binuclear inner-sphere surface complexes of phosphate on aluminum hydroxide, and an uncondensed aluminum phosphate polymer, in which one phosphate anion is bound to two aluminum cations, similar to the wavellite structure. Since the Al-P connectivity differs only marginally between the surface complexes and the uncondensed polymer, only a slight difference in solubility of phosphate is expected.

Interestingly, another broad peak is observed in the difference spectrum, centered at d = 3 ppm. Apparently, Al-P connectivities also exist in the calcium phosphate phase, probably at the interface with aluminum hydroxide polymers or as ternary complexes of aluminum at the surface. This demonstrates once more the heterogeneity of the material and the broad range of possible phosphate species in PL, which make an approach using several complementary, molecular spectroscopic techniques necessary.

3.5.3. Effect of storage on the NMR spectra of PL

Single-pulse MAS NMR experiments were repeated with two PL samples, one unamended and one alum-amended, after seven months of storage at room temperature. The spectra before and after storage are shown in Figure 34. The spectrum of the alum-amended sample PL 125 recorded in January exhibits the previously discussed four overlapping signals: physically bound orthophosphate (6.4 ppm), a calcium phosphate phase (3 ppm), unresolved organic and inorganic phosphate species (broad signal at about 0 ppm), and phosphate associated with aluminum, either adsorbed to aluminum hydroxide or as an uncondensed aluminum phosphate phase such as a poorly ordered wavellite ((-4) - (-10) ppm). After seven months of storing the sample at room temperature, the signal of the physically bound phosphate has completely disappeared, while the signal of the calcium phosphate phase has increased relative to the other signals. Furthermore, the broad signal of phosphate associated with aluminum has become more distinct. A shift of the signal of the calcium phosphate phase from 3.0 ppm to 3.4 ppm can also be observed. This might be indicative of a transformation to octacalcium phosphate (OCP) (Elliott, 1994), but the change is small compared to the margin of error.

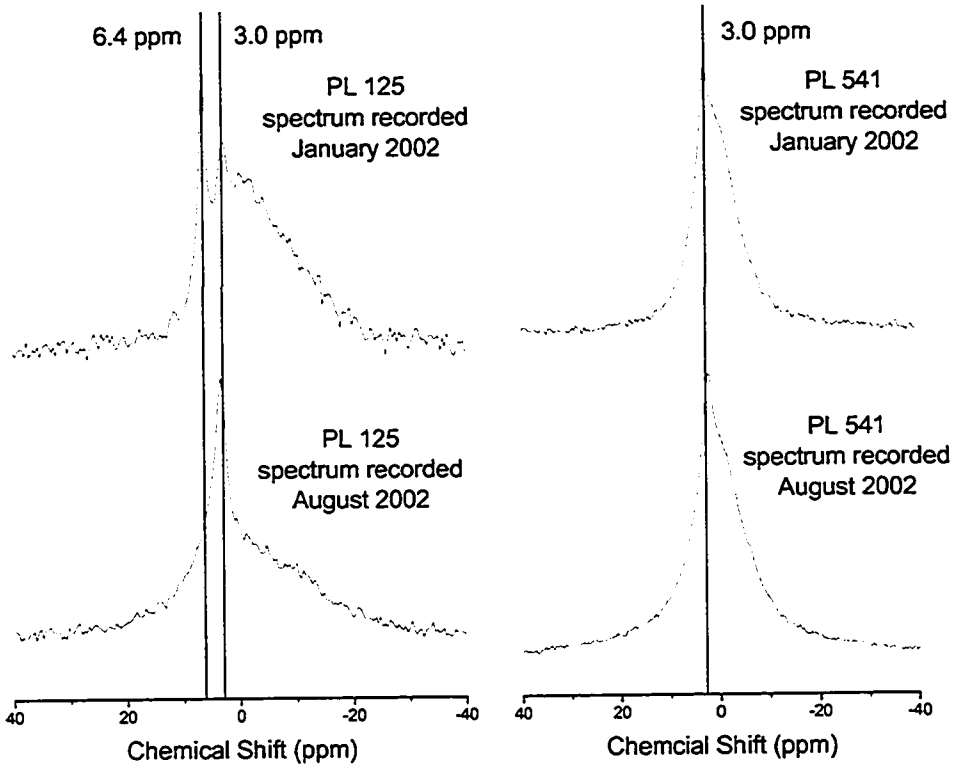

Figure 34. Single-pulse MAS NMR spectra of samples PL 125 (left column) and PL 541 (right column) before and after seven months of storage time.

The spectrum of the unamended sample PL 541 can be deconvoluted into the same two peaks before and after storage: A calcium phosphate phase (3.0 ppm) and a mixture of unresolved organic and inorganic phosphate species (broad signal at about 0 ppm). However, storage changes their ratio, increasing the signal of the calcium phosphate phase in comparison with the broad residual peak. Furthermore, the peak assigned to a calcium phosphate phase shifts upfield to 2.3 ppm.

Both sets of spectra indicate an increase of the more stabile species calcium phosphate and phosphate associated with aluminum over time, while the more labile species (physically bound phosphate and unresolved organic and inorganic phosphate) decrease. These results imply that mere storage of the material can lead to a reduction of water-soluble phosphate in both unamended and alum-amended PL. The results are, however, preliminary. A further investigation of the transformations of alum-amended PL over longer time scales under controlled conditions (temperature, humidity, suppression of microbial processes) is needed to make scientifically sound recommendations on the use of alum-amended PL in agriculture and its contribution towards a more environmentally sustainable poultry industry.

3.5.4. Combination of sequential chemical extraction of poultry litter with ^{31}P-NMR spectroscopy

The amounts of phosphorus, calcium, iron, and aluminum extracted from the two size fractions of PL sample 181 with each extraction step are presented in Figure 35 through Figure 38. Most of the phosphorus is acid-extractable or recalcitrant to extraction, but phosphorus is released during each extraction step. 3.1 mg/g and 3.4 mg/g of phosphorus (17 % and 15 %) are extracted from the coarse and the fine fraction with deionized water and sodium bicarbonate, corresponding to the presumably plant-available phosphorus fraction (Dou et al., 2000). Small amounts of both calcium (Figure 36) and iron (note that the scale in Figure 37 differs by three orders of magnitude from the scales for phosphorus, calcium and aluminum) are concomitantly released. This indicates that calcium and iron in these fractions were either not associated with phosphorus, e.g. as complexes with organic matter and as exchangeable calcium, or present as colloidal calcium and iron phosphate, which did not settle during centrifugation and passed through the filter.

This sample had received alum and a significant amount of phosphorus was therefore expected to be associated with aluminum. Indeed, 1.5 mg/g and 4.5 mg/g of phosphorus (8.4 % and 19 %) are extracted from the coarse and the fine fraction, respectively, by sodium hydroxide, concomitant with 7.2 mg/g and 29 mg/g of aluminum (Figure 38), respectively. More aluminum is present in the fine fraction than in the coarse fraction, which indicates that most of the aluminum hydroxide formed by hydrolysis of alum is present as clay-size particles. The fact that much more aluminum

than phosphorus is released by sodium hydroxide indicates that the fraction of aluminum associated with phosphorus makes up only a small part of the total amount of aluminum in the samples, supporting the hypothesis that aluminum hydroxide forms in the alum-amended litter. The aluminum to phosphorus ratio of the uncondensed aluminum phosphate mineral wavellite (1.3) is lower than that of the sodium hydroxide extractable fraction (4.8 and 6.4 in the coarse and fine fraction, respectively).

These calculations are however of no practical value since significant amounts of aluminum are also extracted by hydrochloric acid (Figure 38). This acid-extractable aluminum fraction is either a different aluminum phase or aluminum hydroxide that was not extracted by sodium hydroxide due to saturation. No attempt was made to exhaustively extract each fraction by repeated treatment with the extractant, a very time-consuming procedure developed by Dou and coworkers (2000).

Most of the calcium in the samples is acid-extractable; some however is present in the residual fraction (Figure 36). Similar results are seen for iron, with an even higher proportion being recalcitrant to extraction. This has been attributed to insoluble or only slowly soluble crystalline calcium and iron phosphate minerals (Dou et al., 2000; Hedley et al., 1982). The major part of acid-extractable Ca can be attributed to calcium carbonate, which is contained in poultry feed. Ca not absorbed during digestion precipitates as calcium carbonate under open atmosphere conditions and acts as a sorbent for phosphate (Kuo and Lotse, 1972; Griffin and Jurinak, 1973; 1974; Hinedi et al., 1992). Consequently, 37 % and 39 % of P are concomitantly extracted. The insoluble

phosphorus not associated with metals has been attributed to occluded and complex organic phosphate species, such as ribonucleic acids (Hedley et al., 1982).

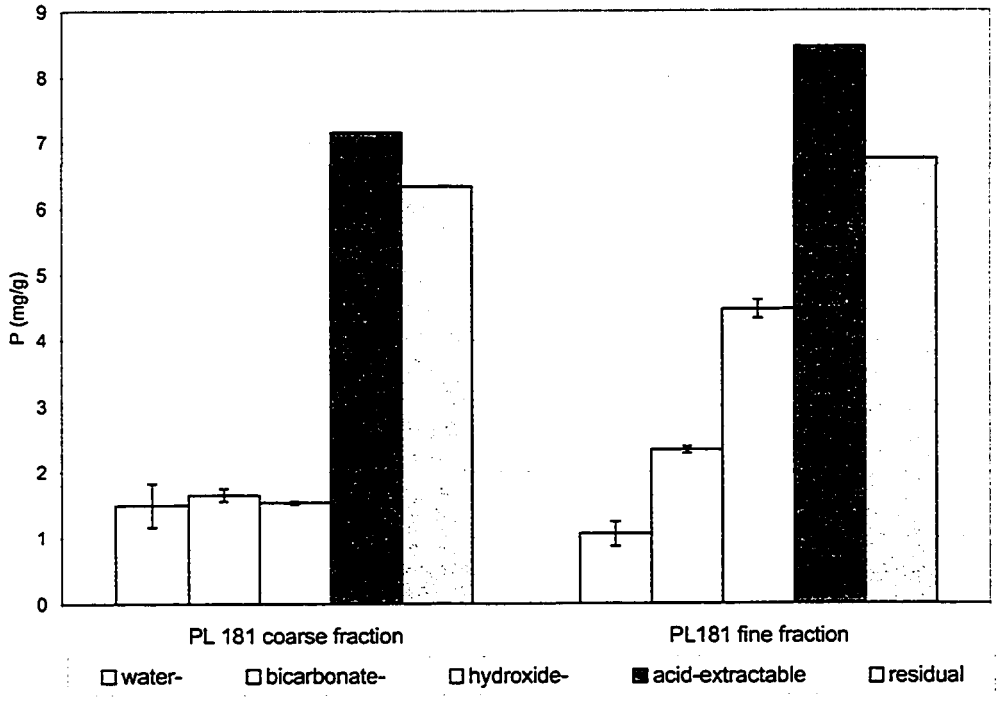

Figure 35. Phosphate fractions in the alum-amended PL sample 181.

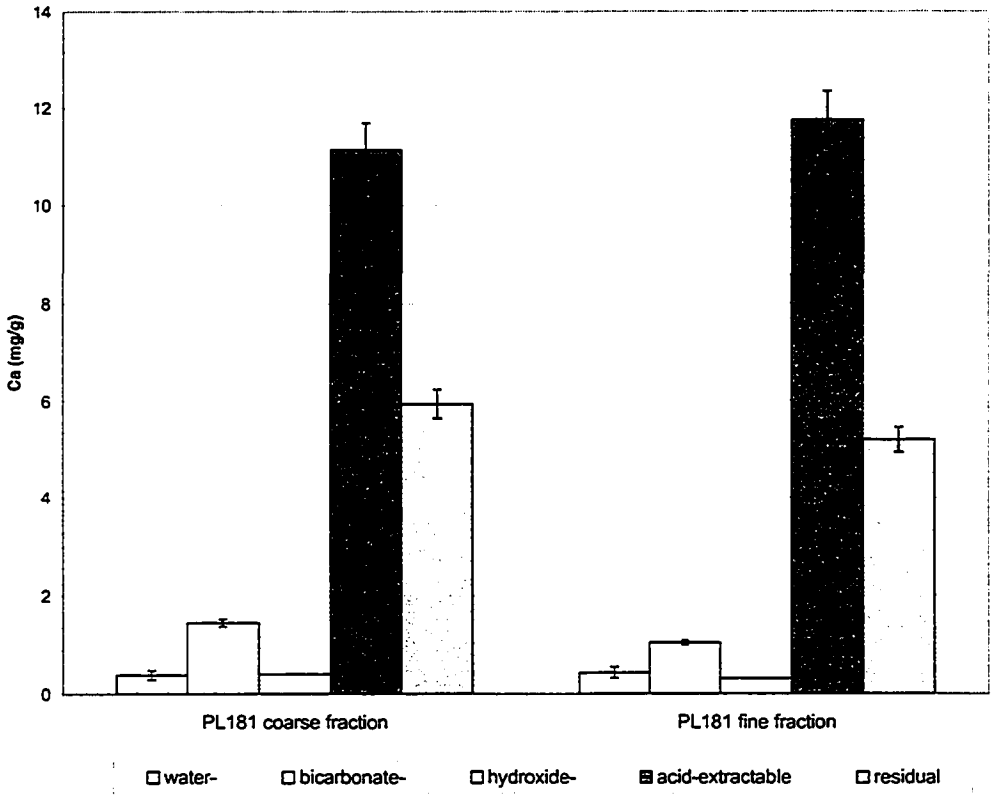

Figure 36. Calcium fractions in the alum-amended PL sample 181.

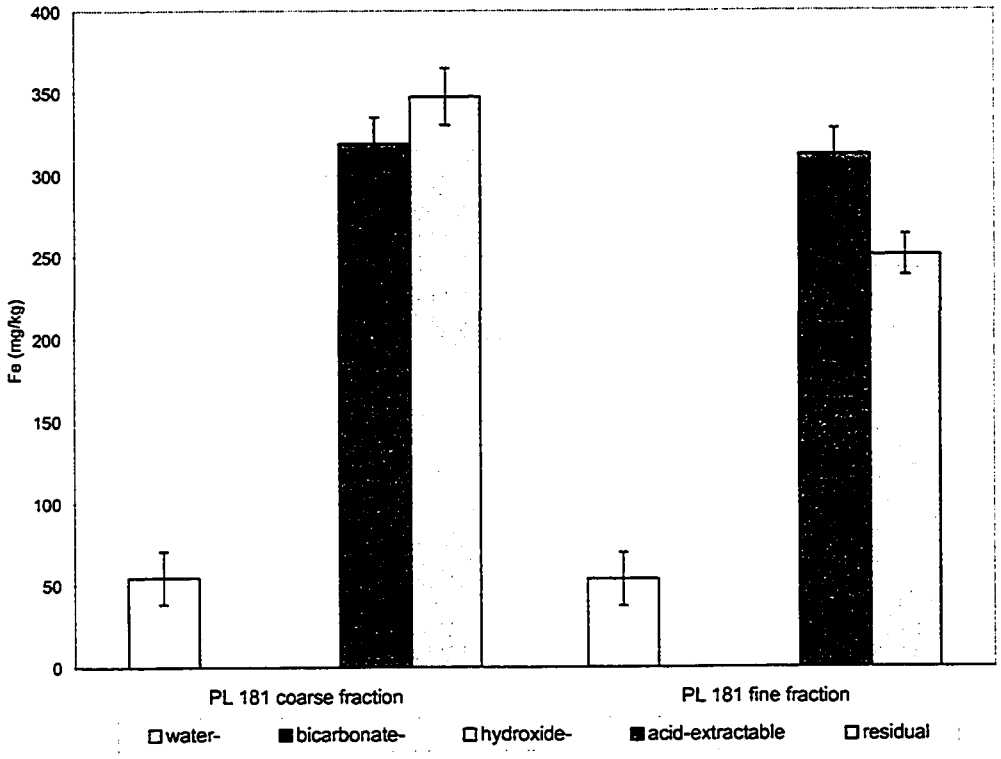

Figure 37. Iron fractions in the alum-amended PL sample 181.

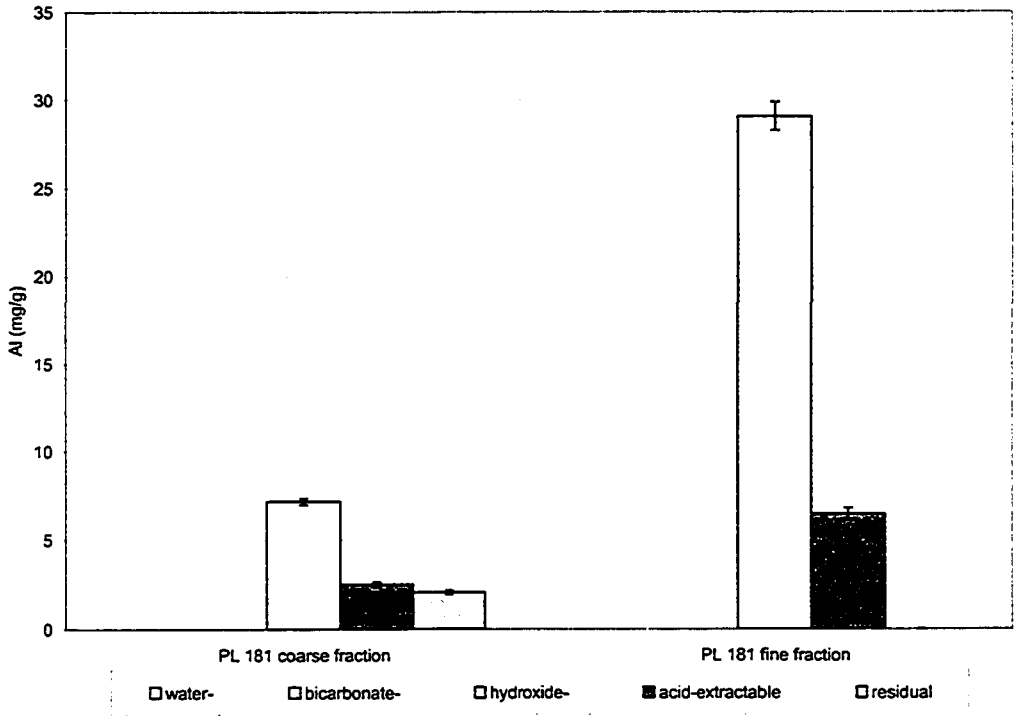

Figure 38. Aluminum fractions in the alum-amended PL sample 181.

The ^{31}P-NMR spectra of the sequentially extracted coarse and fine fraction of PL sample 181 are presented in Figure 39 and Figure 40, respectively. The phosphorus concentrations of the samples after extraction with hydrochloric acid were too low to give spectra of good quality in an acceptable experiment time. Of these spectra only the CP-MAS NMR spectrum of the fine fraction after acid-extraction is therefore presented in Figure 41.

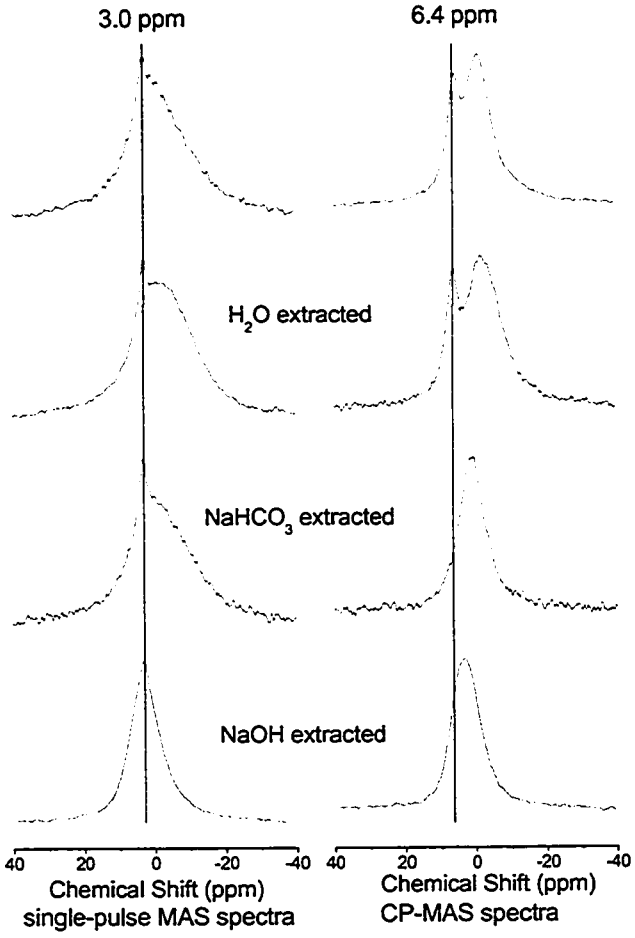

Figure 39. Single-pulse, proton-decoupled MAS NMR spectra (left column) and CP-MAS spectra (right column) of the coarse fraction of PL 181. Samples are sequentially extracted from top to bottom up to the extraction step indicated.

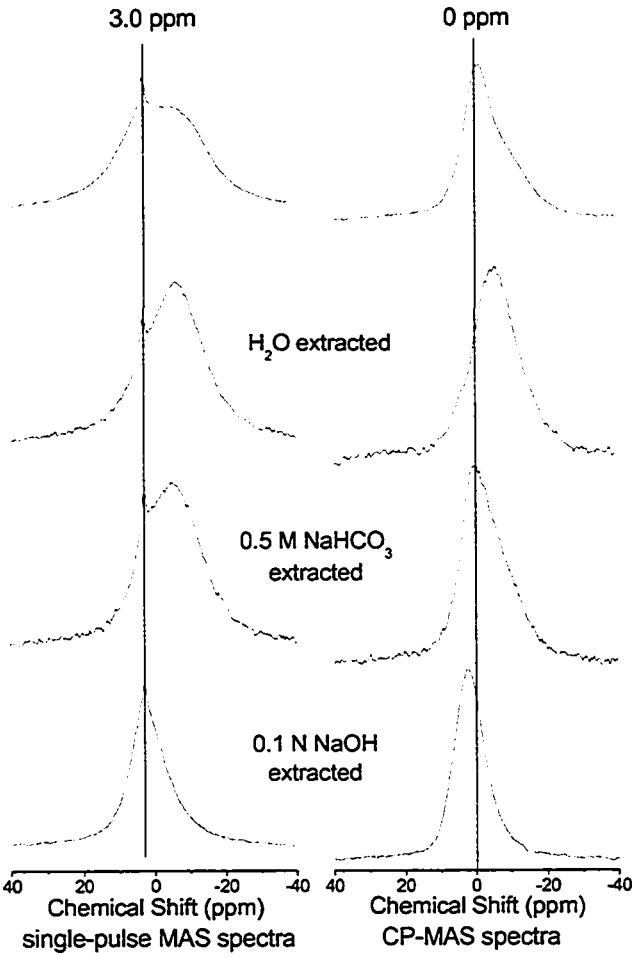

Figure 40. Single-pulse, proton-decoupled MAS NMR spectra (left column) and CP-MAS spectra (right column) of the fine fraction of PL 181. Samples are sequentially extracted from top to bottom up to the extraction step indicated.

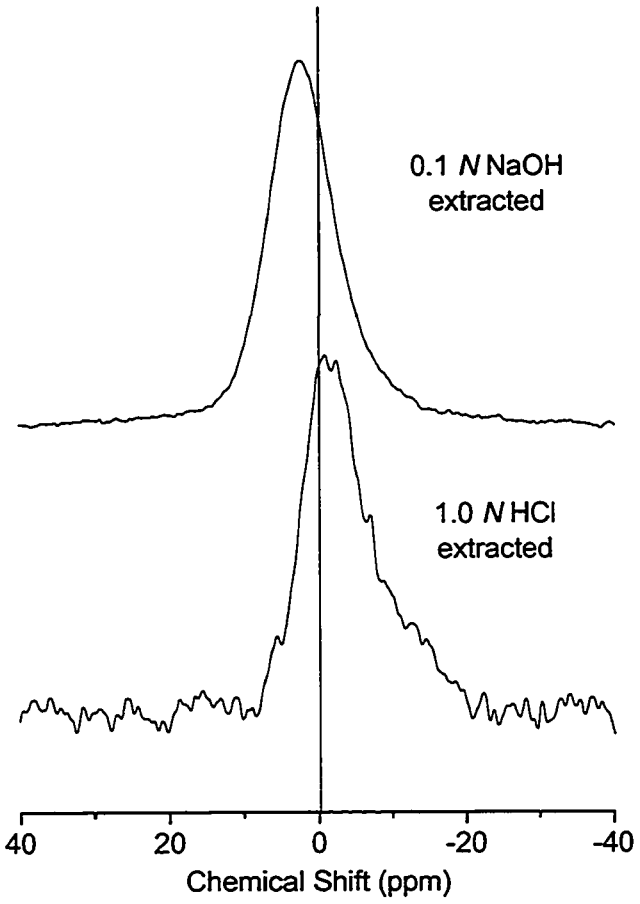

Figure 41. CP-MAS ^{31}P-NMR spectra of the fine fraction of PL 181 after extraction with: Top 0.1 *N* NaOH; Bottom 1.0 *N* HCl.

The spectra of the unextracted samples are similar to the spectra observed earlier (Figure 24, Figure 25, Figure 27, and Figure 28) in that they show complex unresolved resonances. The single-pulse MAS spectra contain a sharp peak at ca. 3.0 ppm that can be attributed to tribasic calcium phosphate. This peak is suppressed in the CP-MAS spectra. The CP-MAS spectrum of the coarse fraction of PL 181 contains a peak at 6.4 ppm, which was attributed to phosphate bound by hydrogen bonds to water molecules in

the sample. Interestingly, this peak does not disappear upon extraction with deionized water, but is only extracted by sodium bicarbonate.

There are several possible explanations for this behavior, the most obvious one being that the assignment is incorrect. Another explanation is that this phosphate species is occluded, either in remnants of biological compartments, such as plant or microbial cells, or in humified organic matter that is not dispersed in deionized water alone. The fact that the extractant with a high ionic strength removes this species favors the latter explanation. The fact that humified organic matter was extracted by both extractants, evidenced by the dark color of the extract, favors the former explanation.

In general, the NMR spectra of the extracted samples confirm some of the molecular assignments of the macroscopic phosphorus fractionation. Phosphate associated with aluminum in the fine fraction, which can be detected as a shoulder on the upfield side of the broad peak in the right column of Figure 40, is extracted by sodium hydroxide. More phosphate is associated with aluminum in the fine fraction than in the coarse fraction, because the NMR spectra of the coarse fraction are lacking the peak in the corresponding chemical shift region. This agrees with the observation made in the macroscopic fractionation that less aluminum and phosphorus are extracted by sodium hydroxide from the coarse fraction.

Furthermore, the calcium phosphate phase is present in all extracted samples (left column of Figure 39 and Figure 40) and is only removed by hydrochloric acid (Figure 41). The peak of the calcium phosphate phase is suppressed in the CP-MAS NMR spectra and not as sharp as in the single-pulse spectra, but the shift to more negative

values is clearly visible in the bottom spectra of Figure 41. The CP-MAS NMR spectrum of the sample after extraction further reveals that the residual phosphorus fraction contains a rather uniform chemical species, as evidenced by the narrow peak.

Extraction of the samples with deionized water narrows the complex peaks in the NMR spectra. Since only a small fraction of phosphorus was removed during this step, this indicates that removal of soluble metal cations has simplified the chemical environment of both inorganic and organic phosphate. Further extraction with sodium bicarbonate and especially so with sodium hydroxide shifts the peaks to more positive values, centering them on the calcium phosphate peak at 3.0 ppm in the single-pulse MAS spectra and slightly lower values in the CP-MAS spectra. These extractants efficiently remove organic phosphate compounds and inorganic orthophosphate not bound in a solid phase (Cade-Menun and Preston, 1996).

Deconvolution of the signals in the single-pulse spectra was not possible to the extent achieved previously. Only the peak at d = 3.0 ppm was reproducible. Therefore only the fraction of calcium phosphate was determined from the single-pulse ^{31}P NMR spectra of the residues of the coarse and fine fractions after each extraction step (Table 4). The expected enrichment of the calcium phosphate phase during the course of the extraction is only observed in the coarse fraction. The changes in both fractions, however, are well inside the error margin (± 5 %) and therefore not significant.

Table 4. Determination of the calcium phosphate contents by 31P-NMR

	Proportion of calcium phosphate[a] (%)[b]	
	PL 181 (125 μm - 420 μm)	PL 181 (<125 μm)
Before extraction	4.3	3.6
H_2O-extracted	4.9	2.7
$NaHCO_3$-extracted	7.3	4.4
NaOH-extracted	8.8	3.2

The acid-extractable phosphate fraction, which presumably contains predominantly calcium phosphate, was 39 % and 37 % in the coarse and fine fractions, respectively. The calcium phosphate content determined by ^{31}P NMR, however, is 4.3 % and 3.6 %, respectively. Clearly, sequential chemical extraction overestimates the calcium phosphate content by one order of magnitude. Possible acid-extractable species that were not accounted for by ^{31}P-NMR are complexes of phytic acid (inositol hexakisphosphate) with a variety of metal cations.

Since poultry is lacking the enzymes necessary to hydrolyze the phytic acid contained in the grain that makes up most of its diet, poultry manure and litter have therefore long been known to contain phytic acid (Taylor, 1965). Calcium and transition metal cations form complexes with phytate which are only soluble at low pH values

[a] Determined as the fraction that the peak at d = 3.0 ppm occupies of the total signal-area.
[b] Estimated error range: ± 5 %.

(Bedot-Brigaud et al., 1999; Seaman et al., 2003). Due to the multitude of metals present in the litter (Moore et al., 2000; Moore et al., 1995a), no single complex is formed with both orthophosphate and phytate and consequently only a broad, unresolved resonance was observed in the ^{31}P-NMR spectra. The acid-extractable fraction therefore probably also contains phytic acid.

In conclusion, these results verified the assumption that aluminum and calcium phosphate phases are mostly extracted by sodium hydroxide and hydrochloric acid, respectively. Aluminum phosphate phases are, however, present even after extraction with sodium hydroxide, as evidenced by the elevated concentrations of aluminum in the acid-extract and the peaks in the chemical shift range of d = -5 to -20 ppm in the NMR spectra of the residues after extraction with 0.1 *N* NaOH and 1.0 *N* HCl. A more thorough, repeated extraction is therefore necessary for a complete assessment of aluminum-associated phosphate species. Calcium phosphate species, on the other hand, are overestimated by the extraction sequence due to extraction of phytate at low pH values. Although chemical sequential extraction is a valuable tool to assess phosphate fractions of differing availability, it is inadmissible to draw conclusions about phosphate species in the material extracted.

IMPLICATIONS FOR FUTURE RESEARCH NEEDS

Chapter 2 demonstrated the use of a combination of spectroscopic and macroscopic techniques to investigate phosphate sorption in systems simulating natural environments. The results offer several starting points for further explorations. One important aspect about the fate and mobility of phosphate in soil environments is the remobilization of sorbed phosphate and an investigation of phosphate desorption from the model systems studied here will give insight in its dependence on reaction conditions, such as pH, reaction time, or co-adsorbing or competing ions. Solid-state ^{31}P NMR spectroscopy will allow a better understanding of the mobility of the phosphate species observed. Chapter 2.5.4 above showed that the mechanism of phosphate sorption in systems containing several sorbents differs from that in simpler systems. This has important implications for the applicability of the results to natural environments, because of the presence of solid phases competing for phosphate in soils (calcite, aluminum hydroxides, iron (oxy)hydroxides, etc.). Sorption and particularly desorption in mixed solid systems certainly needs closer investigation.

Few solid-state ^{31}P NMR spectroscopic studies of whole soils have been published so far (McDowell et al., 2002; 2003), and it has been shown that the application of solid-state ^{31}P NMR spectroscopy to whole soils or size fractions offers challenges and has its limitations but is not impossible. The results of this work can provide a data base to aid in the interpretation of solid-state NMR data and may be an incentive for future NMR studies of whole soils of different origin, under different management practices or climates.

Solid-state ^{31}P NMR spectroscopy has been shown to be a versatile tool for the analysis of animal wastes, especially in combination with chemical extraction. This work has shed some light on P-species in natural and alum-amended poultry litter samples and demonstrates the differences in litter chemistry. It has also been shown, however preliminarily, that some of the labile species are transformed to more stable phases (aluminum phosphate and calcium phosphate phases) with storage. The chemical transformations over time under different storage conditions (composting, dry storage, etc.) are of great importance under economical and ecological aspects (Dao et al., 2001; Frossard et al., 2002; Sharpley and Moyer, 2000; Sinaj et al., 2002). Conversion of labile to stable phosphate species reduces the risk of loss via erosion and run-off after field application. Composting leads to a reduction in weight and to fixation of a number of nutrients, increasing the value of the litter as a fertilizer and making storage and transport easier. A more detailed investigation of the effects of storage on the organic and inorganic phosphorus species is desirable and can be accomplished using solid-state ^{31}P NMR (inorganic P-species) and extraction followed by liquid-state ^{31}P NMR (organic P-species).

BIBLIOGRAPHY

Amelung, W., Rodionov, A., Urusevskaja, I. S., Haumaier, L., and Zech, W. (2001). Forms of organic phosphorus in zonal steppe soils of Russia assessed by ^{31}P NMR. *Geoderma* **103**, 335-350.

Anderson, S. J., Sanders, K. E., and Steyer, K. J. (1996). Effect of Colloidal Goethite and Kaolinite on Colorimetric Phosphate Analysis. *Journal of Environmental Quality* **25**, 1332 - 1338.

Arai, Y., and Sparks, D. L. (2001). ATR-FTIR Spectroscopic Investigation on Phosphate Adsorption Mechanisms at the Ferrihydrite-Water Interface. *Journal of Colloid and Interface Science* **241**, 317-326.

Araki, T., and Zoltai, T. (1968). The crystal structure of wavellite. *Zeitschrift für Kristallographie* **127**, 21-33.

Aramendía, M. A., Borau, V., Jiménez, C., Marinas, J. M., Romero, F. J., and Ruiz, J. R. (1998a). Characterization by XRD, DRIFT, and MAS NMR spectroscopies of a $Mg_2P_2O_7$ catalyst. *Journal of Colloid and Interface Science* **202**, 456-461.

Aramendía, M. A., Borau, V., Jiménez, C., Marinas, J. M., Romero, F. J., and Ruiz, J. R. (1998b). XRD and solid-state NMR study of magnesium oxide-magnesium orthophosphate systems. *Journal of Solid State Chemistry* **135**, 96-102.

Barrow, N. J. (1983a). A mechanistic model for describing the sorption and desorption of phosphate by soil. *Journal of Soil Science* **34**, 733 - 750.

Barrow, N. J. (1983b). On the reversibility of phosphate sorption by soils. *Journal of Soil Science* **34**, 751 - 758.

Barrow, N. J. (1984). Modelling the effects of pH on phosphate sorption by soils. *Journal of Soil Science* **35**, 283 - 297.

Bertsch, P. M., and Hunter, D. B. (2001). Applications of Synchrotron-Based X-ray Microprobes. *Chemical Reviews* **101**, 1809-1842.

Bleam, W. F., Pfeffer, P. E., and Freye, J. S. (1989a). ^{31}P and ^{27}Al solid-state nuclear magnetic resonance study of taranakite. *Physics and Chemistry of Minerals* **16**, 809 - 816.

Bleam, W. F., Pfeffer, P. E., and Freye, J. S. (1989b). ^{31}P solid state nuclear magnetic resonance spectroscopy of aluminum phosphate minerals. *Physics and Chemistry of Minerals* **16**, 455 - 464.

Bleam, W. F., Pfeffer, P. E., Goldberg, S., Taylor, R. W., and Dudley, R. (1991). A ^{31}P solid-state nuclear magnetic resonance study of phosphate adsorbtion at the boehmite/ aqueous solution interface. *Langmuir* **7**, 1702 - 1712.

Blumberg, W. E. (1960). Nuclear spin-lattice relaxation caused by paramagnetic impurities. *Physical Review* **119**, 79-84.

Bolan, N. S., Barrow, N. J., and Posner, A. M. (1985). Describing the effect of time on sorption of phosphate by iron and aluminum oxides. *Journal of Soil Science* **36**, 187 - 197.

Burkholder, J. M., and Glasgow Jr, H. B. (1997). *Pfiesteria piscicida* and other *Pfiesteria*-like dinoflagellates: Behavior, impacts, and environmental controls. *Limnology and Oceanography* **42**, 1052-1075.

Burkholder, J. M., Mallin, M. A., Glasgow Jr, H. B., Larsen, L. M., McIver, M. R., Shank, C., Deamer-Melia, N., Briley, D. S., Springer, J., Touchette, B. W., and Hannon, E. K. (1997). Impacts to a coastal river and estuary from rupture of a large swine waste holding lagoon. *Journal of Environmental Quality* **26**, 1451-1466.

Burkholder, J. M., Noga, E. J., Hobbs, C. H., and Glasgow Jr, H. B. (1992). New 'phantom' dinoflagellate is the causative agent of major estuarine fish kills. *Nature* **358**, 407-410.

Cade-Menun, B. J., Liu, C. W., Nunlist, R., and McColl, J. G. (2002). Soil and litter phosphorus-31 nuclear magnetic resonance spectroscopy: Extractants, metals, and phosphate relaxation times. *Journal of Environmental Quality* **31**, 457-465.

Cade-Menun, B. J., and Preston, C. M. (1996). A Comparison of Soil Extraction Procedures for ^{31}P NMR Spectroscopy. *Soil Science* **161**, 770-785.

Castro, B., and Torrent, J. (1998). Phosphate sorption by calcareous vertisol and inceptisols as evaluated from extended P-sorption curves. *European Journal of Soil Science* **49**, 661-667.

Christoph, G. G., Corbato, C. E., Hofmann, D. A., and Tettenhorst, R. T. (1979). Crystal-structure of boehmite. *Clays and Clay Minerals* **27**, 81-86.

Cody, G. D., Mysen, B., Saghi-Szabo, G., and Tossell, J. A. (2001). Silicate-phosphate interactions in silicate glasses and melts: I. A multinuclear (^{27}Al, ^{29}Si, ^{31}P) MAS

NMR and ab initio chemical shielding (^{31}P) study of phosphorous speciation in silicate glasses. *Geochimica et Cosmochimica Acta* **65**, 2395-2411.

Condron, L. M., Goh, K. M., and Newman, R. H. (1985). Nature and distribution of soil phosphorus as revealed by a sequential extraction method followed by ^{31}P nuclear magnetic resonance analysis. *Journal of Soil Science* **36**, 199-207.

Crouse, D. A., Sierzputowska-Gracz, H., and Mikkelsen, R. L. (2000). Optimization of sample pH and temperature for phosphorus-31 nuclear magnetic resonance spectroscopy of poultry manure extracts. *Communications in Soil Science and Plant Analysis* **31**, 229-240.

Dalal, R. C. (1977). Soil organic phosphorus. *Advances in Agronomy* **29**, 83-117.

Dao, T. H., Sikora, L. J., Hamasaki, A., and Chaney, R. L. (2001). Manure phosphorus extractability as affected by aluminum- and iron by-products and aerobic composting. *Journal of Environmental Quality* **30**, 1693-1698.

Delgado, A., Ruíz, J. R., del Carmen del Campillo, M., Kassem, S., and Andreu, L. (2000). Calcium- and iron-related phosphorus in calcareous and calcareous marsh soils: Sequential chemical fractionation and ^{31}P Nuclear Magnetic Resonance study. *Communications in Soil Science and Plant Analysis* **31**, 2483-2499.

Delgado, A., and Torrent, J. (2000). Phosphorus forms and desorption patterns in heavily fertilized calcareous and limed acid soils. *Soil Science Society of America Journal* **64**, 2031-2037.

Diaz-Barrientos, E., Madrid, L., Contreras, M. C., and Morillo, E. (1990). Simultaneous adsorption of zinc and phosphate on synthetic lepidocrocite. *Australian Journal of Soil Research* **28**, 549-557.

Ding, M., de Jong, B. H. W. S., Rossendaal, S. J., and Vredenberg, A. (2000). XPS studies of the electronic structure of bonding between solid and solutes: Adsorption of arsenate, chromate, phosphate, Pb^{2+}, and Zn^{2+} ions on amorphous black ferric oxyhydroxide. *Geochimica et Cosmochimica Acta* **64**, 1209-1219.

Dou, Z., Toth, J. D., Galligan, D. T., Ramberg, C. F., and Ferguson, J. D. (2000). Laboratory procedures for characterizing manure phosphorus. *Journal of Environmental Quality* **29**, 508-514.

Drago, R. S. (1992). "Physical methods for chemists," 2/Ed. Saunders College Publishing, New York.

Duffy, S. J., and van Loon, G. W. (1995). Investigations of aluminum hydroxyphosphates and activated sludge by ^{27}Al and ^{31}P MAS NMR. *Canadian Journal of Chemistry* **73**, 1645-1659.

Elliott, J. C. (1994). "Structure and chemistry of the apatites and other calcium orthophosphates," Elsevier, Amsterdam.

Elzinga, E. J., Peak, D., and Sparks, D. L. (2001). Spectroscopic studies of Pb(II)-sulfate interactions at the goethite-water interface. *Geochimica et Cosmochimica Acta* **65**, 2219-2230.

Fendorf, S. E., Sparks, D. L., Lamble, G. M., and Kelley, M. J. (1994). Applications of X-ray absorption fine structure spectroscopy to soils. *Soil Science Society of America Journal* **58**, 1583-1595.

Fernandez, C., and Amoureux, J.-P. (1995). 2D multiquantum MAS-NMR spectroscopy of ^{27}Al in aluminophosphate molecular sieves. *Chemical Physics Letters* **242**, 449 - 454.

Fernandez, C., Amoureux, J. P., Chezeau, J. M., Delmotte, L., and Kessler, H. (1996). ^{27}Al MAS NMR Characterization of $AlPO_4$-14. Enhanced resolution and information by MQMAS. *Microporous Materials* **6**, 331 - 340.

Freese, D., van Riemsdijk, W. H., and van der Zee, S. E. A. T. M. (1995). Modelling phosphate sorption kinetics in acid soils. *European Journal of Soil Science* **46**, 239 - 245.

Frossard, E., Tekely, P., and Grimal, J. Y. (1994). Characterization of phosphate species in urban sewage sludges by high-resolution solid-state ^{31}P-NMR. *European Journal of Soil Science* **45**, 403-408.

Frossard, E., Skrabal, P., Sinaj, S., Bangerter, F., and Traore, O. (2002). Forms and exchangeability of inorganic phosphate in composted solid organic wastes. *Nutrient Cycling in Agroecosystems* **62**, 103-113.

Fyfe, C. A., Mueller, K. T., Grondey, H., and Wong-Moon, K. C. (1993). Solid-State Double-Resonance NMR Experiments Involving Quadrupolar and Spin 1/2 Nuclei. *J. Phys. Chem.* **97**, 13484 - 13495.

Fyfe, C. A., Wong-Moon, K. C., Huang, Y., Grondey, H., and Mueller, K. T. (1995). Dipolar-Based ^{27}Al -^{29}Si Solid-State NMR Connectivity Experiments in Zeolite Molecular Sieve Frameworks. *Journal of Physical Chemistry* **99**, 8707 - 8716.

Geelhoed, J. S., Hiemstra, T., and van Riemsdijk, W. H. (1998). Competitive Interaction between Phosphate and Citrate on Goethite. *Environmental Science and Technology* **32**, 2119 - 2123.

Geelhoed, J. S., van Riemsdijk, W. H., and Findenegg, G. R. (1999). Simulation of the Effect of Citrate Exudation from Roots on the Plant Availability of Phosphate Adsorbed on Goethite. *European Journal of Soil Science* **50**, 379-390.

Goldberg, S. (1992). Use of Surface Complexation Models in Soil Chemical Systems. *In* "Advances in Agronomy" (D. L. Sparks, ed.), Vol. 47, pp. 234-321. Academic Press, San Diego, London, Boston, New York, Sydney, Tokyo, Toronto.

Goldberg, S., and Sposito, G. (1984a). A chemical model of phosphate adsorption by Soils: 1. Reference oxide minerals. *Soil Sci. Soc. Am. J.* **48**, 772 - 778.

Goldberg, S., and Sposito, G. (1984b). A chemical model of phosphate adsorption by soils: 2. Noncalcareous soils. *Soil Science Society of America Journal* **48**, 779 - 783.

Grey, C. P., Veeman, W. S., and Vega, A. J. (1993). Rotational echo $^{14}N/^{13}C/^{1}H$ triple resonance solid-state nuclear magnetic resonance: A probe of ^{13}C -^{14}N internuclear distances. *Journal of Chemical Physics* **98**, 7711-7723.

Griffin, R. A., and Jurinak, J. J. (1973). The interaction of phosphate with calcite. *Soil Science Society of America Journal* **37**, 847-850.

Griffin, R. A., and Jurinak, J. J. (1974). Kinetics of phosphate interaction with calcite. *Soil Science Society of America Journal* **38**, 75 - 79.

Grossl, P. R., and Inskeep, W. P. (1991). Precipitation of dicalcium phosphate dihydrate in the presence of organic acids. *Soil Science Society of America Journal* **55**, 670-675.

Guest, C., D.G., S., Thompson, I. A., and Huber, D. M. (2002). Correlating manganese X-ray absorption near edge structure spectra with extractable soil manganese. *Soil Science Society of America Journal* **66**, 1172-1181.

Gullion, T., and Schaefer, J. (1989a). Detection of Weak Heteronuclear Dipolar Coupling by Rotational-Echo Double Resonance Nuclear Magnetic Resonance. *In* "Advances in Magnetic Resonance" (S. W. Warren, ed.), Vol. 13, pp. 58 - 84. Academic Press, New York.

Gullion, T., and Schaefer, J. (1989b). Rotational-Echo Double Resonance NMR. *Journal of Magnetic Resonance* **81**, 196 - 200.

Hamad, M. E., Rimmer, D. L., and Syers, J. K. (1992). Effect of iron oxide on phosphate sorption by calcite and calcareous soils. *Journal of Soil Science* **43**, 273-281.

Hartmann, P., Vogel, J., and Schnabel, B. (1994). The influence of short-range geometry on the ^{31}P chemical-shift tensor in protonated phosphates. *Journal of Magnetic Resonance* **111**, 110-114.

Hartmann, S. R., and Hahn, E. L. (1962). Nuclear double resonance in the rotating frame. *Physical Review* **128**, 2042-2053.

Hawthorne, F. C. (1998). Structure and chemistry of phosphate minerals. *Mineralogical Magazine* **42**, 141-164.

He, L. M., Zelazny, L. W., Baligar, V. C., Ritchey, K. D., and Martens, D. C. (1997). Ionic Strength Effects on Sulfate and Phosphate Adsorption on γ-Alumina and Kaolinite: Triple-Layer Model. *Soil Sci. Soc. Am. J.* **61**, 784 - 793.

He, Z. L., Baligar, V. C., Martens, D. C., and Ritchey, K. D. (1998). Determination of Soluble Phosphorus in the Presence of Organic Ligands or Fluoride. *Soil Sci. Soc. Am. J.* **62**, 1538 - 1541.

Hedley, M. J., Stewart, J. W. B., and Chauhan, B. S. (1982). Changes in inorganic and organic soil phosphorus fractions induced by cultivation practices and by laboratory incubations. *Soil Science Society of America Journal* **46**, 970-976.

Hiemstra, T., and van Riemsdijk, W. H. (1999). Surface structural ion adsorption modeling of competitive binding of oxyanions by metal (hydr)oxides. *Journal of Colloid and Interface Science* **210**, 182 - 193.

Hiemstra, T., Yong, H., and van Riemsdijk, W. H. (1999). Interfacial charging phenomena of aluminum (hydr)oxides. *Langmuir* **15**, 5942-5955.

Hinedi, Z. R., and Chang, A. C. (1989). Solubility and phosphorus-31 magic angle spinning nuclear magnetic resonance of phosphorus in sludge-amended soils. *Soil Sci. Soc. Am. J.* **53**, 1057 - 1061.

Hinedi, Z. R., Chang, A. C., and Lee, R. W. K. (1988). Mineralization of phosphorus in sludge-amended soils monitored by phosphorus-31-nuclear magnetic resonance spectroscopy. *Soil Science Society of America Journal* **52**, 1593-1596.

Hinedi, Z. R., Chang, A. C., and Lee, R. W. K. (1989a). Characterization of phosphorus in sludge extracts using phosphorus-31 nuclear magnetic resonance spectroscopy. *Journal of Environmental Quality* **18**, 323 - 329.

Hinedi, Z. R., Chang, A. C., and Yesinowski, J. P. (1989b). Phosphorus-31 magic angle spinning nuclear magnetic resonance of wastewater sludges and sludge-amended soil. *Soil Science Society of America Journal* **53**, 1053 - 1056.

Hinedi, Z. R., Goldberg, S., Chang, A. C., and Yesinowski, J. P. (1992). A ^{31}P and ^{1}H NMR study of phosphate sorption onto calcium carbonate. *Journal of Colloid and Interface Science* **152**, 141-160.

Hoch, A. R., Reddy, M. M., and Aiken, G. R. (2000). Calcite crystal growth inhibition by humic substances with emphasis on hydrophobic acids from the Florida Everglades. *Geochimica et Cosmochimica Acta* **64**, 61-72.

Inskeep, W. P., and Bloom, P. R. (1986). Kinetics of calcite precipitation in the presence of water-soluble organic ligands. *Soil Science Society of America Journal* **50**, 1167-1172.

Inskeep, W. P., and Silvertooth, J. C. (1988). Inhibition of hydroxyapatite precipitation in the presence of fulvic, humic and tannic acids. *Soil Science Society of America Journal* **52**, 941 - 946.

Iyamuremye, F., Dick, R. P., and Baham, J. (1996a). Organic amendments and Phosphorus dynamics: 1. Phosphorus chemistry and sorption. *Soil Science* **161**, 426 - 435.

Iyamuremye, F., Dick, R. P., and Baham, J. (1996b). Organic amendments and phosphorus dynamics: 2. Distribution of soil phosphorus fractions. *Soil Science* **161**, 436 - 443.

Iyamuremye, F., Dick, R. P., and Baham, J. (1996c). Organic amendments and Phosphorus dynamics: 3. Phosphorus speciation. *Soil Science* **161**, 444 - 451.

Jones, D. L. (1998). Organic acids in the rhizosphere - a critical review. *Plant and Soil* **205**, 25 - 44.

Jones, D. L., and Darrah, P. R. (1994). Role of root derived organic acids in the mobilization of nutrients from the rhizosphere. *Plant and Soil* **166**, 247 - 257.

Kniep, R., Mootz, P., and Vegas, A. (1977). Variscite. *Acta Crystallographica B* **33**, 263-265.

Kraus, H., Prins, R., and Kentgens, A. P. M. (1993). A ^{27}Al MQMAS and Off-Resonance Nutation NMR Investigation of Mo-P/γ-Al_2O_3 Hydrotreating Catalyst Precursors. *J. Phys. Chem.* **100**, 16336 - 16345.

Kuo, S. (1986). Concurrent sorption of phosphate and zinc, cadmium, or calcium by a hydrous ferric oxide. *Soil Science Society of America Journal* **50**, 1412-1419.

Kuo, S., and Lotse, E. G. (1972). Kinetics of phosphate adsorption by calcium carbonate and Ca-kaolinite. *Soil Science Society of America Journal* **36**, 725-729.

Kuo, S., and McNeal, B. L. (1984). Effects of pH and phosphate on cadmium sorption by a hydrous ferric oxide. *Soil Science Society of America Journal* **48**, 1040-1044.

Laiti, E., Persson, P., and Oehman, L.-O. (1996). Surface complexation and precipitation at the H^+-orthophosphate-aged γ-Al_2O_3/ water interface. *Langmuir* **12**, 2969 - 2975.

Laiti, E., Persson, P., and Oehman, L.-O. (1998). Balance between surface complexation and surface phase transformation at the alumina/ water interface. *Langmuir* **14**, 825 - 831.

Lang, D. P., Alam, T. M., and Bencoe, D. N. (2001). Solid-State $^{31}P/^{27}Al$ and $^{31}P/^{23}Na$ TRAPDOR NMR Investigations of the Phosphorus Environments in Sodium Aluminophosphate Glasses. *Chemistry of Materials* **13**, 420-428.

Leinweber, P., Haumaier, L., and Zech, W. (1997). Sequential extractions and 31-P-NMR spectroscopy of Phosphorus forms in animal manures, whole soils and particle-size separates from a densely populated livestock area in northwest Germany. *Biology and Fertility of Soils* **25**, 89 - 94.

Ler, A., and Stanforth, R. (2003). Evidence for surface precipitation of phosphate on goethite. *Environmental Science and Technology* **37**, 2694-2700.

Li, L., and Stanforth, R. (2000). Distinguishing Adsorption and Surface Precipitation of Phosphate on Goethite (α-FeOOH). *Journal of Colloid and Interface Science* **230**, 12-21.

Lindsay, W. L. (1979). "Chemical Equilibria in Soils."

Lookman, R., Geerts, H., Grobet, P., Merckx, R., and Vlassak, K. (1996). Phosphate speciation in excessively fertilized soil: a ^{31}P and ^{27}Al MAS NMR spectroscopy study. *European Journal of Soil Science* **47**, 125 - 130.

Lookman, R., Grobet, P., Merckx, R., and van Riemsdijk, W. H. (1997). Application of ^{31}P and ^{27}Al MAS NMR for phosphate speciation in soil and aluminum hydroxides: Promises and constraints. *Geoderma* **80**, 369 - 388.

Lookman, R., Grobet, P., Merckx, R., and Vlassak, K. (1994). Phosphate sorption by synthetic amorphous aluminum hydroxides: a ^{27}Al and ^{31}P solid state MAS NMR spectroscopy study. *European Journal of Soil Science* **45**, 37 - 44.

Maguire, R. O., and Sims, J. T. (2002). Measuring agronomic and environmental soil phosphorus saturation and predicting phosphorus leaching with Mehlich 3. *Soil Science Society of America Journal* **66**, 2033-2039.

Mahieu, N., Olk, D. C., and Randall, E. W. (2000). Analysis of Phosphorus in Two Humic Acid Fractions of Intensively Cropped Lowland Rice Soils by ^{31}P - NMR. *European Journal of Soil Science* **51**, 391 - 402.

McDowell, R. W., Condron, L. M., Mahieu, N., Poulton, P. R., and Sharpley, A. (2002). Analysis of potentially mobile phosphorus in arable soils using solid state nuclear magnetic resonance. *Journal of Environmental Quality* **31**, 450-456.

McDowell, R. W., Mahieu, N., Brookes, P. C., and Poulton, P. R. (2003). Mechanisms of phosphorus solubilization in a limed soil as a function of pH. *Chemosphere* **51**, 685-692.

McDowell, R. W., and Sharpley, A. (2003). Phosphorus solubility and release kinetics as a function of soil test P concentrations. *Geoderma* **112**, 143-154.

Millero, F., Huang, F., Zhu, X., Liu, X., and Zhang, J.-Z. (2001). Adsorption and desorption of phosphate on calcite and aragonite in seawater. *Aquatic Geochemistry* **7**, 33-56.

Moore, Jr., P.A. , and Miller, D. M. (1994). Decreasing Phosphorus Solubility in Poultry Litter with Aluminum, Calcium and Iron Amendments. *Journal of Environmental Quality* **23**, 325 - 330.

Moore, Jr., P.A. , Daniel, T. C., Edwards, D. R., and Miller, D. M. (1995a). Effect of Chemical Amendments on Ammonia Volatilization from Poultry Litter. *Journal of Environmental Quality* **24**, 293 - 300.

Moore, Jr., P.A., Daniel, T. C., and Edwards, D. R. (2000). Reducing Phosphorus Runoff and Inhibiting Ammonia Loss from Poultry Manure with Aluminum Sulfate. *Journal of Environmental Quality* **29**, 37-49.

Moore, Jr., P.A., Daniel, T. C., Gilmour, J. T., Shreve, B. R., Edwards, D. R., and Wood, B. H. (1998). Decreasing Metal Runoff from Poultry Litter with Aluminum Sulfate. *Journal of Environmental Quality* **27**, 92-99.

Moore, Jr., P.A., Daniel, T. C., Sharpley, A. N., and Wood, C. W. (1995b). Poultry manure management: Environmentally sound options. *Journal of Soil and Water Conservation* **50**, 321-327.

Mortlock, R. F., Bell, A. T., and Radke, C. J. (1993). ^{31}P and ^{27}Al NMR investiagtions of the effect of pH on aqueous solutions containing aluminum and phosphorus. *Journal of Physical Chemistry* **97**, 775-782.

Murphy, J., and Riley, H. P. (1962). A modified single solution method for the determination of phosphate in natural waters. *Analytica Chimica Acta* **27**, 31-36.

Nanny, M. A., Minear, R. A., and Leenheer, J. A. (1997). "Nuclear Magnetic Resonance Spectroscopy in Environmental Chemistry," Oxford University Press, New York, Oxford.

Nanzyo, M. (1984). Diffuse reflectance infrared spectra of phosphate sorbed on alumina gel. *Journal of Soil Science* **35**, 63 - 69.

Nanzyo, M. (1986). Infrared Spectra of Phosphate sorbed on Iron Hydroxide Gel and the Sorption Products. *Soil Science and Plant Nutrition* **32**, 51 - 58.

Nanzyo, M., and Watanabe, Y. (1982). Diffuse Reflectance Infrared Spectra and Ion-Adsorption Properties of the Phosphate Surface Complex on Goethite. *Soil Science and Plant Nutrition* **28**, 359 - 368.

Newman, R. H., and Tate, K. R. (1980). Soil phosphorus characterization by ^{31}P nuclear magnetic resonance. *Communications in Soil Science and Plant Analysis* **11**, 835-842.

Nilsson, N., Persson, P., Lövgren, L., and Sjöberg, S. (1996). Competitive surface complexation of o-phthalate and phosphate on goethite (α-FeOOH) particles. *Geochimica et Cosmochimica Acta* **60**, 4385 - 4395.

Ohno, T. (1997). Inhibitory effects of crop residue-derived organic ligands on phosphate adsorption kinetics. *Journal of Environmental Quality* **26**, 889 - 895.

Ohno, T., and Crannell, B. S. (1996). Green and Animal manure-derived dissolved organic matter effects on Phosphorus sorption. *J. Environ. Qual.* **25**, 1137 - 1143.

Pant, H. K., Warman, P. R., and Nowak, J. (1999). Identification of soil organic phosphorus by ^{31}P nuclear magnetic resonance spectroscopy. *Communications in Soil Science and Plant Analysis* **30**, 757-772.

Parfitt, R. L. (1978). Anion adsorption by soils and soil minerals. *In* "Advances in Agronomy" (D. L. Sparks, ed.), Vol. 30, pp. 1-50. Academic Press, San Diego, London, Boston, New York, Sydney, Tokyo, Toronto.

Parker, J. C., Zelazny, L. W., Sampath, S., and Harris, W. G. (1979). A critical evaluation of the extension of zero point of charge (ZPC) theory to soil systems. *Soil Science Society of America Journal* **43**, 668-674.

Paul, E. A., and Clark, F. E. (1996). "Soil Microbiology and Biochemistry," 2nd/Ed. Academic Press, San Diego, London, Boston, New York, Sydney, Toronto, Tokyo.

Pautler, M. C., and Sims, J. T. (2000). Relationship Between Soil Test Phosphorus, Soluble Phosphorus, and Phosphorus Saturation in Delaware Soils. *Soil Science Society of America Journal* **64**, 765-773.

Peak, D., Sims, J. T., and Sparks, D. L. (2002). Solid-state speciation of natural and alum-amended poultry litter using XANES spectroscopy. *Environmental Science and Technology* **36**, 4253-4261.

Persson, P., Nilsson, N., and Sjöberg, S. (1996). Structure and bonding of orthophosphate ions at the iron oxide-aqueous interface. *Journal of Colloid and Interface Science* **177**, 163 - 275.

Pines, A., Gibby, M. G., and Waugh, J. S. (1973). Proton-enhanced NMR of dilute spins in solids. *Journal of Chemical Physics* **59**, 569-590.

Rietra, R. P. J. J., Hiemstra, T., and van Riemsdijk, W. H. (2001). Interaction between Calcium and Phosphate Adsorption on Goethite. *Environmental Science and Technology* **35**, 3369-3374.

Robinson, J. S., Johnston, C. T., and Reddy, K. R. (1998). Combined Chemical and ^{31}P-NMR Spectroscopic Analysis of Phosphorus in Wetland Organic Soils. *Soil Science* **163**, 705-713.

Rong, C., Wong-Moon, K. C., Li, H., Hrma, P., and Cho, H. (1998). Solid-state NMR investigation of phosphorus in aluminoborosilicate glasses. *Journal of Non-Crystaline Solids* **223**, 32 - 42.

Rothwell, W. P., Waugh, J. S., and Yesinowski, J. P. (1980). High-resonance variable-temperature ^{31}P-NMR of solid calcium phosphates. *Journal of the American Chemical Society* **102**, 2637-2643.

Saalfeld, H., and Wedde, M. (1974). Refinement of the crystal-structure of gibbsite, Al(OH)3. *Zeitschrift für Kristallographie* **139**, 129-135.

Schaller, T., Rong, C., Toplis, M. J., and Cho, H. (1999). TRAPDOR NMR investigations of phosphorus-bearing aluminosilicate glasses. *Journal of Non-Crystalline Solids* **248**, 19 - 27.

Scheidegger, A. M., Fendorf, M., and Sparks, D. L. (1996). Mechanisms of nickel sorption on pyrophyllite: Macroscopic and microscopic approaches. *Soil Science Society of America Journal* **60**, 1763-1772.

Scheidegger, A. M., Strawn, D. G., Lamble, G. M., and Sparks, D. L. (1998). The kinetics of mixed Nickel-Aluminum hydroxide formation on clay and Aluminum oxide minerals: A time resolved XAFS study. *Geochimica et Cosmochimica Acta* **62**, 2233 - 2245.

Seaman, J.C., J.M. Hutchison, B.P. Jackson, and V.M. Vulava. 2003. In situ treatment of metals in contaminated soils with phytate. Journal of Environmental Quality 32:153-161.

Sharpley, A., Foy, B., and Withers, P. (2000). Practical and Innovative Measures for the Control of Agricultural Phosphorus Losses to Water: An Overview. *Journal of Environmental Quality* **29**, 1-9.

Sharpley, A. N., Chapra, S. C., Wedepohl, R., Sims, J. T., Daniel, T. C., and Reddy, K. R. (1994). Managing agricultural phosphorus for protection of surface waters: Issues and options. *Journal of Environmental Quality* **23**, 437-451.

Sharpley, A. N., Daniel, T., Sims, J. T., Lemunyon, J., Stevens, R., and Parry, R. (1999). "Agricultural Phosphorus and Eutrophication." United States Department of Agriculture, Agricultural Research Service.

Sharpley, A., and Moyer, B. (2000). Phosphorus forms in manure and compost and their release during simulated rainfall. *Journal of Environmental Quality* **29**, 1462-1469.

Shreve, B. R., P.A. Moore, J., Daniel, T. C., Edwards, D. R., and Miller, D. M. (1995). Reduction of Phosphorus in Runoff from Field-Applied Poultry Litter Using Chemical Amendments. *Journal of Environmental Quality* **24**, 106 - 111.

Sibanda, H. M., and Young, S. D. (1986). Competitive adsorption of humus acids and phosphate on goethite, gibbsite and two tropical soils. *Journal of Soil Science* **37**, 197 - 204.

Sims, J. T., and Luka-McCafferty, N. J. (2002). On-farm evaluation of aluminum sulfate (alum) as a poultry litter amendment: Effects on litter properties. *Journal of Environmental Quality* **31**, 2066-2073.

Sinaj, S., Traore, O., and Frossard, E. (2002). Effect of compost and soil properties on the availability of compost phosphate for white clover (Trifolium repens L.). Nutrient Cycling in Agroecosystems 62, 89-102.

Smernik, R. J., and Oades, J. M. (2002). Paramagnetic effects on solid state carbon-13 nuclear magnetic resonance spectra of soil organic matter. *Journal of Environmental Quality* **31**, 414-420.

Smith, S. A., and Read, D. J. (1997). "Mycorrhizal Symbiosis," 2nd/Ed. Academic Press, San Diego, London, New York, Boston, Sydney, Tokyo, Toronto.

Sparks, D. L. (1995). "Environmental Soil Chemistry," Academic Press, San Diego, New York, Boston.

Sposito, G. (1981). The Operational Definition of the Zero Point of Charge in Soils. *Soil Science Society of America Journal* **45**, 292 - 297.

Sposito, G. (1984). "The Surface Chemistry of Soils," Oxford University Press, New York.

Sposito, G. (1989). "The Chemistry of Soils," Oxford University Press, New York.

Staunton, S., and Leprince, F. (1996). Effect of pH and some organic anions on the solubility of soil phosphate: implications for P bioavailability. *European Journal of Soil Science* **47**, 231 - 239.

Stumm, W. (1986). Coordinative Interactions between Soil Solids and Water - an Aquatic Chemist's point of view. *Geoderma* **38**, 19 - 30.

Stumm, W. (1997). Reactivity at the mineral-water interface: dissolution and inhibition. *Colloids and Surfaces A: Physicochemical and Engineering Aspects* **120**, 143-166.

Stumm, W., and Morgan, J. J. (1996). "Aquatic chemistry," 3rd/Ed. Wiley Interscience, New York, Chichester, Brisbane, Toronto, Singapore.

Sutter, B., Taylor, R. E., Hossner, L. R., and Ming, D. W. (2002). Solid state 31-phosphorus nuclear magnetic resonance of iron-, manganese-, and copper-containing synthetic hydroxyapatites. *Soil Science Society of America Journal* **66**, 455-463.

Taylor, T. G. (1965). The availability of the calcium and phosphorus of plant materials for animals. *Prceedings of the Nutrition Society* **24**, 105-112.

Tejedor-Tejedor, M. I., and Anderson, M. (1990). Protonation of Phosphate on the Surface fo Goethite as studied by CIR-FTIR and Electrophoretic Mobility. *Langmuir* **6**, 602 - 611.

Tejedor-Tejedor, M. I., and Anderson, M. A. (1986). "In situ" Attenuated Total Reflectance Fourier Transform Infrared Studies of the Goethite-Aqueous Solution Interface. *Langmuir* **2**, 203 - 210.

Traina, S. J., Sposito, G., Hesterberg, D., and Kafkafi, U. (1986). Effects of pH and organic acids on orthophosphate solubility in an acidic, montmorillonitic soil. *Soil Science Society of America Journal* **50**, 45 - 52.

Tunesi, S., Poggi, V., and Gessa, C. (1999). Phosphate adsorption and precipitation in calcareous soils: The role of calcium ions in solution and carbonate minerals. *Nutrient Cycling in Agroecosystems* **53**, 219-227.

Turner, G. L., Smith, K. A., Kirkpatrick, R. J., and Oldfield, E. (1986). Structure and Cation Effects on Phosphorus-31 NMR Chemical Shifts and Chemical-Shift Anisotropies of Orthophosphates. *Journal of Magnetic Resonance* **70**, 408-415.

van Eck, E. R. H., Kentgens, A. P. M., Kraus, H., and Prins, R. (1995). A solid state double resonance NMR investigation of phosphorus-impregnated γ-Alumina. *Journal of Physical Chemistry* **99**, 16080 - 16086.

van Riemsdijk, W. H., Boumans, L. J. M., and de Haan, F. A. M. (1984). Phosphate sorption by soils: 1. A model for phosphate reaction with metal-oxides in soils. *Soil Science Society of America Journal* **48**, 537 - 541.

Venema, P., Hiemstra, T., and van Riemsdijk, W. H. (1997). Interaction of cadmium with phosphate on goethite. *Journal of Colloid and Interface Science* **192**, 94-103.

Voegelin, A., Scheinost, A. C., Bühlmann, K., Barmettler, K., and Kretzschmar, R. (2002). Slow formation and dissolution of zinc precipitates in soil: A combined column transport and XAFS study. *Environmental Science and Technology* **36**, 3749-3754.

Wilson, M. A. (1987). "NMR-Techniques and Applications in Geochemistry and Soil Chemistry.," Pergamon Press, Oxford.

Yoza, N., Ueda, N., and Nakashima, S. (1994). pH-Dependence of ^{31}P-NMR spectroscopic parameters of monofluorophosphate, phosphate, hypophosphate, phosphonate, phosphinate and their dimers and trimers. *Fresenius Journal of Analytical Chemistry* **348**, 633 - 638.

Zhang, T. Q., Mackenzie, A. F., and Sauriol, F. (1999). Nature of Soil Organic Phosphorus as affected by long-term Fertilization under Continuous Corn (*Zea Mays* L.): A ^{31}P NMR Study. *Soil Science* **164**, 662-670.